NATIONAL AERONAUTICS AND SPACE ADMINISTRATION

Technical Memorandum 33-768

Mu-II Ranging

W. L. Martin
A. I. Zygielbaum

JET PROPULSION LABORATORY
CALIFORNIA INSTITUTE OF TECHNOLOGY
PASADENA, CALIFORNIA

May 15, 1977

Prepared Under Contract No. NAS 7-100
National Aeronautics and Space Administration

Preface

The work described in this report was performed by the Telecommunications Division of the Jet Propulsion Laboratory.

Contents

Tables

Figures

Abstract

This report describes the Mu-II Dual-Channel Sequential Ranging System designed as a model for future Deep Space Network ranging equipment. A list of design objectives is followed by a theoretical explanation of the digital demodulation techniques first employed in this machine. Thereafter, both hardware and software implementation are discussed, together with the details relating to the construction of the device. The report concludes with a section describing the system's performance in both the field and laboratory, with the authors' recommendations for future ranging equipment. Finally, in the interest of completeness, two appendixes are included relating to the programming and operation of this equipment to yield the maximum scientific data.

MU-II Ranging

I. Introduction

Ranging with sequential components was first suggested in 1969 (Ref. 1). Advantages intrinsic to serial transmission of a range code, together with an increased efficiency resulting from harmonically related code components, made the scheme appear most attractive. Calculations predicted a 40 to 1 improvement in acquisition time over previous designs. A prototype was built to test the concept and used to support both the Mariner 1969 and 1971 missions. Throughout these two programs, ranging data was employed for navigation and to test Einstein's Theory of General Relativity. Additionally, performance and evaluation checks were made while the equipment was in a Deep Space Network (DSN) environment. Usage-upheld theoretical predictions and the results of several tests, together with a description of the design criteria, are summarized in Refs. 2 and 3.

During the 4 years in which the prototype was supplying ranging information to the two Mariner missions, certain operational deficiencies became apparent. A unique opportunity was presented in late 1972 when the need arose for a two-channel, S- and X-band, ranging machine to support the Mariner Venus/Mercury 1973 (MVM'73) radio science experiments. While work had been going forward in the design of an improved ranging subsystem, the commitment to a project provided the impetus and opportunity to translate many new ideas into reality. These ideas, their rationale, and their

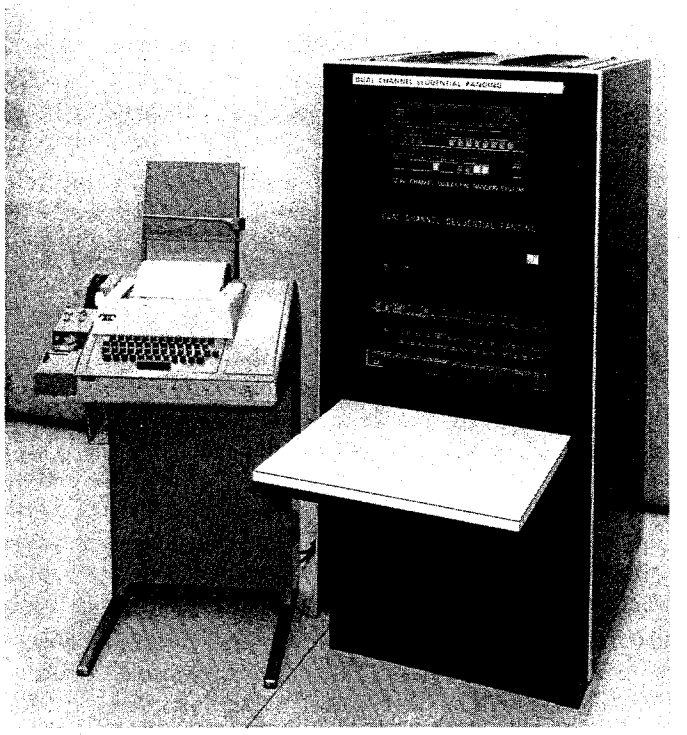

Fig. 1. Dual-Channel Sequential Ranging System (Mu-II)

translation into the finished product (Fig. 1) are the subjects of this report.

The report is subdivided into six remaining sections. Section II sets forth the design objectives. Experience gained during the Mariner 1969 and 1971 missions, together with discussions with station operating personnel, led to a formulation of this set of design objectives. A statement of these features, together with a succinct explanation, appears in this section.

Section III discusses the range measurement and the principles of the machine's operation. Equations representing the calculation of carrier phase and the computation of range are included.

Section IV describes the ranging hardware and contains a detailed explanation of the system's block diagram and subunits. Included are performance and test data on critical components, together with a commentary on design philosophy, to maximize stability and reliability.

Section V explains the capability provided by the software. The objective is to familiarize the potential user with the rather extensive number of options available in order that he may maximize the return on his experimental investment. This section also describes how the machine is operated and provides operational instructions for the user.

Section VI is concerned with the finished product. Photographs of the ranging and interface units are included to illustrate the packaging of these subsystems. The accompanying description sets forth the objectives which led to this package design.

Section VII concludes the report and presents performance data gathered under both laboratory and field conditions. Extensive stability and repeatability tests conducted in the laboratory show the effects of various subsystems upon performance of the composite system. Field data, collected over several months at Deep Space Station (DSS) 14, is also included to demonstrate stability under actual operating conditions.

II. Design Objectives

Ranging is basically a measurement of elapsed time between the transmission and return of an encoded signal, as described in Section III. Thus, superficially, there appears to be an identity among equipment designed for range determination. However, both the underlying philosophy and the mechanization can vary substantially between systems, rendering this apparent similarity illusory. So it is with this machine, wherein a cursory examination deceptively leads one to the inference of commonality with its predecessor. To forestall such conclusions, a list of features has been compiled which distinguishes this from other systems. This list, together with a succinct description of each characteristic, is presented here to provide the reader with a concise summary of capability while allowing him to seek greater depth in later sections if he so desires.

(1) *Ease of operation.* An entire day's operating sequence, including multiple reacquisitions, can be entered hours before a pass, and the machine automatically performs all functions at the proper time.

(2) *Flexibility of operating modes.* 32,268 different operating modes ensure that the machine can support virtually any experimental objective.

(3) *Multiple reacquisitions.* Up to 10 separate acquisitions can be "strung out" between spacecraft and Earth, facilitating rapid acquisition of multiple independent range points without loss of data.

(4) *Automatic calibration.* Automatic measurement and calibration of the receivers' 10-MHz IF carrier phase for each range point ensures optimal performance from the demodulator.

(5) *Automatic level control.* A wideband automatic gain control (AGC) amplifier automatically controls the input signal level without affecting group delay, relieving the operator of making periodic adjustments.

(6) *All-digital signal processing.* A high-speed, 40-MHz analog-to-digital converter ensures stability by digitizing the 10-MHz carrier, eliminating the need for analog signal processing with mixers, filters, and demodulators.

(7) *High accuracy, stability, and reliability.* Wide bandwidths, coupled with high-speed logic, minimize delays, thereby promoting stability. Careful symmetry control of all code waveforms eliminates distortion which can cause a spacecraft transponder's "apparent" delay to be affected by ground hardware changes.

(8) *True two-channel operation.* Complete, separate and independent channels allow simultaneous ranging on S-band, X-band, or any combination of these or any other frequencies.

(9) *High-resolution code option.* Extended range provides codes up to 8 MHz for improved accuracy

when compatible spacecraft hardware becomes available.

(10) *Compatibility with Block III-Block IV ground receivers.* The phase inversion existing between the two receivers can be compensated by simply setting a computer parameter inverting the digital demodulation process.

(11) *Adaptability to other computer types.* A generalized interface design allows connection with other computer types with minimal changes.

(12) *Fault indication and simplicity of repair.* Status monitors on important functions provide immediate visual indication of erratic behavior. Modular design allows for swift replacement of malfunctioning part.

(13) *Unitized packaging.* Compact design results in economy of floor space, portability, and simplicity of operation.

(14) *Human-readable local data output.* In addition to providing backup for the primary data handling system, local data output gives the operator a real-time indication of system operation.

(15) *Code servo option.* Optimal automatic adjustment of phase relationship between local reference code and received code ensures maximum sensitivity to group delay changes. Simple mode change allows servo to be disabled when plasma activity is high.

Because of space limitation, the foregoing list is necessarily incomplete. Additional information on each item will be found in the following text.

III. Principles of Ranging

A. Theory of Ranging

Range is essentially a determination of the period of time a radio wave takes in traversing the round-trip distance from the Earth to a spacecraft. Commonly called the round-trip light time (RTLT), this period is measured through the use of a turn-around transponder on the spacecraft. The uplink carrier is modulated by some repetitious code, termed a range code. Transponded, the code is returned to Earth on the downlink carrier. The returned code appears phase delayed from that being transmitted due to the round-trip travel time. This phase offset is the basis for the range determination.

The phase offset translates directly into a measure of distance if the code's period is greater than the RTLT. On the other hand, if the code period is some fraction of the RTLT, then the range measurement is ambiguous. For example, if the transmitted and returned codes have periods of 1 s, and differ in phase by 180 deg, then the RTLT to the spacecraft could be 0.5, 1.5, 2.5 ...$(n + 0.5)$ s (for any integer n). This ambiguity results from repetition of the code. RTLTs are on the order of tens of minutes for neighboring planets and hours for distant bodies such as Uranus. Unambiguous resolution of such distances would require codes of comparable periods. Both the generation and the phase measurement of such codes are impractical. Fortunately, one can make an a priori estimate of the spacecraft's range, which reduces the distance that must be resolved. The code period now need only be greater than the uncertainty of the a priori estimate since the number of code periods within the predicted distance can be computed. Adding the predicted number of code periods to the fractional period measured by the Mu-II results in the unambiguous range estimate.

Although measurement precision is a concept quite distant from ambiguity, it too is related to the code frequency. Unlike ambiguity, the precision to which code phase measurement can be made improves as the code period decreases. For example, if a precision of 10 ns is required and the code period is 100 s, then phase must be resolved to one part in 10^{10}. This is a difficult if not impossible task. If however, the code period is 2 μs, the same precision only requires measurement to within one part in 200.

The Mu-II balances the conflicting requirements of ambiguity resolution and measurement precision through the use of several square wave range codes. Related by powers of two, these codes are transmitted sequentially, starting with the highest frequency, which establishes the precision of the measurement, and ending with the lowest, which has minimum ambiguity. The Mu-II makes available codes from about 8 MHz to approximately 1 Hz. This gives the system a maximum ambiguity resolution of 3×10^8 m and a precision in the neighborhood of a fraction of a nanosecond.

B. Mu-II Ranging

The Mu-II is operated as part of a DSN tracking station. Its relation to other ground-based subsystems and to the spacecraft is shown in Fig. 2. The ranging process starts with the generation of the range code in the transmitter coder. Derived from a 66- or 132-MHz frequency reference by successive division by powers of two, the appropriate code is selected by the ranging computer. This code is phase-modulated onto the uplink carrier and transmitted to the spacecraft. A transponder aboard the spacecraft, which is phase-locked to the uplink carrier,

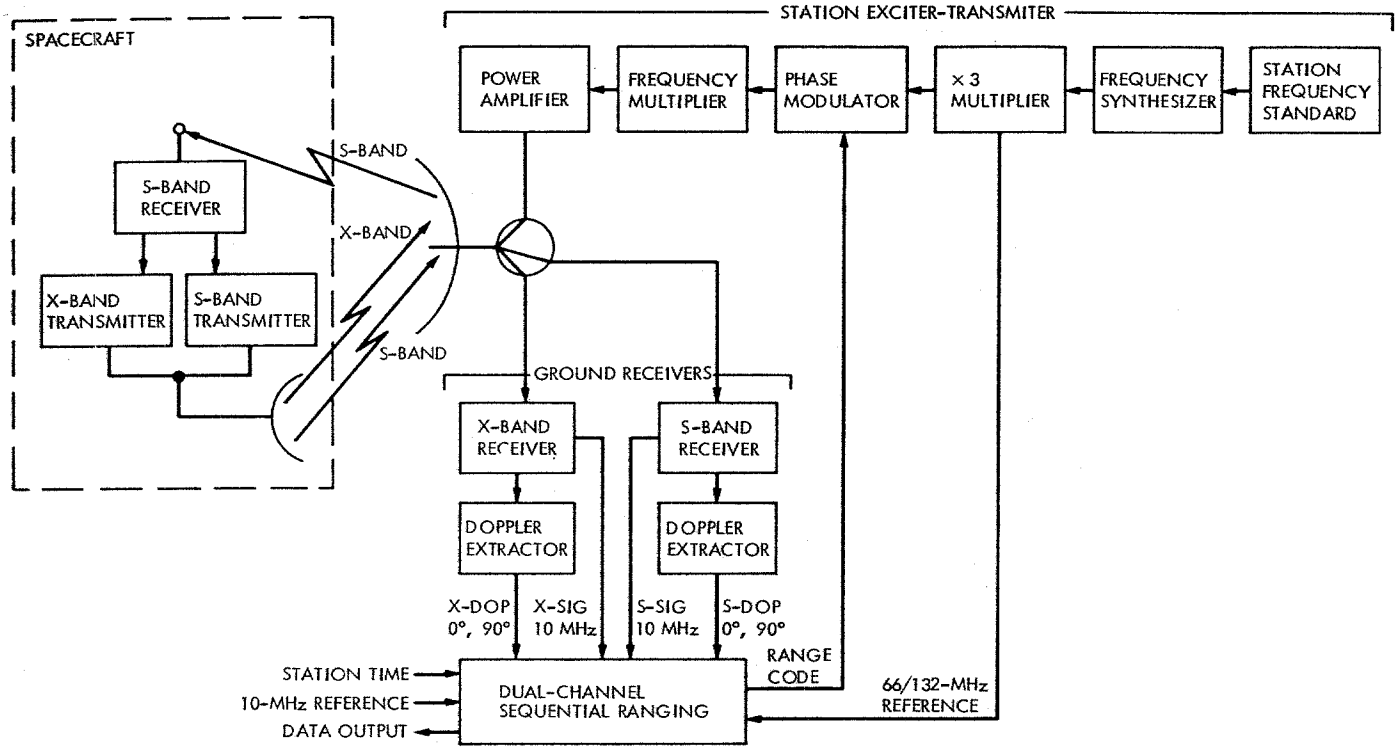

Fig. 2. Station–spacecraft configuration

multiplies the carrier frequency by 240/221 and 880/221 to develop, respectively, S- and X-band downlink carriers. Concurrently, the received range code is coherently detected, filtered in a 1-MHz passband channel, hard-limited, and used to remodulate the two downlink carriers. Note that two-way doppler will be affected by the carrier frequency multiplication, whereas the range code will not. The downlink signals are received by two identical Block IV receivers, phase-locked respectively to the S- and X-band carriers. These receivers provide 10-MHz IF signals modulated with the range code to the Mu-II. Utilizing these codes, the Mu-II independently measures the S- and X-band range. The Mu-II has two separate and identical receiving channels, one for S-band and one for X-band. In the discussions following, the range measurement algorithm will be explicitly examined. It is to be understood that the discussion applies equally to both channels.

The range code received differs from that transmitted by (1) phase delay due to range, (2) frequency change due to Earth–spacecraft relative doppler, and (3) lesser phase and frequency variations due to the transmission medium. It is impossible to determine the phase difference of two square waves whose frequencies are not identical. Before range can be determined, the doppler effect must be

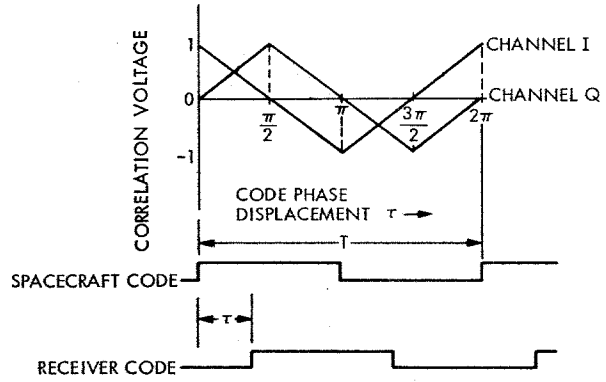

Fig. 3. Code correlation characteristics

removed. The Mu-II uses a second coder, termed the receiver coder, to accomplish this. This coder is identical to the transmitter coder in all respects. The codes it generates are based upon the same 66- or 132-MHz reference. Just prior to completion of a RTLT after start of the ranging transmit sequence, the receiver coder is synchronized to the transmitter coder. Their respective outputs are made identical. Following synchronization, however, the receiver coder's count rate is modified by adding properly scaled doppler from the Block IV (or III) doppler extractor to the 66- or 132-MHz reference. This process, known as doppler rate aiding, causes the receiver

coder to instantaneously become a frequency coherent model of the received signal. In other words, it becomes identical to what the transmitted code would be if the transmitted code were modified by doppler. The necessary code phase measurement can now be made at leisure since the received code and the receiver coder output remain in a fixed phase relationship. The resulting range determination is equivalent to the "backward looking" time of flight at the instant that the receiver coder becomes rate-aided. This instant is called TØ.

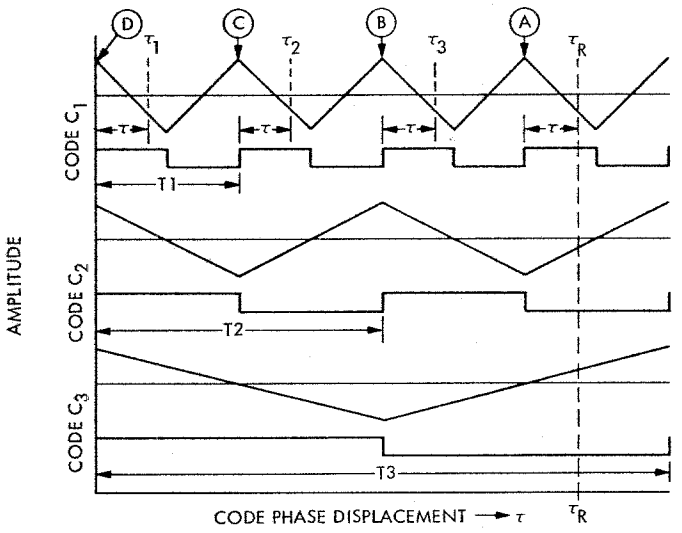

Fig. 4. Relative code correlation characteristics

Table 1. Time delay calculations from correlation voltages for range determination

Quadrant	Given	Equation
$0 \le \phi_c < \frac{\pi}{2}$	$I > 0, Q > 0$	$\tau = \frac{T}{4}\frac{Q}{I+Q}$
$\frac{\pi}{2} \le \phi_c < \pi$	$I < 0, Q > 0$	$\tau = \frac{T}{4}\left(\frac{I}{I-Q} + 1\right)$
$\pi \le \phi_c < \frac{3\pi}{2}$	$I < 0, Q < 0$	$\tau = \frac{T}{4}\left(\frac{Q}{I+Q} + 2\right)$
$\frac{3\pi}{2} \le \phi_c < \pi$	$I > 0, Q < 0$	$\tau = \frac{T}{4}\left(\frac{I}{I-Q} + 3\right)$

where

$$T = \frac{16 \times 2^N}{3 \times F_S}$$

N = component number (1 4-MHz code, 23 1-Hz code)

F_S = exciter synthesizer frequency (approx. 44 MHz)

To mechanize the code phase measurement, two correlation voltages are computed for each channel. The first voltage, called the in-phase voltage, is a direct comparison of the received code with the receiver coder output. The second voltage, called quadrature voltage, is an analogous comparison of the received code with the receiver coder output delayed by one quarter of a code period. Figure 3 shows how the in-phase (I) and quadrature (Q) correlation voltages vary as a function of τ, the phase difference. Further, given any values of I and Q, the equations in Table 1 may be used to determine τ in microseconds. The ranging algorithm first determines the phase delay for the highest-frequency code to establish the range measurement precision. The same determination on a series of lower-frequency codes resolves the range ambiguity. Because each code is derived from the same binary counter, they are phase coherent. Therefore it is not necessary to actually measure the phase of any component except the first one.

Refer to Fig. 4 for the correlation functions for three successive codes. Naturally, their respective correlation functions are coherent. Assume that the original (highest-frequency) measurement $C1$ indicates a phase delay of τ. Any of the points marked $\tau_i (i = 1 \ldots R)$ satisfy this condition. Let us now put the value τ into the range tally. Retarding the receiver coder by the same amount moves the observed point on the correlation function to a peak for the highest-frequency code (one of the points labeled A, B, C, or D). Because the correlation functions are coherently related, the $C2$ function will now be at either a positive or negative peak. If the peak is positive, the component can be ignored since it is already in phase and makes no contribution to the range tally. If, on the other hand, it is negative, then one half of the code period is added to the range tally, and once again the receiver coder is delayed by the same amount. This is illustrated by assuming the $C1$ measurement to be at τ_R. The first retard would leave the coder at A. $C2$ is negative; therefore the coder would be moved to point B after it is delayed by half of the period of $C2$. Since $C3$ is negative at this point, half of the period of $C3$ would be added to the tally, and again the coder would be delayed. This final shift leaves the coder at point D. The code phase delay is then determined to be equal to τ_R. Note that while the first component must be explicitly measured, the succeeding component measurements consist only of determining the sign of the in-phase correlation voltage.

So far, only ideal conditions were discussed. In the real world, charged particle plasmas, both ionospheric and interplanetary, corrupt the received signal (Refs. 4 and 5). The range measurement is affected in two ways by a

plasma medium. First the range modulation is decreased in frequency (thereby corrupting code phase), and second the carrier is increased in frequency by a like amount (thereby corrupting doppler). This causes a slow drift of the measured phase delay.

The measured drift, known as differential range versus integrated doppler (DRVID), can be used to determine the time rate of change of the total columnar electron content of the ray path. Both to measure this drift and to redetermine the initial phase measurement, after the range acquisition is complete, the ranging program repeats the highest-frequency component and remeasures its phase delay. Although these remeasurements can be performed at the correlation function peak, up to a 5-dB improvement in performance is obtained by retarding the receive coder by one eighth of the code period (Ref. 6). Note from Fig. 2 that this is the "equal-power" point, where both the quadrature and in-phase voltages have equal magnitude. To further increase the amount of DRVID data, the highest-frequency component is, at the experimenter's option, transmitted concurrently with all low-frequency components, except the second, during the resolution of range ambiguity. DRVID data is then available throughout the ranging acquisition.

If the charged-particle-induced drifts are large enough, the code phase will be driven significantly from its proper operating point on the correlation function. To prevent this, a code servo, implemented in software, with loop gain of 0.25 is employed to retain proper code phase alignment. The servo routine provides a correction factor to the range calculation so that coder moves, i.e., servo actions, do not mask or corrupt the real charged particle effects.

While the ranging algorithm has remained essentially unchanged, the Mu-II represents a marked advance and departure from earlier systems in the mechanization of the range code demodulation and correlation. Whereas earlier systems, including Mu-I and the Planetary Ranging Assembly (PRA), were purely analog, the Mu-II is wholly digital. The next subsection will, for clarity, present a general discussion of demodulation/correlation techniques. Following, in the last part of this section, the Mu-II mechanization will be presented in some detail.

C. Range Code Demodulation/Correlation in General

The process by which the returned range code is compared to the transmitted code is shown functionally in Fig. 5. (This functional diagram is not intended to portray a possible implementation and is presented only for demonstration.) A 10-MHz IF signal is obtained from the

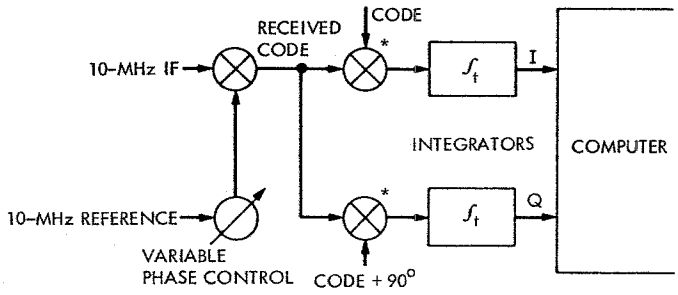

*MIXER OUTPUT FUNCTION

RECEIVED CODE	CODE (+90°)	CODE MIXER OUTPUT
-1	-1	1
-1	1	-1
1	-1	-1
1	1	1

Fig. 5. General code demodulation/correlation

station receiver. To demodulate the range code, a 10-MHz reference is adjusted to quadrature with the IF carrier, and both signals are applied to a mixer. The mixer product, after filtering, is the baseband code signal.

Two additional mixers are used to multiply the baseband square wave against (1) the receiver coder output and (2) the receiver coder output delayed by 90 deg. If two square waves are allowed to take on the values ±1 and input to the mixer, the output takes on the product values ±1 according to the table in Fig. 5. It is easy to visualize that if the phase difference between the two signals is 0, then the output is +1. If it is 90 deg, the output is a square wave with half the code period. Given a phase difference of 180 deg, the output is -1. For any other phase, the output is a pulse train whose ±1 duty cycle is proportional to the phase offset. Integration of the mixer output results in a number related to the duty cycle and integration time. Normalizing the integrated values by their maximum yields the I and Q correlation functions given in Fig. 3. Integration also averages the received random noise components in the I and Q values. The demodulation and correlation of the range code are now complete.

The phase adjustment of the 10-MHz reference is critical to best performance of the system. Any misadjustment degrades the magnitude of the I and Q voltages with respect to noise. Prior to ranging, the phase control is "calibrated" or set so as to null the 10-MHz component in the first mixer output. This is the quadrature point required for phase demodulation. Calibration was achieved manually in the Mu-I and semi-automatically in the PRA. Carrier-phase calibration of the Mu-II is fully automatic, and will be described in the next subsection.

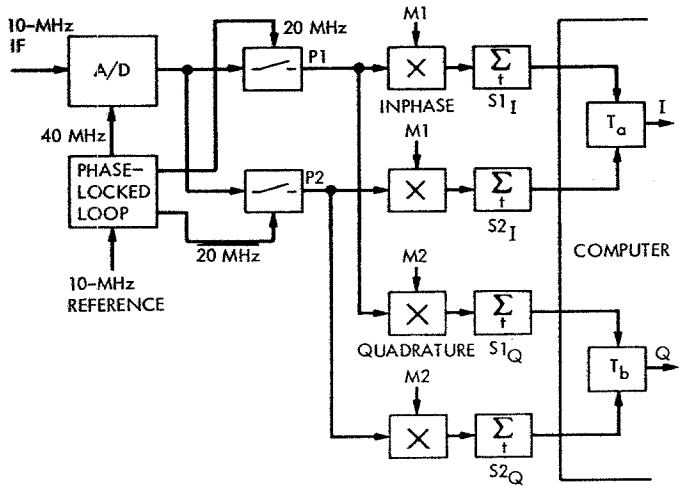

Fig. 6. Functional equivalent: digital demodulator

D. Mu-II Digital Demodulation/Correlation

The demodulation/correlation process in the Mu-II is digital, realizing two advantages over analog techniques: stability and fully automatic operation. In this subsection, a schematic view will be taken. For more detail, the reader is referred to the sections on system hardware and software.

A functional equivalent to the digital demodulation/correlation scheme is shown in Fig. 6. The important distinction between this scheme and that represented in Fig. 5 is that the incoming IF signal is immediately coherently sampled with the 10-MHz reference and digitized by an A/D converter. Discrete samples thereby created are processed to produce the same I and Q voltages previously discussed. The samples are routed and controlled by 40-, 20-, and 10-MHz reference signals developed by a phase-locked loop synchronized to the 10-MHz station standard. As shown in Fig. 7, the A/D is controlled by the 40-MHz reference. Four samples, $A1$, $B1$, $A2$, and $B2$, are taken for each cycle of the 10-MHz IF carrier. Samples $A1$ and $A2$ are routed to path $P1$ under control of the 20-MHz reference. Similarly, $B1$ and $B2$ appear on $P2$ under control of the complement of the 20-MHz reference.

Figure 7 shows a phase offset ϕ between the 10-MHz station reference and the 10-MHz IF carrier. Sample $A1$ is then taken at the point $\phi + \pi/4$. If $\phi + \pi/4$ is designated as α, the following equations may be written for each of the samples (ignoring noise):

$$A1 = D\sin(\alpha + M(t))$$

$$A2 = D\sin(\alpha + \pi + M(t))$$

$$B1 = D\sin\left(\alpha + \frac{\pi}{2} + M(t)\right)$$

$$B2 = D\sin\left(\alpha + \frac{3\pi}{2} + M(t)\right)$$

where D is the signal amplitude and $M(t)$ is the range code modulation $k\sin[\omega_x t]$, with k being the modulation index.

Assume that the multiplication terms $M1$ and $M2$ in Fig. 6 are the 10-MHz reference from the phase-locked loop. The effect is to multiply samples $A1$ and $B1$ by 1 and samples $A2$ and $B2$ by -1. Under noise-free conditions, the discrete integrators $S1_I$, $S2_I$, $S1_Q$, and $S2_Q$ contain the following values over a 10-MHz cycle (note that a primed term henceforth designates the unprimed term taken over one 10-MHz cycle):

$$S1_I' = S1_Q' = A1 - A2 = 2D\sin(\alpha + M(t)) \qquad (1)$$

$$S2_I' = S2_Q' = B1 - B2 = 2D\cos(\alpha + M(t)) \qquad (2)$$

The output I and Q terms are computed through transformations T_a and T_b, which are defined by

$$T_a: \quad I = S1_I\cos\alpha - S2_I\sin\alpha \qquad (3)$$

$$T_b: \quad Q = S1_Q\cos\alpha - S2_Q\sin\alpha \qquad (4)$$

Simple trigonometry yields

$$I' = Q' = 2DM(t) = 2Dk\sin[\omega_x t] \qquad (5)$$

It should be apparent that the range code has been demodulated.

The remaining task is to correlate the demodulated range code against the output of the receiver coder. If we allow the I' or Q' value given by Eq. (5) to be integrated for time t,

$$I = \sum_t I' = \sum_t 2Dk\sin[\omega_x t] \qquad (6)$$

For t sufficiently large, $I = Q \cong 0$. Now assume that the right side of (6) is multiplied by the ±1 square wave

$$\sin[\omega_x(t + \tau)]$$

If $\tau = 0$, then I is equal to

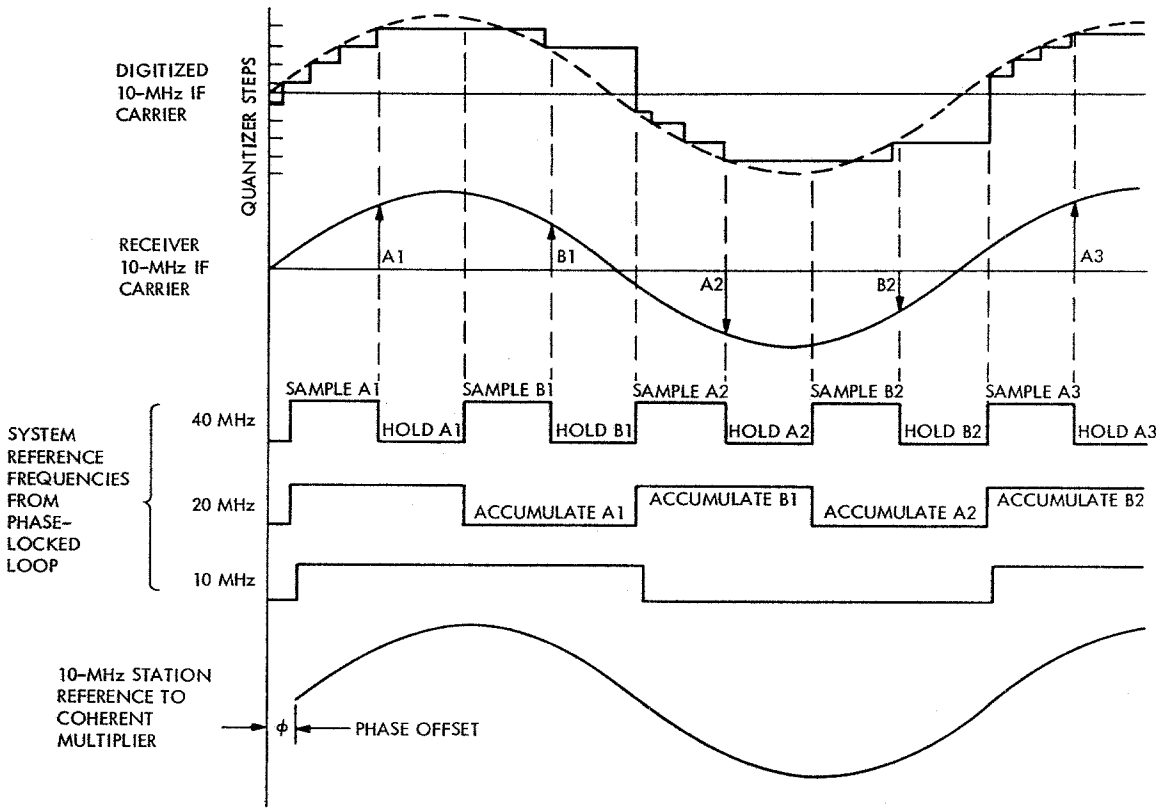

Fig. 7. Digital sampling of IF carrier

$$\sum_t 2Dk$$

If, however, τ is equal to one fourth of the code period, then

$$I = \sum_t 2Dk \sin[\omega_x t] \sin\left[\omega_x t + \frac{\pi}{2}\right]$$

$$= \sum_t 2Dk \frac{1}{2} \sin[2\omega_x t] \cong 0 \text{ for large } t$$

If τ is equal to half of the code period,

$$I = \sum_t 2Dk \sin[\omega_x t] \sin[\omega_x t + \pi]$$

$$= \sum_t 2Dk \sin[\omega_x t](-1) \sin(\omega_x t)$$

$$= -\sum_t 2Dk \text{ for large } t$$

Observe that if the multiplying square wave is the receiver coder output, then the correlation curve in Fig. 3 is obtained.

To mechanize this multiplication, $M1$ is defined to be the 10-MHz square wave reference times the receiver coder output. Similarly, $M2$ becomes the reference multiplied by the receiver coder output delayed by one fourth of the code period. Therefore, T_a (Eq. 3) applied to $S1_I$ and $S2_I$ yields the in-phase correlation voltage, while T_b (Eq. 4) applied to $S1_Q$ and $S2_Q$ yields the quadrature correlation voltage.

One thing remains to be done: the determination of cos α and sin α for use in T_a and T_b. First, from Eqs. (1) and (2), if $M1$ and $M2$ are the 10-MHz reference,

$$S1_I = S1_Q = \sum_t 2D \sin[\alpha + M(t)] = 2D \sin\alpha \text{ for large } t$$

$$S1_Q = S2_Q = \sum_t 2D \cos[\alpha + M(t)] = 2D \cos\alpha \text{ for large } t$$

From these equations,

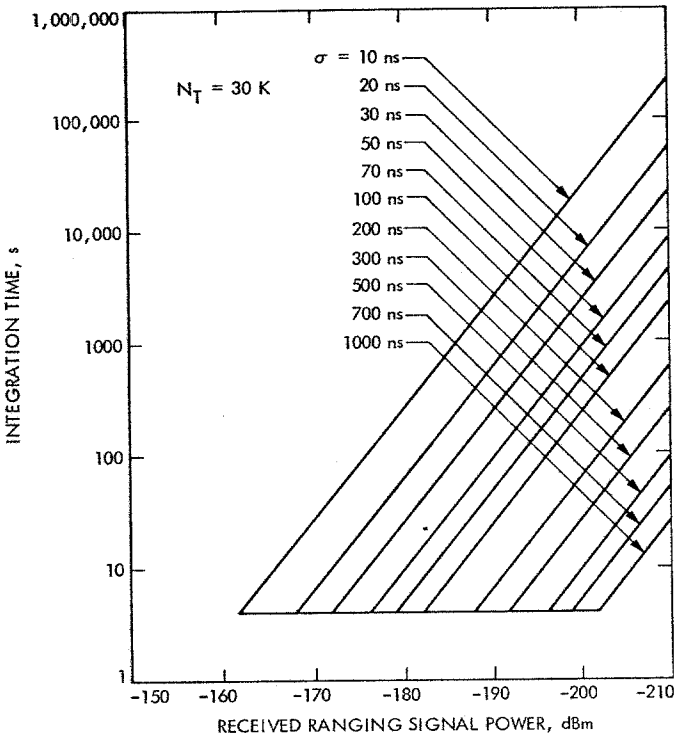

Fig. 8. Mu ranging constant phase jitter contours

$$\sin\alpha = \frac{S1_I}{\sqrt{S1_I^2 + S2_I^2}} = \frac{S1_Q}{\sqrt{S1_Q^2 + S2_Q^2}} \tag{7}$$

$$\cos\alpha = \frac{S2_I}{\sqrt{S1_I^2 + S2_I^2}} = \frac{S2_Q}{\sqrt{S1_Q^2 + S2_Q^2}} \tag{8}$$

The determination of sin α and cos α is equivalent to the calibration of the station reference. It is done automatically under computer control at the start of each range acquisition by forcing the coder output factor in $M1$ and $M2$ to be 1. The resulting $S1$ and $S2$ values are input to the computer and Eqs. (7) and (8) applied. After calibration, $M1$ and $M2$ again become a product of the coder output and the 10-MHz reference. The necessary hardware/software controls will be discussed later in this report.

It should be noted that noise-free signals were assumed throughout this subsection. Noise is, of course, part of any real signal. Since the sampling of the 10-MHz IF signal is sufficiently fast to characterize the additive noise in this signal as well as the range-code signal, the digitally computed I and Q voltages become a good representation of the I and Q voltages which would be obtained from an ideal analog demodulator/correlator. Hence, the previously published results for the signal and noise performance of sequential component ranging may be used to predict the performance of the Mu-II (Ref. 1; Figs. 8 and 9).

E. Power Meter

To facilitate evaluating Mu-II performance and estimate range precision, the software calculates an approximate ranging-signal-power-to-noise-density ratio. This calculation utilizes the fact that the input automatic gain control amplifier provides constant total (signal plus noise) power to the A/D converters. If we designate this total power to the A/D as P_T, the ranging signal power to the A/D as P_R, and the carrier power to the A/D as P_c, then the total noise power to the A/D is given by

$$N_T \approx P_T - P_R - P_c$$

Hence

$$\frac{P_R}{N_T} \approx \frac{P_R}{P_T - P_R - P_c}$$

Because $N_T = N_0 W_{IF}$, where N_0 is the noise density and W_{IF} the receiver IF bandwidth, we obtain

$$\frac{P_R}{N_0} \approx \frac{P_R W_{IF}}{P_T - P_R - P_c} \tag{9}$$

Note that W_{IF} = 4 MHz on the Block III receiver and 8 MHz on the Block IV receiver.

The carrier power P_c can be determined during the 10-MHz calibration. Specifically, the average carrier "voltage" at each 10-MHz sample is given by the total integrated voltage divided by the number of samples; that is,

$$A = \frac{\sqrt{S1^2 + S2^2}}{TC \times (20 \times 10^6)}$$

where TC is the integration time in seconds and 20×10^6 is the number of $S1$ and $S2$ samples per second. P_c is proportional to the square of the peak voltage; i.e.,

$$P_c = K\left(\frac{A}{\sqrt{2}}\right)^2$$

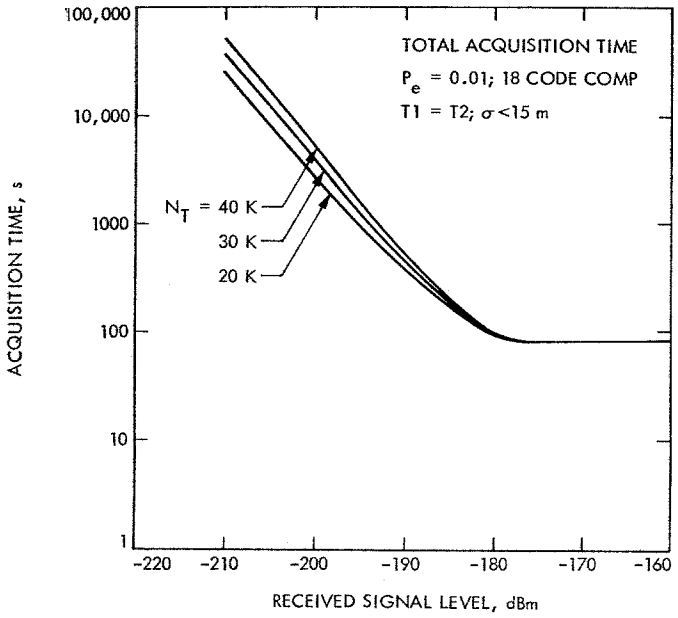

Fig. 9. Mu ranging acquisition time

The constant proportionality factor K is in units of inverse impedance.

Similarly, the ranging power is given by

$$P_R = K\left(\frac{B}{\sqrt{2}}\right)^2$$

where

$$B = \frac{|I| + |Q|}{T \times (20 \times 10^6)}$$

I,Q are the correlation voltages and T is the integration time.

In the same manner, P_T can be written as

$$P_T = K\left(\frac{v}{\sqrt{2}}\right)^2$$

where v is the average voltage applied to the A/D.

The AGC amplifier is set to produce an average count of 2.3 from the A/D. This count is averaged by an eight-stage counter prior to the accumulators accessed by the computer. Therefore, the average "voltage" v per 10-MHz cycle is $2.3/2^8$ or 8.984×10^{-3}. Because the value is dependent on AGC peculiarities, the actual number used is determined from laboratory measurement.

The final form of Eq. (9) is then

$$\frac{P_R}{N_0} \approx \frac{P_R W_{IF}}{P_T - P_R - P_c} = \frac{B^2 W_{IF}}{v^2 - B^2 - A^2}$$

This number is converted to and output as a ratio in decibels.

IV. Hardware Implementation

A simplified block diagram of the Dual-Channel Sequential Ranging System appears in Fig. 10. It is apparent that this diagram is approximately symmetrical about a horizontal line drawn through the coherent multiplier. The upper half represents the first channel, while the lower half depicts the remaining channel. Note that both of these channels are complete and equivalent, giving rise to truly independent operation on any set of frequencies.

Since there is a single S-band uplink, only one transmitter coder is required. Code generation is accomplished by dividing 132 MHz from the exciter (see Fig. 2) by 8 and applying the resultant 16.5-MHz frequency to a 24-stage binary counter. Unlike the Block III exciter, 66 MHz was not available initially in the Block IV, and the choice narrowed to a selection of 44 or 132 MHz.

Because the step size and positioning accuracy of the local code are determined by this reference frequency, it was felt that the 23-ns granularity imposed by the 44 MHz was too great. Accordingly, a decision was made to utilize 132 MHz, which provided a 7.5-ns step. Additionally, since 132 MHz is a multiple of 66 MHz, utilization of the former would make the system compatible with either Block III or Block IV exciters—a feature which would prove invaluable during the MVM'73 mission.

A. Coders

The coders consist of 24 flip-flops arranged as 8-bit binary counters on each of three printed circuit cards (Fig. 11). Repeater flip-flops at the output of each card resynchronize the code with 16.5 MHz from the divide-by-8 module, effectively tying the code to the exciter reference and thus promoting stability.

Efficiency of design and repair dictated that all nine coder cards used in the system be identical. Therefore, those used in the transmitter include the quadrature (90-deg) output even though it is not required in this application. Code frequencies are user selectable by loading a 0 into the appropriate flip-flop in the code

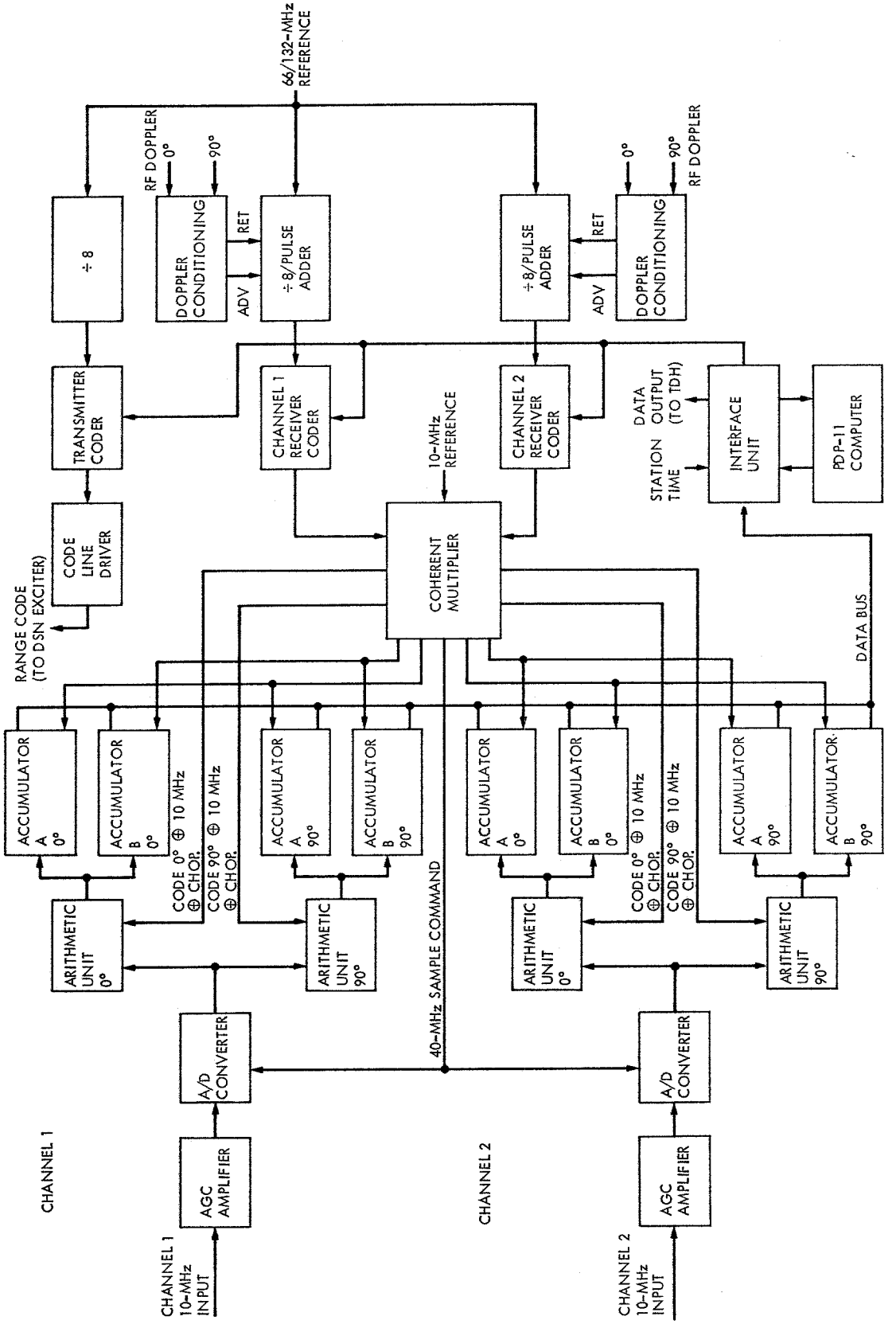

Fig. 10. Simplified block diagram of Dual-Channel Sequential Ranging System

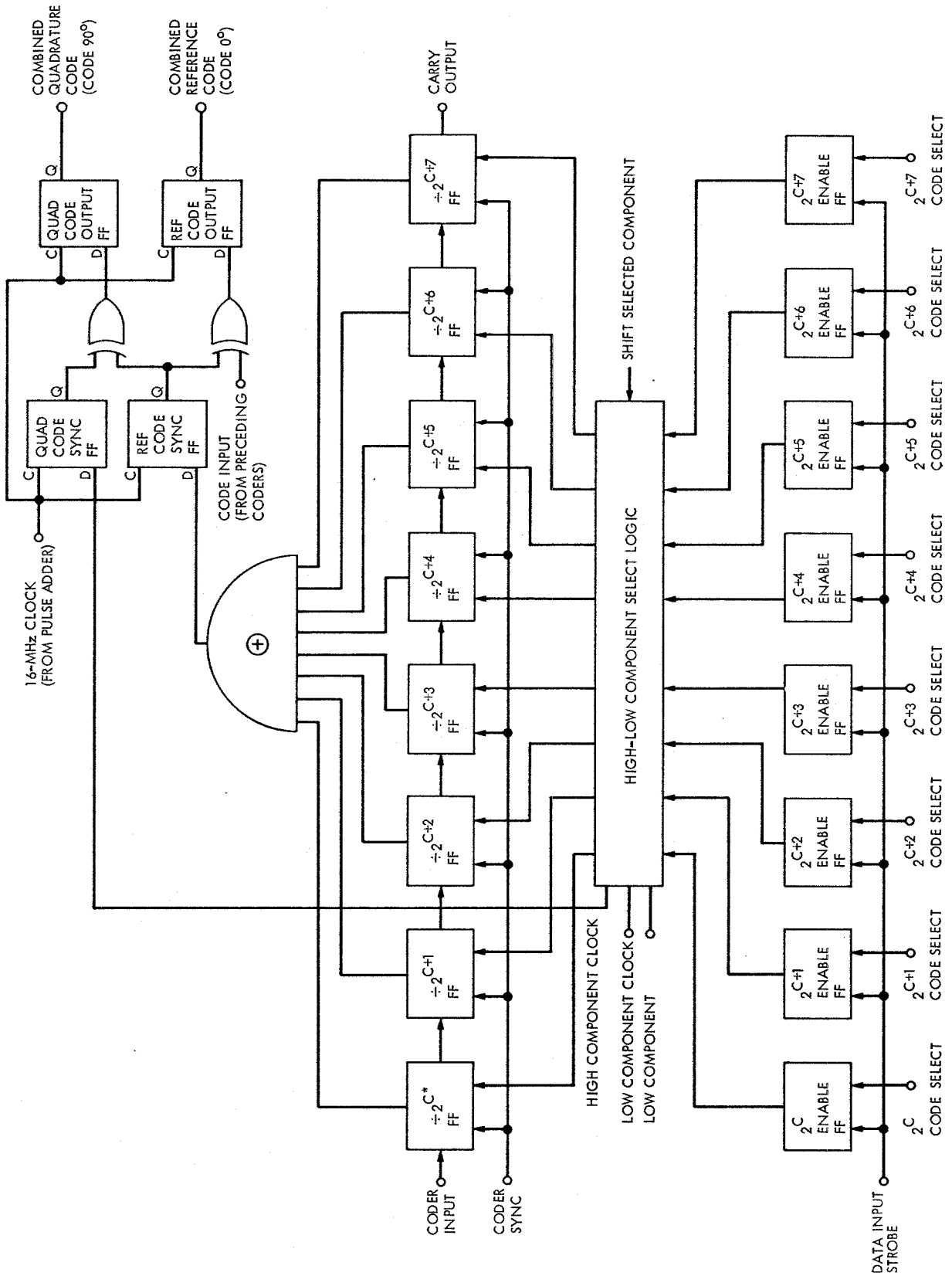

Fig. 11. Eight-bit coder logic diagram

enable register (a 1 inhibits the associated code component). Frequencies beginning with 1 Hz and extending to 8 MHz are available. Thus, the machine makes provision for high-precision ranging when transponders capable of handling these higher code frequencies become available.

Any combination of the 24 codes can be called simultaneously according to the relationship

$$C_T = C_0 \oplus C_1 \oplus C_2 \oplus C_3 \oplus \cdots \oplus C_N$$

This facility for combining many code frequencies may be of interest to those concerned with "discrete spectrums" resulting from modulation with a single code frequency.

High-Low Component Select Logic, again required only in the receiver coders, determines which of the 24 code components is the highest and the lowest in frequency. The clock (or predecessor) for the highest-frequency component is used to generate the quadrature phase by simple modulo-2 addition:

$$C_{T-90} = C_n \oplus C_{n-1}$$

During acquisition, it is sometimes necessary to invert the phase of a particular code component. This is accomplished by inhibiting the clock to a particular counter stage for one cycle with the result that the code component is now delayed by π. To prevent carries from propagating in the synchronous pairs (from first to second flip-flop), it is necessary to inhibit the selected flip-flop only when its predecessor is in a "1" state. Low component and low component clock are used to accomplish this function.

Shift selected component is the command used to inhibit the lowest-frequency code currently in use in the receiver coder and hence to delay its phase by π. Obviously, all successive codes are also delayed by a like amount.

Coder synchronization is accomplished by setting all counter flip-flops to a 1 state in response to a computer-generated command. The receiver coders are held in this reset state until a word detector on the transmitter coder, which continues to run undisturbed, indicates that it too is in the all 1's state, whereupon the receiver coders are released. Independent control allows separate or simultaneous synchronization of the coders in both channels.

B. Code Line Driver

The transmitter coder's combined reference code output is supplied to a high-precision line driver for transmission to the exciter phase modulator (Fig. 12). This driver has adjustable symmetry and dc offset controls to compensate for errors induced either in code generation or within the exciter. Rise and fall times are designed to be less than 2 ns, ensuring high stability once the adjustments have been made. By connecting a spectrum analyzer to the exciter's output, it may be possible to adjust the entire system for the best balance and symmetry of modulation sidebands.

C. Pulse Adder

Both receiver coders are preceded by the pulse adder/ ÷8 circuit, depicted schematically in Fig. 13. This card functions not only to reduce the 132 MHz to 16.5 but also as a phase shifter for the two receiver coder strings.

Three independent divide-by-8 counters provide separate control for the two channels relative to the transmitter coder. MECL III digital logic is used to implement the dividers to ensure minimum delay time and, hence, maximum stability. Additionally, the first two counter stages operate synchronously to further minimize this delay. Less than 5 ns are required for the signal to propagate from input to output.

As part of the overall coder synchronization scheme, the two receiver dividers can be synchronized to the transmitter section. A word detector on the transmitter divider enables a synchronization flip-flop to be set for one clock period, forcing the two receiver dividers to a reset (000) condition. Coincidentally, the transmitter divider is also in the all 0's state, although it has remained undisturbed throughout the entire process.

The pulse adder is used to adjust the phase of the receiver coders with respect to the transmitter coder. Adjustment commands may come from either the computer or from the RF doppler. Advance-Retard Priority Logic allows these commands to be mixed randomly and asynchronously without confusion. This logic serves to delete a clock pulse in the retard mode or to delete the 100 counter state, thus shortening the count sequence, in the advance mode.

Doppler rates in excess of 16 MHz at S-band and 60 MHz at X-band can be handled by the system. While in theory the pulse adder can simultaneously process computer commands at a 16-MHz rate, a machine has yet to be found which will tax this capability.

Because phase errors resulting from missed or extra shift commands are fatal to high-precision ranging, this card was extensively tested. Both pulse adder and associated

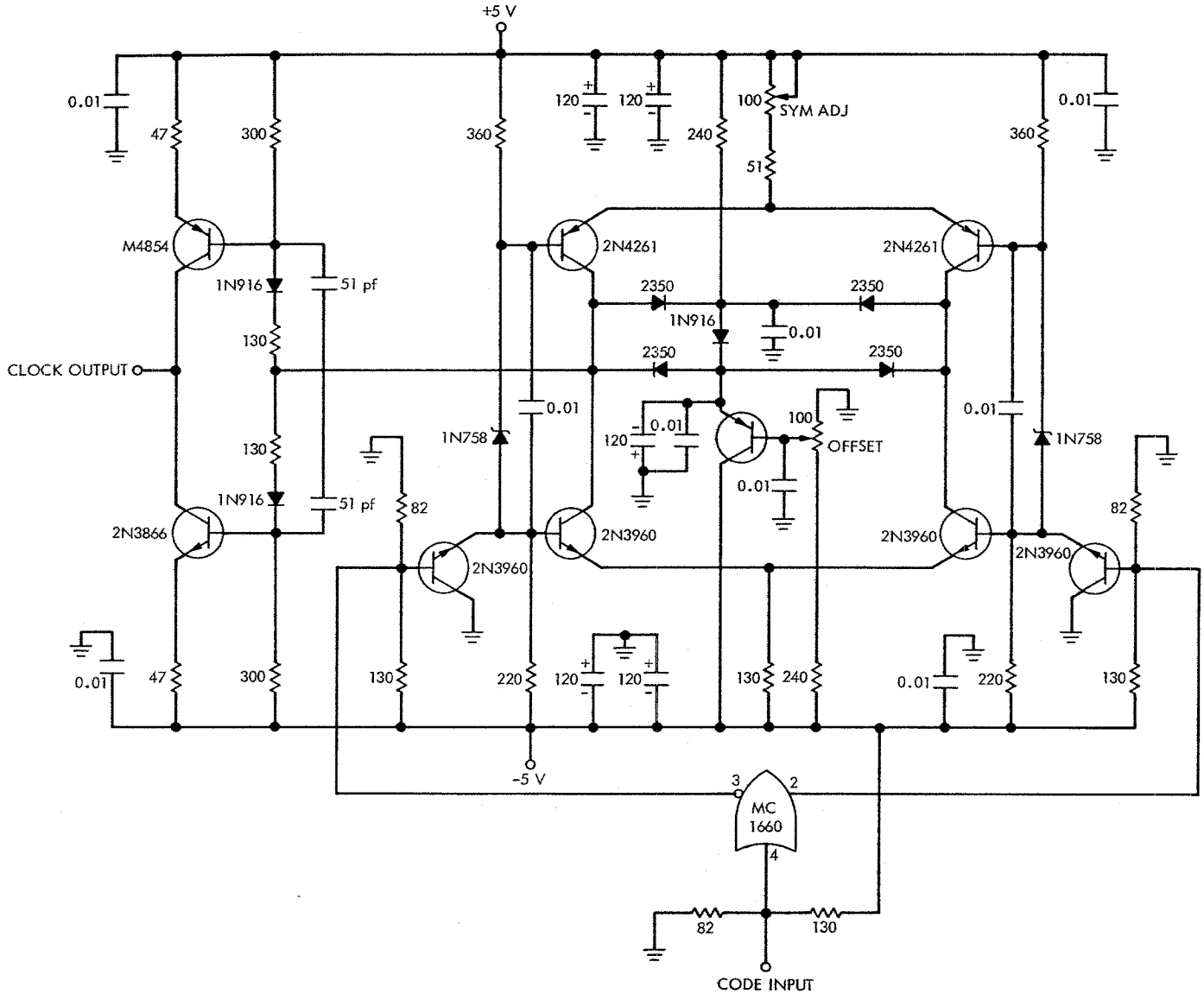

Fig. 12. Code line driver logic diagram

coder strings were subjected to more than 1,000,000,000 consecutive shifts without error prior to acceptance.

D. Doppler Conditioning

From the foregoing, it is obvious that the range code is a subharmonic of the transmitted carrier. This relationship is a condition precedent to using the RF doppler for rate aiding the receiver coders (Ref. 2). However, because the RF link through the spacecraft involves frequency multiplication (240/221 for S-band or 880/221 for X-band), the received doppler must be properly scaled before it can be used. Scaling is accomplished by applying the inverse multiplier and dividing until the doppler frequency has been reduced to one corresponding to the rate aiding frequency (either 66 or 132 MHz).

Figure 14 is a functional block diagram of the doppler conditioning card. Because the scaling ratio normally depends upon the carrier frequency, it is difficult to make a general-purpose device. The one employed here contains scaling for two channels. While the scalar in the upper half of Fig. 14 can be used only on S-band, that in the lower half can be employed on either S- or X-band by simply changing a jumper wire. Thus, the card allows the system to operate as two independent S-band channels or, in the alternative, as an S-band channel and an X-band channel.

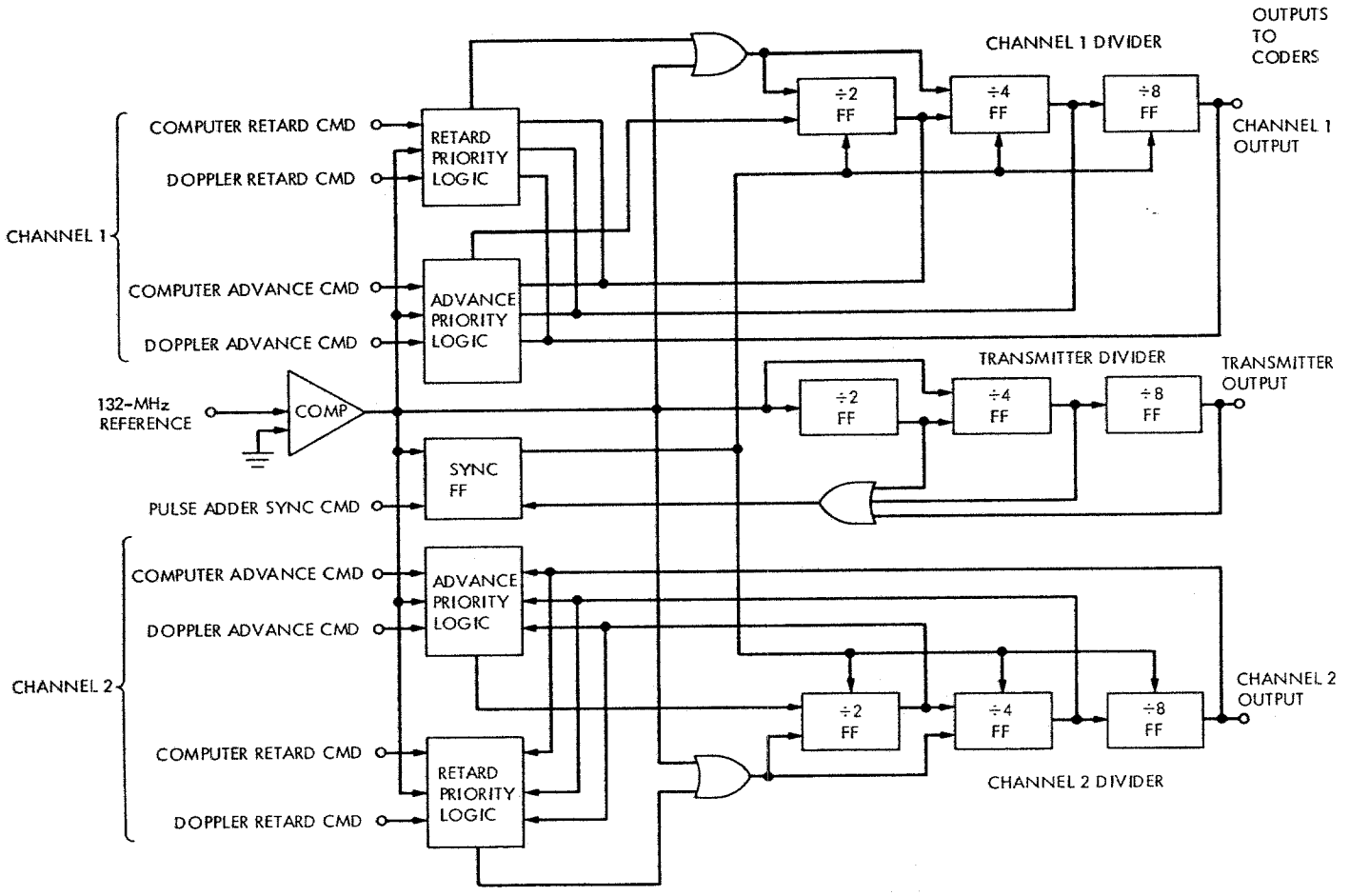

Fig. 13. Pulse adder/÷8

S-band scaling is accomplished by deleting 19 of every 240 doppler cycles, providing the ratio 221/240. Two sequence generators—one of length 15, the other of length 16—whose combined period is 240, are used for the task. Each time a particular word vector appears in the 15 generator, it causes the ÷8/÷16 scalar to slip a clock cycle. This results in 16 evenly spaced deletions for every 240 doppler clock cycles. The additional three deletions are obtained by selecting three word pairs from both 15 and 16 generators which are conveniently, and evenly, spaced throughout the 240-cycle period. The result is that for every 240 input doppler cycles, only 221 are supplied to the scaling counter.

To be useful, the doppler frequency must be further reduced to that which would be found at the rate aiding frequency. Again the desire for a general-purpose machine dictated that the capability exist for rate aiding at either 66 MHz (Block III) or at 132 MHz (Block IV). Thus, the scalar has additional jumpers, providing a divide by 8 (Block III) or a divide by 16 (Block IV). A simple wire change allows the machine to be used with either type of receiver.

X-band scaling is obtained by employing the S-band scalar as a basic building block and adding an additional 3/11 generator. This device produces three pulses for every 11 which it receives. When connected in series with the clock to the S-band scalar, it effectively provides the 221/880 as required for X-band. A jumper wire, depicted in Fig. 14, allows the inhibit pulse from the 3/11 generator to be readily inserted or removed, making the conversion from an X-band to an S-band channel a simple matter.

Direction of spacecraft travel is determined by the phase relationship between the 0- and 90-deg RF doppler signals. In one case, the 90-deg channel leads the reference, whereas in the other, it lags the reference. Under poor signal-to-noise conditions or where the receiver is operating improperly, these doppler signals

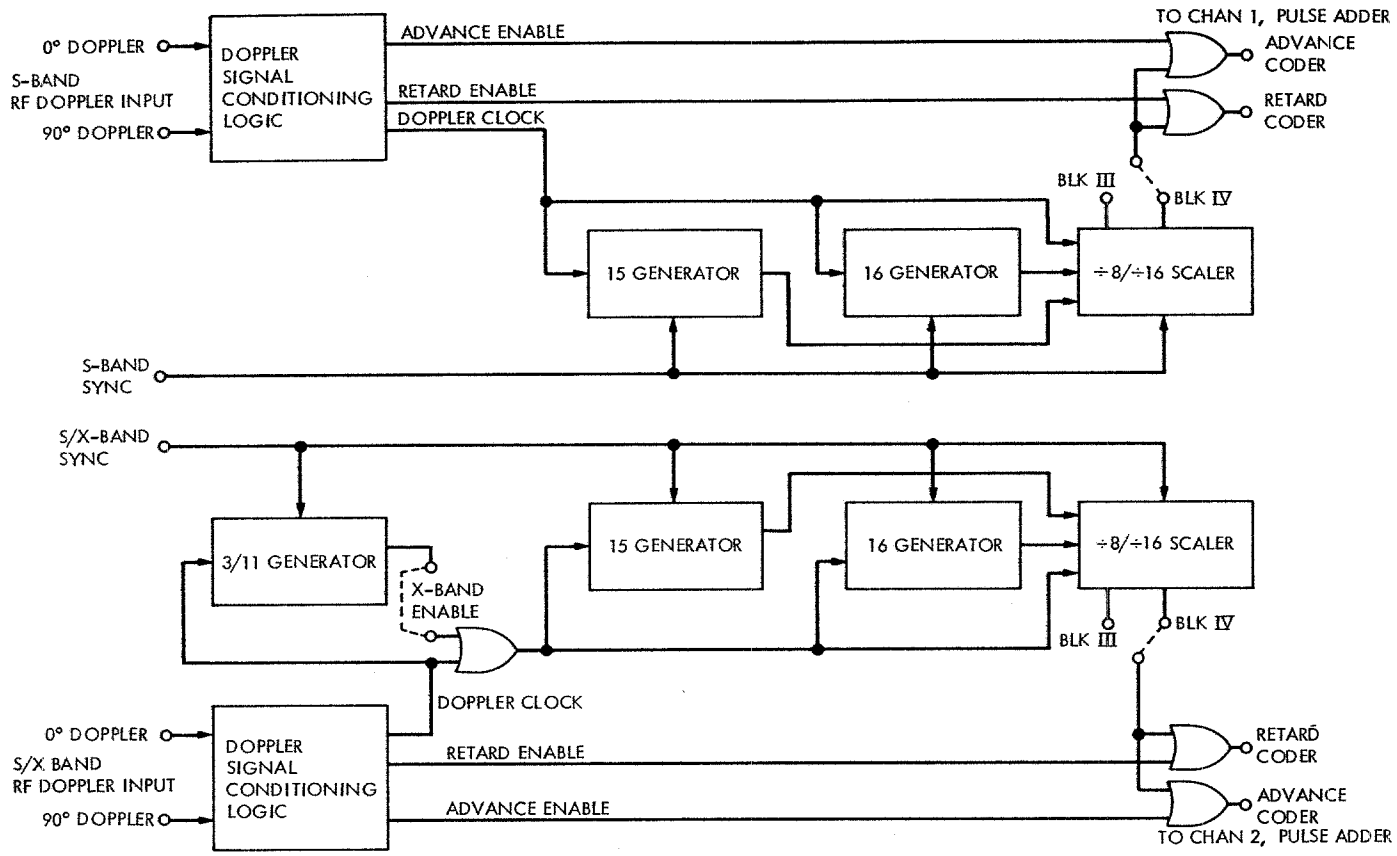

Fig. 14. Doppler conditioning diagram

may have substantial phase and/or amplitude noise. Here the 0-deg doppler channel serves as a clock for the doppler conditioning card. This noise, coupled with the relatively small hysteresis of digital logic, may cause multiple clock pulses where only one was proper. Improper rate aiding results, causing the receiver coder to slip in phase with respect to the received code.

To forestall this failure mode, doppler signal conditioning logic was developed which makes use of both 0- and 90-deg doppler to provide a high degree of noise immunity. This circuitry proved invaluable during the MVM'73 mission. On numerous occasions, good ranging data was acquired when the doppler data was so noisy that improper counts were obtained using conventional measurement techniques. Tests of the doppler conditioner have shown that correct scaling is obtained even with phase noise as great as ±89 deg on one of the channels.

E. Code Correlation

Earlier sequential ranging equipment comprised both analog and digital modules constructed in separate slide-out drawers. Cross-correlation of received and local codes was done at 10 MHz using balanced mixers (Fig. 15; Ref. 2). Since the code had not been demodulated from the IF carrier and the system bandwidths were relatively wide, small phase instabilities in the analog hardware did not affect the group delay. However, the system did require daily adjustment of two phase shifters used to align the 10-MHz reference in quadrature to the receiver's IF carrier. Moreover, these adjustments had to be made under strong signal conditions to prevent noise from obscuring the desired null at the respective outputs. Thus, as the received signal became weaker, and the DSN receiver adjusted its gain to compensate, phase shifts occurred in its 50-MHz IF amplifier, rendering the previous phase adjustment improper. While the resultant losses were small, they nevertheless represented a system deficiency. Furthermore, phase adjustments were made but once a day, and changes occurring throughout the pass would not be detected until the following day. To overcome these and other problems, it was decided to depart radically from the former design.

Comparison of Fig. 10 with Fig. 15 will make the changes apparent. The amount of analog equipment has

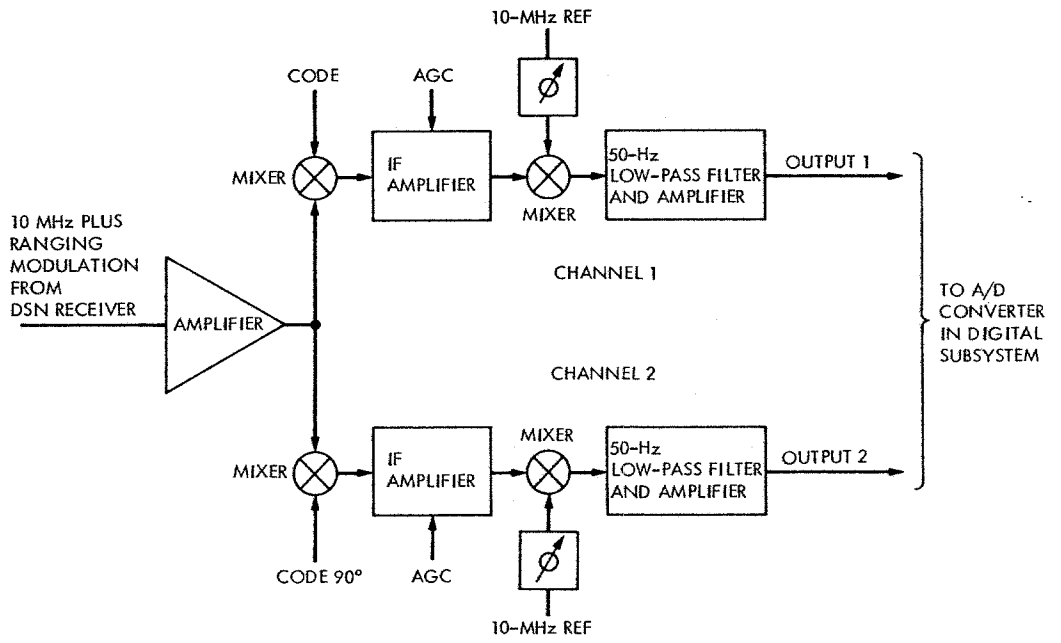

Fig. 15. Ranging receiver simplified block diagram

been drastically reduced and consists of only a single wideband AGC amplifier and a portion of an analog-to-digital (A/D) converter. While the two channels (0 and 90 deg) are retained, they are now digital, and code correlation is accomplished using high-speed arithmetic units. Thereafter, numbers representing the degree of code correlation are collected in four accumulators and transferred at regular intervals to a dedicated PDP-11 computer.

F. AGC Amplifier

The AGC amplifier's characteristics are critically important to the ranging system's performance, and, therefore, considerable time and effort was expended in the design and testing of this device. The amplifier consists of three transformer-coupled, variable-gain stages and a power stage (Fig. 16). Feedback is obtained by using a MECL 1650 comparator as a peak detector and converting its variable pulse width to an equivalent dc voltage. After amplification, this control voltage is used to adjust the gain stages.

The amplifier is designed to accept input levels from +10 to −80 dBm while holding its output power constant at 0 dBm within ±0.2 dB. This invariant level is required to ensure that the A/D converter is always operating at an optimal level. Rapid fluctuations in input signal level are allowed to pass because of a time constant of several seconds in the feedback loop. Thus, only long-term signal changes, and not high-frequency noise bursts, result in a gain adjustment.

Figure 17 shows the open-loop frequency response at several different input levels. Generally, the output is constant within ±1.5 dB from 250 kc to better than 25 MHz at any input level from +10 to −60 dBm. While the nominal operating frequency is 10 MHz, this wide bandwidth is desirable to minimize changes in group delay with received signal level fluctuation.

Figure 18 shows the test configuration used to measure group delay variation in the AGC amplifier. Tests were conducted in the Telecommunications Development Laboratory (TDL) using a conventional DSN Block III exciter and receiver. An attenuator, B, at the input to the AGC amplifier, allowed the input power level to be varied from +10 to −80 dBm. The amplifier gain was then manually set, using an external control voltage, such that the amplifier output was constant at 0 dBm. Its output was then connected to the earlier sequential ranging equipment, designated Mu-I, whose purpose it was to measure the total system group delay.

After setting the amplifier input to a strong signal level of +10 dBm and its output to 0, a single ranging acquisition was made and several re-estimations of group delay were obtained. Thereafter, the input level was decreased by 10 dB and the amplifier gain was adjusted to maintain a constant output of 0 dBm. Several more re-

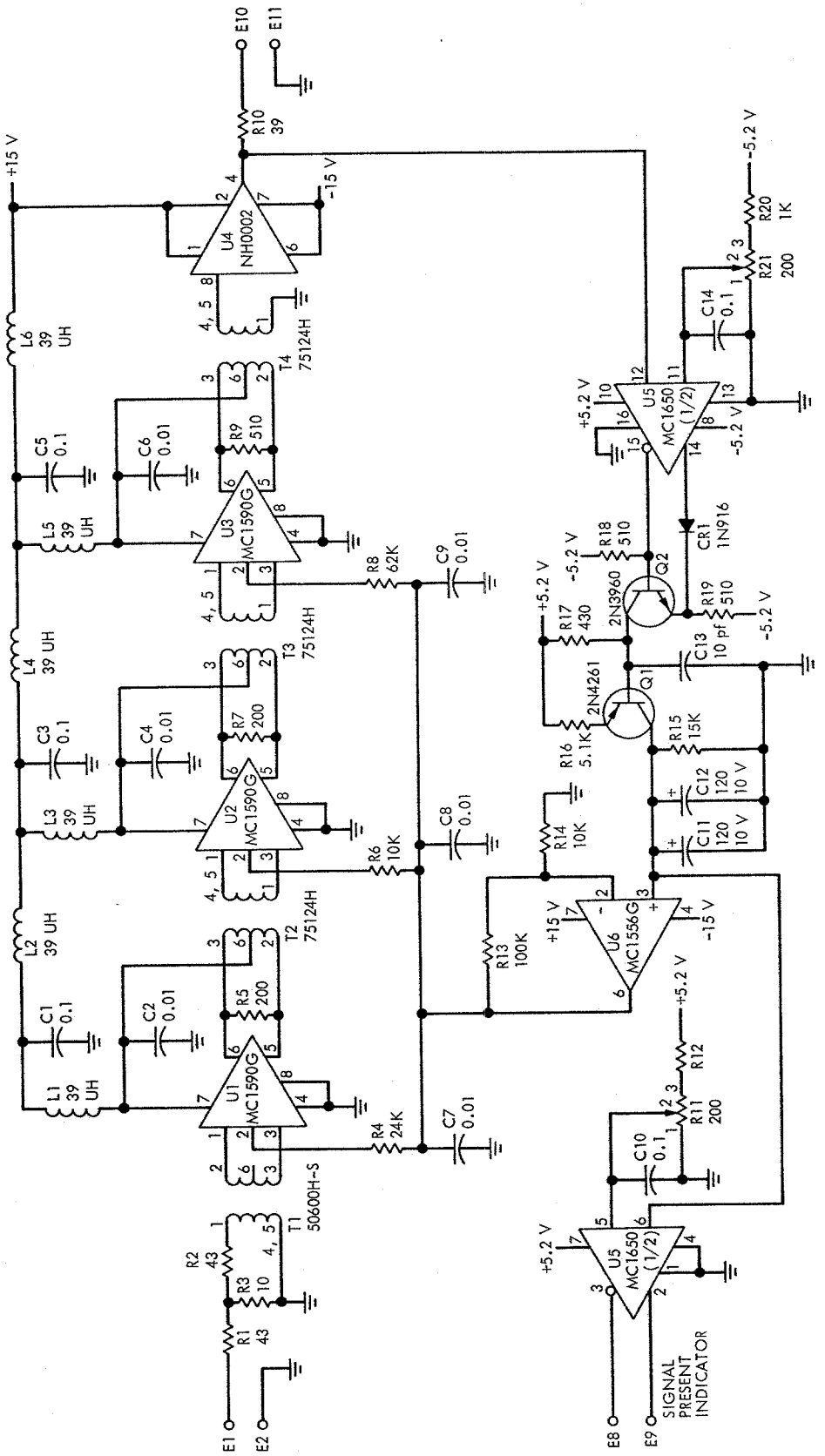

Fig. 16. AGC amplifier schematic

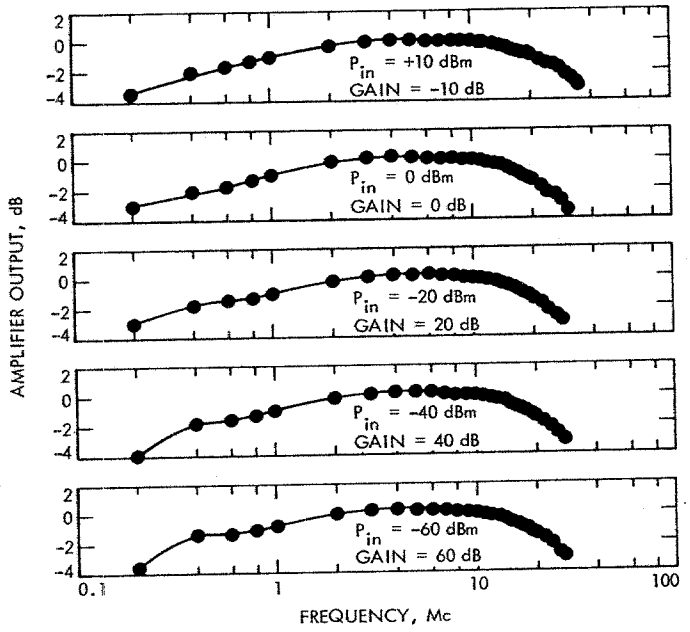

Fig. 17. Frequency response of AGC amplifier

estimations of the group delay were made without breaking lock to minimize the experimental error. This process continued until the full range of +10 to −80 dBm was covered. The re-estimations of group delay for each input level were averaged, and the total group delay variation over the 90-dB range was computed. Thereafter, the entire process was repeated two more times to verify the results.

Figure 19 shows the average group delay variation obtained for the three different tests. Note that the total variation in group delay is less than ±1 ns for a 90-dB change in input signal level. This corresponds to an error of approximately 15 cm (±6 in.) in one-way range for all signal conditions. Since the expected variation within a pass should be considerably less than 10 dB, the amplifier's performance was well within the design objectives.

G. A/D Converter

A high-speed A/D converter follows the AGC amplifier. Since the design objectives placed a premium on system automation as well as reliability, the entire demodulation process is performed digitally. This necessitated measuring the phase of the 10-MHz IF carrier from the DSN receiver relative to the 10-MHz station reference.

Figure 7, discussed earlier, shows the digital sampling points on the 10-MHz IF carrier. Note that there are four samples during each cycle. This ensures sufficient data to compute the IF carrier's phase relative to the 10-MHz reference. A more complete discussion of the phase measurement algorithm will be found in Section III.

From the foregoing, it is apparent that the converter must sample at a 40-MHz rate. Since commercially available units meeting this speed requirement were generally large and bulky, as well as expensive, it was decided to design a new unit on a single card. A study indicated that a 4-bit A/D converter provided the best compromise between converter complexity and performance. Comparing mean and variance at the quantizer output with that present in the unquantized sample, a 4-bit converter with a step size of 0.4 times the rms input voltages provides the best performance over the range of signal-to-noise ratios from 0 to -60 dBm. Since the AGC amplifier output was 0 dBm, a quantizer step size of 100 mV was indicated.

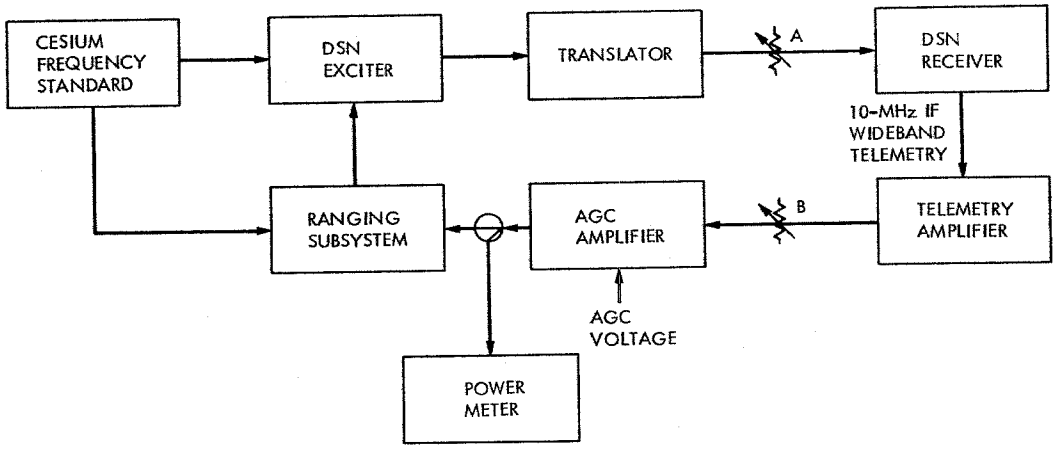

Fig. 18. AGC amplifier group delay variation test configuration

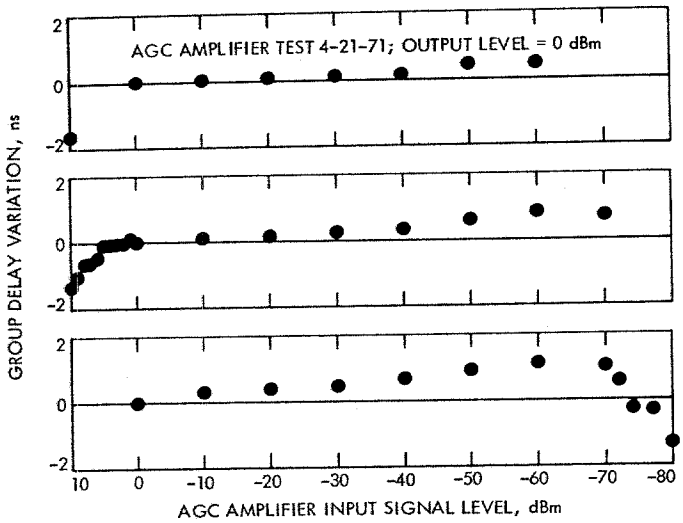

Fig. 19. Group delay variation in AGC amplifier

Figure 20 is a schematic diagram of the A/D converter. The design is an adaptation of a scheme suggested by Motorola several years ago and employs 14 MECL III comparators whose thresholds range from +650 to -650 mV in 100-mV increments. Comparator outputs are decoded into the complement of the familiar binary code. The comparators include a gate which functions as a sample and hold device. Referring to the 40-MHz reference shown in Fig. 7, the comparators follow the input signal while the reference is in the positive or "1" state. When this 40-MHz reference changes to the "0" state, the follower flip-flops are disconnected from the input circuitry, retaining their present value. While the reference is in the 0 or "hold" state, the conversion results are allowed to propagate through the gate decoding structure. In addition to re-enabling the follower flip-flops, the reference's next positive transition strobes the previous 4-bit conversion into a storage register, where it is held for the arithmetic unit.

The converter was constructed on a multilayer printed circuit card and tested at clock frequencies in excess of 100 MHz using a high-speed digital-to-analog converter.

H. Coherent Multiplier

Frequency multiplication from 10 to 40 MHz is handled by the coherent multiplier. Both harmonic generators and phase-locked loops were considered for the purpose. Power considerations, simplicity of failure detection, presence of a system clock in the absence of a 10-MHz reference, and fail-safe data steering led ultimately to a selection of the phase-locked loop. A simplified block diagram of the phase-locked loop designed by L. Constenla appears in Fig. 21.

Integrated circuits are used to implement the loop. A high-speed comparator converts the 10-MHz sine wave reference into an equivalent square wave while insuring minimal phase shift between input and output. The voltage controlled oscillator (VCO) employs a MECL III device timed to operate at 40 MHz. This frequency is divided by a synchronous counter to 10 MHz and compared in the phase detector with the 10-MHz station reference. High–low comparators are used to determine whether the phase detector output lies within the proper range for a locked condition. Status lamps on the system's front panel indicate whether the loop is operating correctly.

System clocks are provided by the coherent multiplier. As shown in Fig. 21, each of the three clock frequencies contains an additional distribution amplifier which may be individually disabled by an appropriate command from the computer. This feature was included to facilitate servicing by allowing the user to shut down certain sections of the machine while operating other parts.

I. Arithmetic Unit

Both coherent multiplier and receiver coders provide inputs to the arithmetic unit shown in Fig. 22. Since a completely digital demodulation scheme was employed, it was necessary to combine the 10-MHz coherent reference with the local code. Additionally, a chopper frequency was included to foreclose contamination of the received signal by leakage from either the coders or the 10-MHz reference.

Unlike earlier systems which had narrowband filters, the broadband character of this machine might allow coupling of both code and/or 10-MHz reference through the power system into the AGC amplifier. The result of such leakage is that the ranging machine measures its own delay rather than the desired round-trip distance to the spacecraft.

The chopper signal is generated by the computer in accordance with a 10-ms station reference, and has a 50% duty cycle with a total period of 20 ms. The effect is to cause the arithmetic unit to alternately add and then subtract. Since the computer is issuing the chopper signal, it knows the current status (i.e., inverted or noninverted) and can decommutate the samples which are transferred from the accumulators (see Fig. 10) at a 10-ms rate. The result is that any leakage occurring prior to the chopper is alternately added, then subtracted, and hence is cancelled,

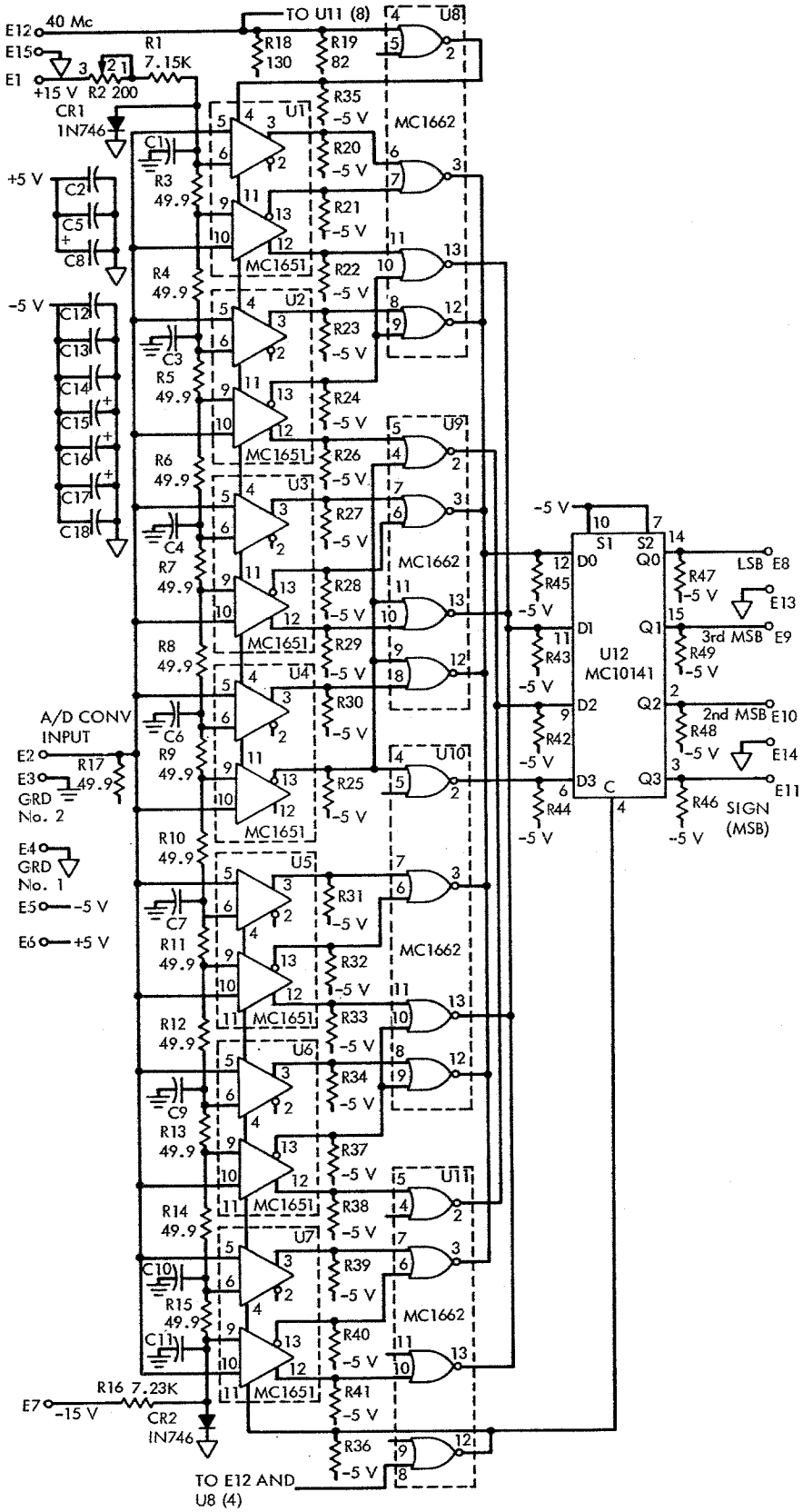

Fig. 20. A/D converter schematic

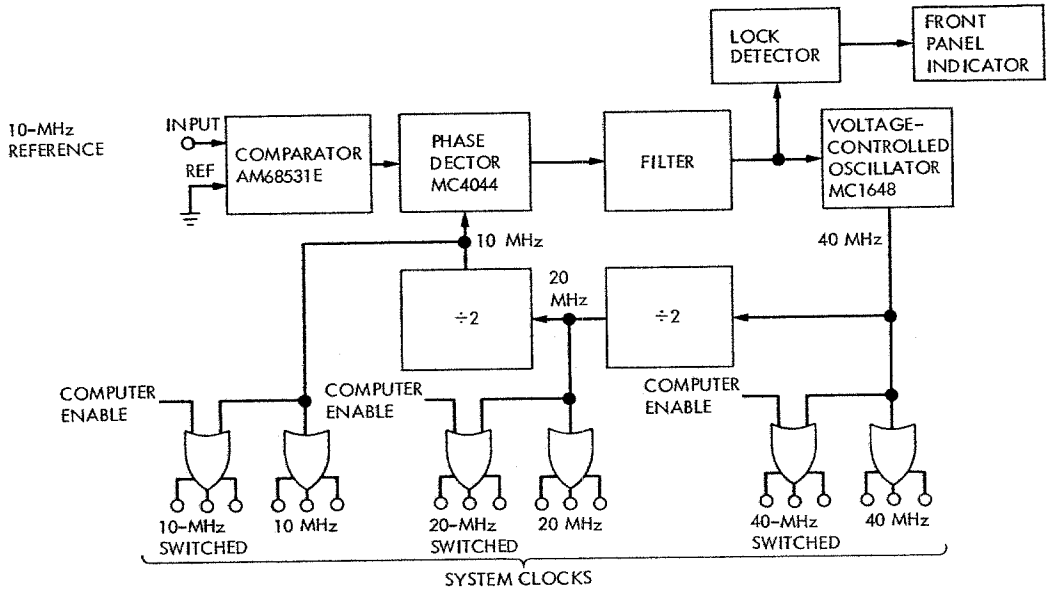

Fig. 21. Coherent multiplier diagram

while the desired signal from the spacecraft is passed. The output of the combiners can be expressed as

$$Y = \text{code} \oplus 10\,\text{MHz} \oplus \text{chopper}$$

Measurements indicate that the leakage is more than 60 dB below the received carrier with the chopper operating.

Synchronization and delay flip-flops are included to align the coder and chopper sample times with those of the A/D converter, which is sampling the receiver's IF carrier. The 4 bits from the A/D converter are simultaneously strobed into a hold register, which provides inputs to both the arithmetic units. During the next sample time, these will either add the new sample to or subtract it from previous values accumulated in the output registers. Operation is according to the expression for Y as set forth above. At the conclusion of the add-subtract cycle, the result is transferred to the first of two output (hold) registers.

Two registers are required by each arithmetic unit to implement the alternate sampling, as shown in Fig. 22. Assuming an initial condition wherein the registers are cleared, the first sample, $A1$, is added or subtracted (depending upon Y) into the first output register. Thereafter, the second sample, $B1$, is likewise transferred to the first output register while $A1$ is shifted to the second register. Note that $A1$ is now available at the second input to the arithmetic unit. Thus, when sample $A2$ is taken, it can be combined with $A1$ and stored in the first register while $B1$ is shifted to the second register. This process continues such that one register contains

$$\sum_{i=1}^{n} A_i$$

while the other holds

$$\sum_{i=1}^{n} B_i$$

Since the two arithmetic section output registers contain only 4 bits and the samples are collected at a 40-MHz rate, additional storage is required. The accumulators consist of 20-stage up-down counters. When the arithmetic operation results in a carry from the least significant 4 bits, an appropriate count command is generated and supplied to the proper accumulator. Three possible alternatives exist: the accumulator may be incremented, decremented, or retain its present value. This decision depends upon the adders' carry output, the sign of the present sample, and the status of the arithmetic unit (add or subtract) as determined by Y. Two control bits, S_1 and S_2, generated by the arithmetic unit, are used to select the count mode according to Table 2.

Arithmetic unit logic for S_1 and S_2 can be expressed as

$$S_1 = C_{N+4}$$

$$S_2 = \text{Add} \cdot B3 + \text{Add} \cdot B3$$

where $B3$ is the sign bit of the present sample. Two control bits for both the 0- and 90-deg channels are stored for one 40-MHz clock period in the count control register.

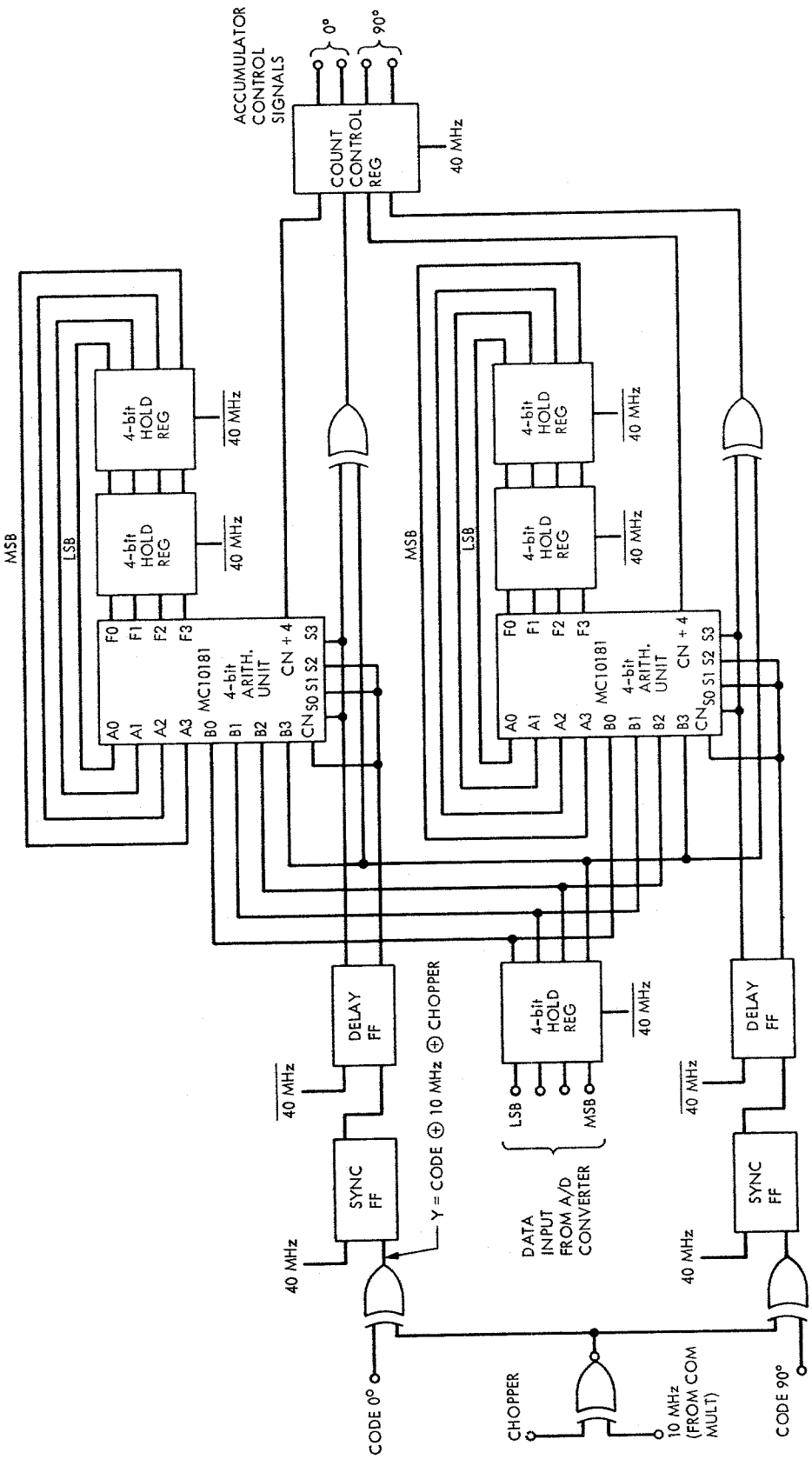

Fig. 22. Arithmetic section logic diagram

Table 2. Count control

S_1	S_2	Operating mode
0	0	Hold (stop count)
0	1	Increment (count up)
1	0	Decrement (count down)
1	1	Hold (stop count)

During the subsequent clock cycle, they are used to retain or change the contents of the accumulators.

J. Accumulators

Accumulation takes place in the 20-bit counters shown in Fig. 23. Mechanization employs a series of Motorola MC10136 synchronous counters with four possible operating modes, as shown in Table 3. Reconciliation of the disparity between S_1, S_2 and S_1, S_2 is included on the accumulator cards according to the relationship

$$S_1 = S_1 + S_2$$

$$S_2 = S_1 + S_2$$

This effectively converts the 00 (parallel load) state into a 11 (hold) condition.

From the foregoing discussion regarding the arithmetic units, it is obvious that, although sampling is at a 40-MHz rate, the collection of

$$\sum_{i=1}^{n} A_i \text{ and } \sum_{i=1}^{n} B_i$$

proceeds at one-half that speed. Reference to the 20-MHz and 40-MHz waveforms on Fig. 7 will clarify the operation. Note that samples are taken during the positive portion of the 40-MHz period and held while in the negative part. The arithmetic operation takes place during this negative period with the result stable and ready to be used by the following positive transition.

Since

$$\sum_{i=0}^{n} A_i \text{ and } \sum_{i=0}^{n} B_i$$

must be separate in order to compute the 10-MHz IF carrier phase, it is necessary to provide two accumulators. The 20-MHz clock can be used to steer the data to the proper accumulator, as shown in Fig. 23. During the negative half cycle, data is guided to accumulator A, whereas the positive half cycle directs the data to accumulator B. Caveat—the above explanation is only illustrative of the principle of operation since the existence of the count control register on the arithmetic unit (Fig. 22) has the effect of delaying accumulation by an additional 40-MHz clock period. This holding register provides insurance against timing problems which can occur when data is transferred from one card to another.

Returning to the accumulator diagram (Fig. 23), it can be seen that accumulator B receives the 20-MHz clock, whereas the complement is directed to accumulator A. Thus, the data is steered to A or B depending upon the clock's phase. Note also that because these clocks are derived from a phase-locked loop, wherein a definite phase relationship exists between all clocks and the 10-MHz reference, it is impossible for the samples to be directed to the improper accumulator. Even if a "glitch" causes an error or inversion of the data in the two hold registers following the arithmetic units, the system will correct itself during the next sample time. As noted earlier, this "corrective action" represents one of the advantages of the phase-locked coherent multiplier over a harmonic multiplier.

Data is accumulated continuously in the 20-bit counter. At 10-ms intervals, the computer issues a register transfer command, causing the most significant 16 bits of the counter to be transferrd to a hold register. Only 16 rather than 20 bits were utilized since they provided adequate precision and facilitated data transfer to the PDP-11, a 16-bit machine.

The hardware represented in Fig. 23 is constructed on a single card and accumulates data from one of the four arithmetic units. A total of four such cards, or eight registers, is needed to collect information from the 0- and 90-deg S-band section and from the 0- and 90-deg X-band channel.

Counter contents are transferred to the hold registers simultaneously for all channels at the conclusion of a 10-MHz cycle. Referring to Fig. 7, this means that the contents of Register A are transferred following sample $A2_n$ and those of Register B are moved following sample $B2_n$, where the sample number n will be the same for both transfers. This amounts to simultaneous sampling and forecloses errors due to nonuniform sample intervals or samples representing partial cycles.

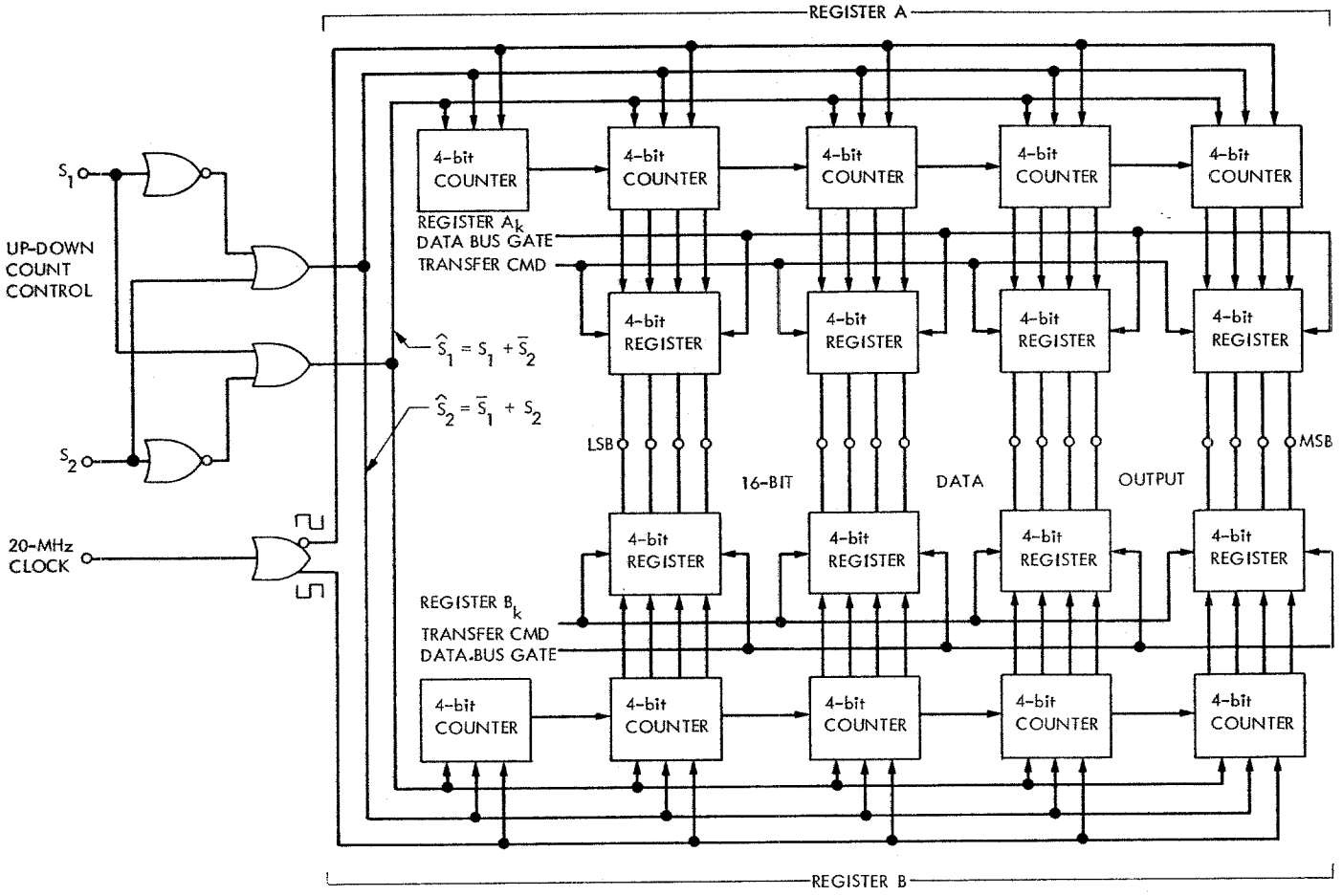

Fig. 23. Diagram of accumulators

Table 3. Truth table for MC10136 counter

S_1	S_2	Operating mode
0	0	Parallel load
0	1	Increment (count up)
1	0	Decrement (count down)
1	1	Hold (stop count)

Corresponding bits from all eight hold registers are bussed in common and transferred, via the interface unit, to the computers. Individual gate controls on the registers allow sequential transfer of data from each register onto the bus.

Numerical data accumulated in these hold registers represents the degree of correlation between the received and reference codes. Using this information, the phase of the received code, and hence the range, can be computed.

K. Minicomputer Control

The dual-channel ranging system was designed as a stand-alone unit. A PDP-11/20 is incorporated as a computer to control the ranging system, perform all calculations, and provide both local and remote output for operators and experimenters. The use of a minicomputer has had a material influence on the portability, versatility, and reliability of the ranging system. Because the system is not tied to a particular computer installation, there were no computer scheduling or interface conflicts in the testing of the machine at JPL or DSS 14. Further, the system's enhanced portability facilitates its use in the calibration and testing of DSN and spacecraft subsystems. During critical phases of the MVM'73 mission, a standby computer was maintained at DSS 14. Computer malfunc-

tions could be corrected by merely replacing a chassis rather than by the expensive process of troubleshooting on-line. The reliability of the ranging system was thereby greatly increased.

L. The Interface

The physical system interfaces may be partitioned into two groups. Those interfaces internal to the system and those mating the system to its environment. The internal interface exists in particular between the ranging chassis and the PDP-11/20 computer. This interface was designed with a view toward making the ranging chassis computer-independent, thereby facilitating system operations with different computers.

The PDP-11/20 is a 16-bit one- or two-address machine. The computer has a single bus-oriented architecture. This "unibus" is a 56-line data and control path. Of these lines, 18 are address, 16 are bidirectional data, and the remainder are control lines. The central processing unit (CPU), memory, and all I/O couplers or interface units are connected via the unibus. Each device is assigned a unibus address which is contiguous with memory addresses. Therefore, a transfer of data between a memory location and a device (e.g., a teletype) or between two memory locations is indistinguishable.

Any device on the bus can become the bus master, with any conflicts being resolved by priority logic in the CPU. As an example, consider the interrupt process, whereby a device connected to the unibus interrupts the central processor. The interrupt takes place in two phases. First, the device requests that it be granted mastership of the bus. Once granted, the device can then request an interrupt on one of four interrupt levels. When the CPU indicates that it is ready to accept the interrupt, the device responds with a 16-bit transfer address to begin the interrupt operation. Data transfers on the unibus are handled by a simple handshake, transferring address and data information via a series of interlocked cycles.

An eight-level priority interrupt circuit card was designed to simplify interrupt processes. Any device can interrupt the CPU by providing a 100-ns pulse to any of the eight input lines. Upon receipt of such a pulse, the interrupter checks all eight of its input levels in a priority polling scheme to select the one of highest priority. In response, the interrupter sends a unique 16-bit transfer address to the CPU. Thereby, each of the eight priority interrupt lines is tied to a particular preset address. These addresses are set via a diode matrix on the interrupter circuit board. The interrupter provides both internal and external interrupt capability to the system.

All timing and time of day information for the software is provided by the frequency and timing subsystem (FTS) at DSS 14. It supplies 1-s and 100-ms timing pulses which are used to synchronize the ranging algorithm and control process. To facilitate the input of time of day information, a unibus address was assigned to gating logic, which then controls the transfer of data from the FTS BCD time code to the unibus.

Ranging data is provided to the Space Flight Operations Facility (SFOF) primarily via the high-speed data line. The ranging system communicates with the high-speed data line through the digital instrumentation system (DIS)/telemetry data handler (TDH) interface. This interface, which is 41 bits wide, conforms to requirements as specified in TRK 2-8 (Ref. 7). The interface is mechanized as a 41-bit buffer, which has a unique unibus address. This buffer is loaded in response to a request pulse from the telemetry data handler. The DIS/TDH formats and commutates the ranging data with data from other systems. These data are sent via the high-speed data line to the SFOF, where an IBM System 360 computer decommutates the data and provides appropriate displays. The development of the DIS/TDH interface was hampered somewhat by the lack of real-time visibility of the commutated data at DSS 14. New monitor and control programs now being installed at DSS 14 should improve this situation.

The interface between the computer and the ranging chassis is primarily an extension of the unibus handshake operation. The 16 bidirectional lines of the unibus are split into 32 unidirectional data lines. The most significant 13 bits of the unibus address are decoded in the interface chassis as a device address. The five remaining least significant bits are decoded to provide 16 unibus addresses to the ranging chassis interface. Of these 16, eight are used as command functions to control operations of the ranging system and to strobe data transfers. The remaining eight are used to gate ranging system data back to the unibus for input into the PDP 11/20.

The computer controls the ranging system by sending a command word to one of two unibus addresses. These unibus addresses are assigned to control and gating logic in the ranging chassis interface. Particular bits and particular combinations of bits of the command word control specific ranging functions. These functions include retarding, advancing, or synchronizing the receive coders, resetting the accumulators, and strobing data from the range accumulators into the data buffers. Particular range codes and combinations of range codes are selected by transferring a coder control word to either of the

addresses assigned, respectively, to the transmit coder and to the receive coders.

The mechanization of the ranging chassis interface required the synchronization of 1-MHz TTL signals to 40-MHz MECL signals. Two important problem areas appeared in the debugging of this interface hardware. First, unexpected delays were found in the propagation of the 40-MHz signals through the ranging chassis backplane. Second, the MECL was found to be susceptible to the noise caused by TTL switching. Solution of the first problem involved reclocking and resynchronizing strobe pulses on one of the interface circuit boards. Solution of the second problem involved keeping lines carrying TTL signals isolated from lines carrying MECL signals. One recommendation for future TTL/MECL interfaces would be to do the actual conversion at the TTL side of the interface and transfer only differential MECL-level signals between TTL and MECL subsystems.

V. Software Implementation

The Mu-II hardware system is orchestrated by an advanced software system dubbed Super Mu-II. Developed and refined from the software supporting Mu-I, this system is designed to support virtually any mission ranging requirement. The primary features of the Super Mu ranging programs are (1) automatic reacquisition of the range code, (2) reacquisition of the range code without disturbing acquisitions already in the ray path, and (3) a flexible, efficient operator interface. The Super Mu-II system will be discussed in some detail in this section. The Systems Operating Instructions can be found in Appendix A.

A. Design Goals

There were four primary design goals for the software:

(1) *Ease of operation.* The operator interface must be easy to learn and simple to operate. It must be amenable to operators of varying degrees of skill and interests.

(2) *Efficient use of operator.* The operator must not be involved in "busy-work" calculations. The program must make efficient use of the operator's time.

(3) *Local visibility.* The operator or experimenters at the tracking station must have sufficient local visibility to confirm and assure proper system operation.

(4) *Modular construction.* The software must be constructed in interrelated but well defined modules to facilitate debugging, reliable operation, and developmental expansion.

Realization of the first three goals involved the direct interaction and cooperation of the ranging operators. The operator interface was designed to satisfy operational conditions rather than the more typical programming constraints. The resulting low probability of human error fully justified the extra programming effort involved.

The fourth goal was met through normal good programming practice. The various modules involved and their interrelation will be the subject of most of the rest of this section.

B. Operator-Supplied Parameters

Before going further, it is necessary to enumerate the operator-supplied parameters. These are broken into general groups as follows:

(1) Physical parameters

(a) TOF — time of flight. This is the time in integral seconds for a signal traveling at light speed to make the round trip from Earth to the spacecraft. To facilitate "zero delay measurements", entering TOF = 0 disables doppler rate aiding.

(b) SYN FREQ — synthesizer frequency. Because the ranging code is derived from a multiple of the station exciter synthesizer, the frequency of the synthesizer is required to calculate the code period.

(2) Component selection. Note that the code components are labeled from 0 to 23. When the Mu-II is connected to a Block IV receiver, code 0 ≈ 8 MHz, 1 ≈ 4 MHz, 2 ≈ 2 MHz, and so on, according to the formula:

$$\text{Code frequency} = \frac{\text{SYN FREQ} \times 3}{2^{4+N}}$$

where SYN FREQ ≈ 44 MHz and N is the component number.

(a) C1 — the highest-frequency code component. This is the initial component as well as the component used during post-acquisition redetermination of the high-frequency code measurement. C1 sets the bound on measurement accuracy.

(b) C2 — the lowest-frequency code component. This component sets the ambiguity resolution of the range measurement.

(c) CN — the number of post-acquisition redeterminations of the high-frequency (C1) code phase.

(3) Integration time (seconds)

(a) T1 — integration time of the initial measurement of C1.

(b) T2 — integration of all acquisition components following C1 and ending with C2.

(c) T3 — integration time of C1 during the post-acquisition redetermination.

(d) TC — integration time with the receiver coders disabled for the 10-MHz calibration (e.g., measurement of the phase relation between the 10-MHz IF carrier and the 10-MHz station reference).

(4) System configuration

(a) MODE. This parameter will be discussed in detail later. Its purpose is to select any of the 65,000 different configurations of the system.

(b) TØ — The time at which the receiver-transmitter coders are synchronized and to which the range point is referred. The operator can request a specific TØ time. The program will then automatically sequence an acquisition such that its TØ corresponds to the requested one.

(c) TX — an optional entry provided for operator convenience. TX is a specific time to start the next ranging acquisition. During the pre-track calibration, for instance, the operator can enter the scheduled time to start ranging. He may then ignore the ranging and go about more critical duties.

C. Time Line

The sequencing of operations is pertinent to the remainder of this section. This time line expands in greater detail the ranging algorithm discussed in Section III.

A timing chart for the Mu-II ranging algorithm is shown in Fig. 24. Note that the receive and transmit routines are timed independently and corresponding states related in time by a TOF. After acquisition is initiated, the transmit routine calculates a bias time which delays the actual start of acquisition so that the TØ time falls on 1 min + 2 s. The reason for this is to assure time compatibility between the range number and doppler data reported to the SFOF.

As discussed previously, the 10-MHz reference and IF signal calibration is done prior to an acquisition. During the receive portion of the calibration, the signal samples are integrated, with the receive coder inhibited, for a period equal to the parameter TC. After the integration, the receive and transmit coders are synchronized. This process takes 5 s. Thus for a period equal to BIAS + TC + 5, the transmit routine has only two tasks: first, to set a time in the scheduler to start the receive acquisition at START TRANSMIT TIME + BIAS + TOF, and second, for automatic reacquisition, to calculate and store the time to start the next acquisition such that all receive requirements are satisfied.

After the delay period has elapsed, the transmit routine activates the first component, C1, for T1 s, the integration time for the first component. The remaining components are turned on in turn for periods of T2 s. After transmission of the lowest-frequency component, C2, is completed, the transmit coder is returned to the first component, C1, and the transmit routine terminated.

The receive routine is activated, as previously mentioned, after a TOF + BIAS following the transmit routine start. The receive routine first disables (inhibits) the receiver coder, then integrates the signal samples for TC s to calculate the 10-MHz calibration. At the end of this period, the coder is enabled and the synchronize (sync) command sent to the ranging system. Within 5 s, the computer receives a coder sync interrupt from the hardware to confirm sync. Coincidentally, the station binary coded decimal (BCD) time clock is sampled to save the TØ time. If 5 s have passed and no interrupt occurs, a warning message is sent to the operator.

Because a 4-s deadband is allowed between acquisition components, the receive routine waits 2 s before configuring the receiver coder to the C1 component and clearing/enabling the accumulators. This deadband simplifies software/hardware timing for output preparation and reconfiguration. The first component is actually integrated for T1 − 4 s. The C1 + 1 through C2 components are integrated for T2 − 4 s. After the C2 integration is completed and the receiver coder returned to C1, the receive routine remeasures the C1 phase CN times. Each of these measurements requires an integration period of T3 s. A complete acquisition sequence, therefore, takes

$$TC + BIAS + 5 + T1 + (C2 - C1)T2 + (CN)T3 \text{ s}$$

Only one complete transmit-receive sequence has been discussed. In reality, there may be time for several such sequences in one round-trip light time. In effect, several

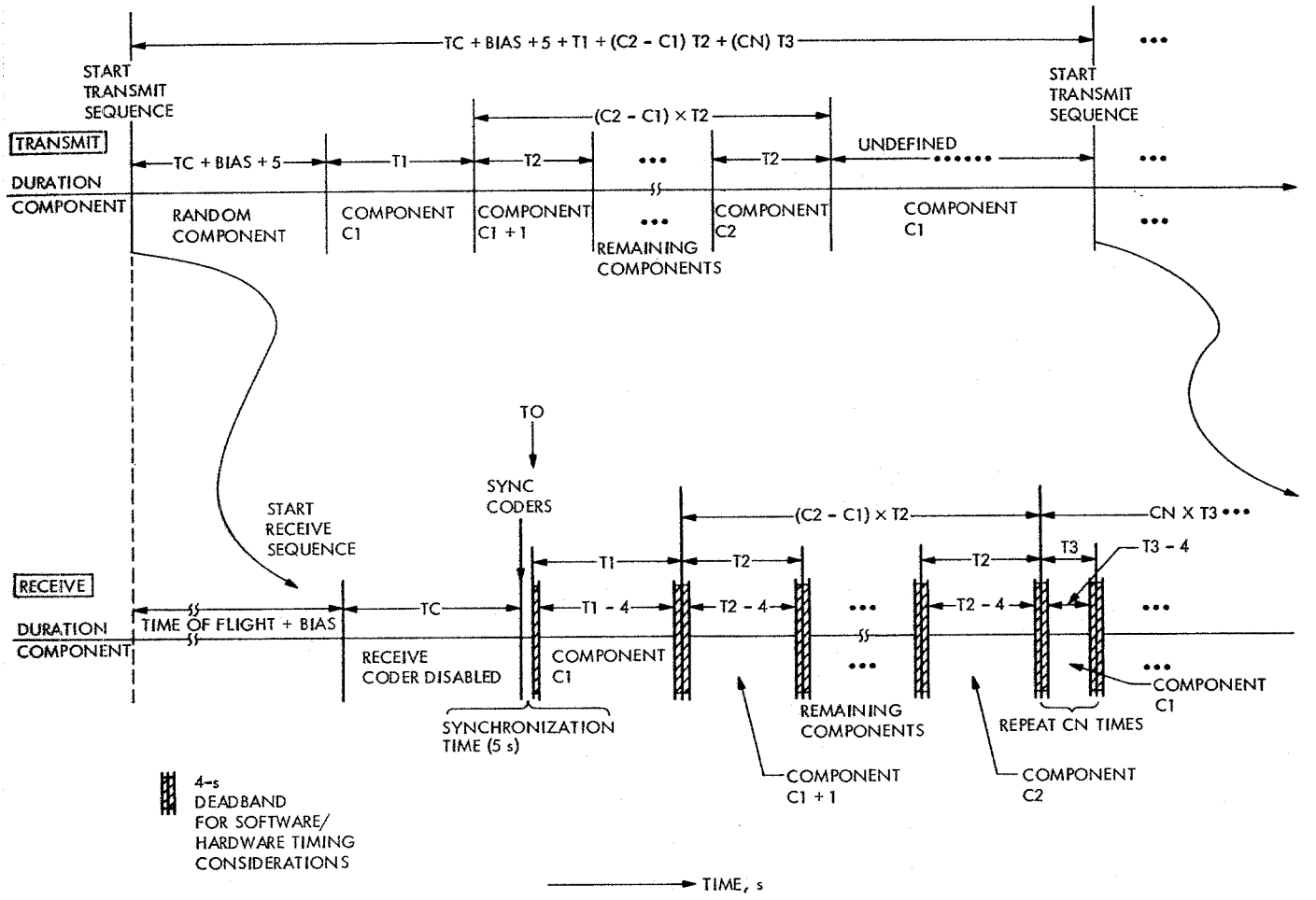

Fig. 24. Acquisition time line

acquisitions can be "strung" or "pipelined" in the Earth–spacecraft–Earth ray path. To take advantage of this possibility, each time the transmit portion of an acquisition is initiated, a time tag is generated for the next possible transmit time using the above formula. At the same time, a time tag is generated for one round-trip light time later to start the receive portion of the current acquisition. Because the operating parameters may be changed between transmit and receive times, it is also necessary to save the parameters used at transmit time so that they can be used again at the appropriate receive time. To accomplish this, a circular list is used to store both the receive time tags and operating parameters. This list is large enough to allow up to 10 acquisitions to be pipelined in the round-trip ray path.

D. A Block Diagram Overview—Scheduler

The Super Mu-II software is organized about a scheduler driving, at proper intervals and in proper sequence, several functional units. As shown in Fig. 25, each functional unit mechanizes a particular required operation. Because of the real-time environment, great care was taken to avoid timing problems in the interaction and control of these functional units.

The scheduler is simply a table of time tags and corresponding transfer locations. During initialization, a software second counter, which is driven by the station 1-s time pulse, is reset to zero and enabled. This counter serves as the time base for all ranging operation. The scheduler compares its time tags with this counter. If the current count equals or exceeds the tag, the scheduler transfers the program to the appropriate corresponding location.

A tag and transfer location are assigned to each functional unit. All communication between functional units is constrained to a data buffer and the scheduler (with the sole exception of the command routine to be discussed later). For instance, consider the operation of outputting data. When the receive routine has completed

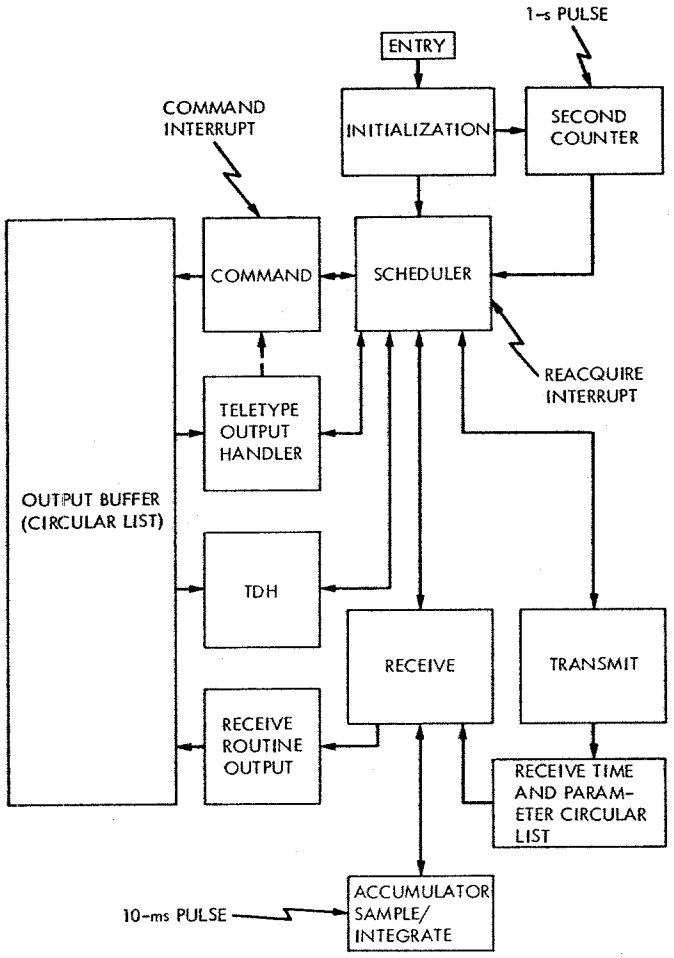

Fig. 25. Software block diagram

a calculation, the result is sent in a specific format to the output buffer. The receive routine then checks to see if the teletype handler and telemetry data handler are active. If they are active, the data will be automatically output. If they are not active, then their respective time tags are set to the current time and their transfer locations to the respective routine initiate locations. Note that all of these operations occur in background so that simultaneity conflicts cannot occur. All returns from the functional units are back to the scheduler.

As a further safeguard, interrupt routines can interact with any background task or functional unit only via the scheduler. The teletype output handler contains an interrupt routine to control the character-by-character output to the teletype machine. When the current teletype buffer has been output, the interrupt routine sets the time tag for the teletype output handler to the current time and the transfer location to the handler's start location. When background returns to or continues in the scheduler, the match between current time and the teletype time tag is found, and the teletype handler terminates its operation if there is no more data or prepares the teletype buffer for the next data transmission.

This use of the scheduler for background/foreground communication precludes a tieup of CPU resources by a particular foreground/background process. It also eliminates the simultaneity problem where both a foreground and background task are accessing the same parameter.

E. Transmit/Receive Functional Units

The operation of the transmit/receive functional units has already been described. Their purpose is to control and sequence the transmitter and receiver coders. The transmit functional unit also calculates the time for the next acquisition sequence and places the time to start receiving the current acquisition and all operating parameters in the circular list shown in Fig. 25 and described earlier.

The receiver functional unit takes all of its operating parameters from the aforementioned circular list. At appropriate times, the receive unit outputs correlation voltages and calculated range, estimated range signal-to-noise ratio, and DRVID. Note that the correlation voltages are obtained from the "accumulator" interrupt routine. This routine, driven by a 10-ms interrupt, samples and integrates data from the hardware accumulators described elsewhere.

Range acquisitions can be started in any of four ways. First, the operator can simply press an interrupt button on the front panel of the ranging system. Second, he can type in a GMT time at which the transmit sequence will be initiated. Third, he can type in a "TØ" time, and the program will calculate the appropriate transmit and receive times to meet that TØ. Fourth and finally, the program will automatically reacquire per the operating parameters supplied by the operator.

F. Command Functional Unit

All data to be output either to the teletype for local printout or to the TDH for transmission to the SFOF is put into the output buffer in a tagged format. Particular tags indicate what the data is and whether the data is for the TDH, the teletype handler, or both. An additional tag is the "Teletype Grab" tag. This tag is used to turn control of the teletype machine over to the command functional unit.

When the operator presses the command interrupt, the command functional unit time tag is set, and its transfer

location is set to the entry address. When the scheduler allows the routine to proceed, a word containing the Teletype Grab tag and an address is put into the output buffer. Then, if the teletype output functional unit is not active, it is activated. Upon its processing a Grab, control is transferred to the address given. This assures that the teletype has completed a line of data and makes a neat break to the command routine. During a command function, ranging processes continue and data is put into the output buffer. When commanding is complete, teletype control is returned to the teletype output handler and data stored during the command period is output.

The technique used to input operating parameters, "Tutorial Input," was discussed in a Progress Report article attached to this report as Appendix B. The technique allows the experienced operator to rapidly input required numbers while providing a helping hand to novice operators. Each command consists of an alphanumeric combination designating a command and the parameter or parameters to be entered. A complete list of commands and parameters is given in Tables 4 and 5.

To begin an input, the operator presses the command interrupt to gain the computer's attention. When the scheduler allows the command routine to proceed, indication is given to the operator by the typing of a pound sign (#). The pound sign is used throughout to indicate that input is required. The initialization of all parameters, for example, can be entered in any of the following ways (computer type-outs are underlined and all lines terminated by a carriage return):

(INTERRUPT)
#A/
TOF:
#1264
SYN FREQ:
#44.1234
T1:
#16
T2:
#16
T3:
#16
TC:
#30

Table 4. Tutorial input commands

Input command	Parameters to be entered
A/	TOF,SYN FREQ,C1,C2,CN,T1,T2,T3,TC,MODE
TF/	TOF
C/	C1,C2,CN
C1/	C1
C2/	C2
CN/	CN
T/	T1,T2,T3,TC
T1/	T1
T2/	T2
T3/	T3
TC/	TC
S/	SYN FREQ
M/	MODE
TX/	Start transmit time
TZ/	T0 time request
Y/	Typewriter printout ON/OFF; i.e., {Y/ON, Y/OFF}

Table 5. Operating parameters

Input parameters	Meaning
TOF	Round-trip light time[a]
SYN FREQ	Exciter synthesizer frequency
T1	First component integration time[a]
T2	Lower-frequency component integration time[a]
T3	Post-acquisition DRVID integration time[a]
TC	10-MHz calibration integration time[a]
C1	Highest-frequency component
C2	Lowest-frequency component
CN	Number of post-acquisition DRVID points before automatic reacquisition
MODE	Select configuration (i.e., Block III or IV receiver phasing, reacquisition with or without coder sync, etc.); "—" results in standard configuration, all flag bits zero.
T0	Coder synchronizer time (optional)[b]
TX	Start transmit time (optional)[b]

[a]These times may be input as integer seconds, HH:MM:SS, H:MM:SS, MM:SS, or M:SS, where H = hours digit, M = minutes digit, S = seconds digit.

[b]These lines may be entered as HH:MM:SS or HH:MM.

C1:

#4

C2:

#19

CN:

#3

MODE:

#-

or

(INTERRUPT)

#A/1264,44.1234,16,16,16,30,4,19,3,-

or

(INTERRUPT)

#A/1264,44.1234,16

T2:

#16

T3:

#16,30,4,19

CN:

#3,-

As can be inferred from the example, if data has been entered on a line, it is used. If it has not been entered, then it is requested. Commands can also be entered contiguously to change two or more sets of parameters. For instance:

(INTERRUPT)

#T/16,16,30,30,S/44.1235

or (equivalently for illustration)

(INTERRUPT)

#T/16,16,30,30,S/

SYN FREQ:

#44.1235

For more information on Tutorial Input, the reader is referred to Appendix B.

The configuration of the ranging system is controlled through the mode parameter. This parameter either sets flag bits in the mode word or transfers the switch states of the PDP-11/20 switch register to the mode word. Each bit of the mode word is assigned to a particular configuration option. Since fifteen flag bits are assigned, there are 2^{15} or 32,768 different system configurations available. The effect of each flag is listed in Table 6, and will be reviewed below.

Table 6. Configuration options

FLAG	"0" state	"1" state
0	Code servo on	Code servo off
1	DRVID during acquisition	Inhibit DRVID during acquisition
2	S-band code normal[a]	S-band code inverted[b]
3	X-band code normal[a]	X-band code inverted[b]
4	Normal reacquisition	Reacquisition without coder synchronization
5	Triangle correlation	Arctangent correlation
6	S-band power meter bandwidth	
	Block III	Block IV
7	X-band power meter bandwidth	
	Block III	Block IV
8	Not assigned	
9	Normal	No transmit code during calibration portion of transmission
10	Calibrate on in-phase channels	Calibrate on quadrature channels
11	Normal	Post-acquisition DRVID tracked at correlation peak
12	Normal	Accumulator dumps instead of carrier phase on local printout
13	Normal	Generate correlation curve during post-acquisition DRVID
14	Normal	Reverse calibrate SIN, COS internally (90-deg phase shift)
15		Set COS = 1, SIN = 0 internally[c]

[a]Normal for Mariner-type spacecraft and Block IV receiver.

[b]Normal for Mariner-type spacecraft and Block III receiver.

[c]TC must be zero for this option. 15 and 14 may be used together for SIN = 1, COS = 0.

Only flags 0 through 9 can be set to "1" from the teletype. The digits corresponding to the flag to be set are typed for the mode entry as a single multi-digit number. For example, consider the following command:

(INTERRUPT)

#M/0324

This would (1) disable the code servo, (2) set up inverted code phasing on both S- and X-bands, and (3) cause reacquisitions to be accomplished without synchronizing the transmit and receive coders. Entering a hyphen (-) sets all flags to zero.

If combinations of flags are required which include flags 10 through 15, then the entire flag word must be entered from the switch register. The operator first sets up the register, with switch number (0–15) corresponding to flag number, then enters "S" for the mode parameter (i.e., #M/S). The command routine then immediately copies the console switch register states into the mode word.

It is instructive at this point to review the various system options in some detail. The options can be separated into two groups, those necessary during normal tracking operations and those used for testing or experiments. The first group can be entered from the teletype or switch register; i.e., they are numbered 0–9. The second group can be entered only from the switch register.

The normally available options are designed to accommodate different operating conditions. Options 2 and 3 are used to compensate for code inversions resulting from different demodulation standards, i.e., local oscillator position, among the various DSN receivers and spacecraft. Options 0, 1, and 4 are used during periods of low signal-to-noise ratios and/or significant charged particle activity. Recall from an earlier discussion that a code servo is used to maintain code phase at an optimal point on the correlation function. During high noise, a phase measurement can be erroneous and the servo could cause the code phase to be removed from the desired point. Option 0 disables the code servo, and the system in effect "takes its chances." As mentioned earlier, DRVID data is taken during an acquisition by combining the high-frequency code with the acquisition's lower-frequency components. The phases of the two components are measured simultaneously. This combining of codes results in both splitting available power between the codes and corrupting the correlation function of the lower-frequency component in such a way as to decrease the probability of successfully determining its phase. During high noise, when optimum performance is desired, option 1 is used to prevent taking DRVID during the acquisition. Option 4 allows the redetermination of the contributions of lower-frequency components without resynchronization. This effectively means that the same range point can be remeasured.

Several experiments are in progress to improve the accuracy of range measurements. One source of range error is the fact that amplifiers, modulators, and filters may nonuniformly delay the fundamental frequency component and harmonics of the square wave code. To solve this problem, one experiment uses a narrowband filter to remove all harmonics so that a fundamental only phase measurement is made. The normal ranging algorithm assumes square waves; hence the correlation function is an approximation to square wave trigonometric functions. The fundamental only measurement, however, involves a sine wave; therefore normal trigonometric functions must be used. Option 5 substitutes the arctangent function for the square wave function.

Recall from the discussion on the power estimator that the routine needs to know the receiver's IF bandwidth. If options 6 and/or 7 are selected, the routine is told to use the Block III bandwidth for S- and/or X-band, respectively. Normally, the Block IV receiver is used, so that options 6 and 7 are not selected.

The special options 9–15 are used either for diagnostics or for particular experimental configurations. The only one of interest to the general user is 13. Option 13 causes the receiver coders to be delayed by 7 ns after each post-acquisition DRVID measurement. The effect is to trace a correlation function in terms of correlation voltage versus code phase. This technique is useful in determining and identifying errors and error sources in the ranging system and associated station/spacecraft hardware.

From both an operational and engineering standpoint, the mode parameter allows the system to be tailored to existing signal conditions and experimenters' desires. The usefulness of this configuration control cannot be overstressed.

G. Output Functional Units

Two output paths are used by the Mu-II. First, for local display, ranging data is printed on the console teletype. Second, data is sent to the SFOF via the TDH/DIS/high-speed-data-line system (Ref. 7). Figure 26 is a teletype printout from a Viking 1 tracking pass.[1] This particular pass was designed to collect a large number of DRVID measurements (highest-frequency phase remeasurements).

[1] Note: Typeout format changes may occur as the Mu-II programming is updated. This example is included only for illustration.

From the section on the timeline, one can see that the receive sequence is initiated one round-trip light time after the transmission start. After the bias time and the 10-MHz calibrate time (TC) have elapsed, the receive routine has completed the calibration and gives the synchronize coders signal to the hardware. The output (Fig. 26) indicates this event by the day of year (DOY) and calibrate measurement printout. As indicated, the S-band 10-MHz phase ($\theta + \pi/4$) has a sine of about –0.482 and a cosine of 0.876. This is an angle of 28.9 deg. The analogous number is given for X-band. The number following "MODE:" is a binary representation of the mode word. If any flag is set, it appears as a 1 in the binary word, where the bits are numbered right to left as 0 through 15. In the present case, no options are selected. The T0 time is given in the next line. This is the epoch to which the range measurement refers.

```
****DOY 198*****
S SIN:   0.48234D 00    COS:  0.87599D 00
X SIN:  -0.59533D 00    COS: -0.80348D 00


MODE:    0 000 000 000 000 000

T0**072202

072300      2.39545D 04  3.97401D 04  3.82543D-01  20.0D 00
   1    4   2.04224D 04 -2.17141D 03 -4.66028D-02  11.0D 00

072340     -3.53649D 04 -2.09975D 03  3.02543D-01  19.0D 00
   2    5   1.36672D 04  3.19426D 02 -4.66028D-02  10.3D 00

072420      3.40092D 04 -6.38330D 01 -7.95977D-03  18.3D 00
   3    6   1.29901D 04  3.24676D 02  5.39028D-03  99.3D-01

072500     -3.30347D 04  1.42867D 02 -9.13941D-03  18.1D 00
   4    7  -1.30398D 04  2.85321D 01 -7.49273D-03  97.9D-01

072540      3.28472D 04 -6.27008D 02 -1.61342D-02  18.2D 00
   5    8   1.22990D 04  6.40598D 02  1.75721D-02  97.1D-01

072620      3.25928D 04  5.07646D 01 -6.29725D-03  17.9D 00
   6    9   1.22201D 04  3.20484D 02  5.95820D-03  94.9D-01

072700      3.18422D 04 -2.77648D 02 -1.12429D-02  17.8D 00
   7   10   1.21599D 04 -2.64468D 02 -9.17919D-03  94.3D-01

072740     -3.18640D 04  1.07921D 03 -2.29368D-02  18.1D 00
   8   11  -1.24390D 04 -4.39537D 02  1.76923D-02  96.8D-01

072820      3.18625D 04 -1.11436D 03 -2.34374D-02  18.1D 00
   9   12   1.26411D 04  2.42679D 02  1.02764D-02  96.8D-01

 72900     -3.17907D 04  1.39803D 02 -1.67511D-02  17.7D 00
  10   13  -1.20392D 04  6.20426D 02 -2.26218D-02  95.6D-01
XMIT****072929

072940      3.16343D 04  7.89158D 02 -2.82578D-03  17.9D 00
  11   14   1.19826D 04 -9.63711D 01 -2.72613D-03  92.4D-01

073020     -3.15146D 04 -1.94670D 02 -1.16511D-02  17.6D 00
  12   15  -1.15185D 04  2.87059D 02 -1.06481D-02  91.0D-01

073100      3.13089D 04 -2.97610D 01 -1.50888D-02  17.5D 00
  13   16   1.17536D 04 -6.78275D 02 -2.53136D-02  94.3D-01

073140      3.07229D 04  4.95255D 02 -6.93529D-03  17.4D 00
  14   17   1.23347D 04 -1.61806D 02 -1.27127D-02  94.7D-01

073220      3.10557D 04  3.42524D 02 -9.33816D-03  17.5D 00
  15   18   1.19565D 04 -4.68944D 02 -2.47348D-02  94.3D-01
***  2.61686965898D 03   2.61652051359D 03

073320      3.24163D 04 -2.62616D 04  1.08030D-02  19.3D 00
  16    4   1.20750D 04 -1.06135D 04  9.18350D-03  11.1D 00

073420      3.11944D 04 -2.91045D 04  1.35175D-03  19.5D 00
  17    4   1.20140D 04 -1.07117D 04  7.45989D-03  11.1D 00

073520      3.04676D 04 -2.79986D 04  3.22101D-03  19.3D 00
```

Fig. 26. Ranging teletype printout

The range acquisition is now printed as blocks with the following format. On the first line, reading column by column, is (1) the completion of measurement time, (2) the S-band in-phase voltage, (3) the S-band quadrature voltage, (4) the DRVID or highest-frequency code phase measurement printed in microseconds, and (5) the S-band range signal-to-noise ratio in decibels. On the second line is (1) a line number, (2) the number of the primary component measured (it may be combined with the highest-frequency code for DRVID), (3) the X-band in-phase voltage, (4) the X-band quadrature voltage, (5) the X-band highest-frequency code phase measurement in microseconds, and finally, (6) the X-band signal-to-noise ratio in decibels. Note that if no DRVID is requested during acquisition, the first DRVID value is repeated. Notice also that the transmission for a new acquisition has started following line 10. Following line 15, the range measurement is printed as indicated by the three asterisks. Both the S-band and the X-band ranges are printed in microseconds.

The use of the printout in determining success or failure of an acquisition can be illustrated by following the acquisition progress. Starting on line 1, the correlation voltages can be essentially random since the phase ambiguity resolved by the first component is very small compared to the time of flight. Once can see that for this particular example, the phase initially measured was 0.303 μs (recall that component 4 is approximately a 2-μs code). The program now shifts the code so that the correlation function is at a peak. This implies that the following component will be at a positive or negative peak. As can be seen, the S-band for component 5 (line 2) is at a negative peak, such that the in-phase voltage is a large negative number while the quadrature voltage is near zero. Reference to the correlation function in Fig. 3 will illustrate this relation. Because the in-phase voltage is negative, half the period of component 5 must be added to the range value. The coder is now shifted by the same period, so that the next component is at a positive or negative peak. If the fifth component were at a positive peak, no contribution would have been made to the range value and no coder shift. In general, then, for a successful acquisition, the absolute value of the in-phase voltage must be much larger than the absolute value of the quadrature voltage.

For illustration, one can calculate the S-band range value from the correlation voltages. The period of a code is given by the formula:

$$P = \frac{2^{N+4}}{\text{SYN FREQ} \times 3}$$

where N is the component number, SYN FREQ is the synthesizer frequency in megahertz, and P is the period in microseconds. Therefore component 4 in this example has a period of about 1.94 μs.

From Fig. 26, the first phase measurement is 0.303 μs. For each succeeding negative in-phase voltage, we add half the period of the corresponding component. There is a contribution from components 5, 7, 11, 13, and 15. The range is thus 0.303 + 1.94 + 7.76 + 124.16 + 496.64 + 1986.56 or ~2.617 μs. This is approximately the value shown in the printout.

One final note on the acquisition. It was arbitrarily decided that the high-frequency code phase would be measured from minus half a period to plus half a period, so that positive and negative DRVID would be shown. However, this raises the possibility of a negative range (which is not esthetically pleasing). Therefore, if the initial phase measurement is negative, one first-component code period is added to the measurement to move it to the positive region. When the receiver coder is shifted to a peak, the shift is commensurate with this positive number, so that the proper peak is obtained.

After the acquisition, the receiver coder is shifted to move the code phase to the equal power point on the correlation function. This is apparent from line 16, where the in-phase and quadrature voltages are nearly the same in magnitude but of opposite sign. The DRVID value for line 16 is about –0.018 μs for S-band. This means that due to noise and charged particle effects, the apparent range differs by ~18 ns from its original measurement. The following acquisition will be similarly received after CN post-acquisition DRVIDs.

The reader is referred to Ref. 7 for a complete explanation of the format and physical data links involved in data transmission to the SFOF. The output consists of a 41-bit buffer, which is loaded upon interrupt from the TDH. These interrupts are at the same rate as the doppler sample rate, typically 10 per second.

Three format blocks are used for data transmission. The first, the "initialize" block, is two 41-bit words, the first containing the time of flight, number of components, and T1, and the second containing T2 and T3. The second block is a "DRVID" block with four words: (1) S-DRVID, S-band $P_R N_0$, and the line number; (2) X-DRVID, X-band $P_R N_0$, and the line number repeated; (3) S correlation voltages, and (4) X-band voltages. The final block is the "range" block. This block has three words: (1) T0 time, number of components, (2) S range, and (3) X range.

The TDH/DIS mechanization for sending data to the SFOF had some major problems. The initialize block which is sent at transmit time causes the programs running in the system 360 at the SFOF to initialize and wait a time of flight before accepting data. This is adequate for the planetary ranging assembly (PRA), which does not have multiple automatic reacquisition capability. The Mu-II, however, may be receiving data from an earlier transmit sequence at the time a new acquisition is transmitted. If the initialization block were sent at transmit time, data from current receive sequences would be lost. To avoid this problem, the initialization block is sent 1 s prior to a receive sequence, with a dummy time of flight equal to 1 s.

Another problem set occurs because the TDH doppler sample rate is independent from ranging system timing. First, if the doppler sample rate is not high enough to sample the range data at a rate commensurate with range processing, data will be lost. Second, no provision is made to send the time tags for DRVID measurements to the SFOF. Thus DRVID data may be catalogued asynchronously with doppler data.

One final problem caused the most data to be lost or adulterated. This involved the use of range units (RU) instead of microseconds for data transmission to the SFOF. Each type of ranging system has its own range units. Given that the transmitter exciter synthesizer frequency (F) is given on the order of 44 MHz, the range in microseconds can be calculated from PRA and Mu-II range units by

$$R_{\mu s} = \frac{R_{\text{RU(Mu-II)}}}{3072 \times F} = \frac{R_{\text{RU(PRA)}}}{24 \times F}$$

where

$R_{\text{RU(Mu-II)}}$ = Mu-II range units

$R_{\text{RU(PRA)}}$ = PRA range units

Though not pertinent to the discussion, there are also unique range units for the Mark 1, Mark 1A, Mu-I, and TAU systems.

It is readily apparent that difficulties are possible when raw data must be analyzed manually. People running the

data processing in the SFOF sometimes mistook range units for seconds or PRA range units for Mu-II range units or vice versa. Given two different range units plus microseconds, there seemed to be a one out of three chance that data manually input into the 360 was correct. Happily, odds improved as experience was gained.

Range measurements using units of time are (1) natural to interpret and (2) universal among ranging systems. It is therefore hoped that future mission operations will restrict any human-readable or -accessible range measurements to units of time.

A final note: The software controls and inputs were designed through cooperation and interaction between the programmer and the ranging operators at DSS 14. The direct result of this effort was Tutorial Input. Indirect results were a strong operator interest in the ranging performance through a high degree of personal involvement. The success of the Mu-II software as indicated by the system performance was largely due to this cooperation between the system operators and the system programmer.

VI. Construction Details

A principal objective was the design of a self-contained ranging machine requiring interfaces with only the DSIF exciter, receiver, timing, and data handling subsystems. Furthermore, the paucity of station floor space made it mandatory that the design be as compact as possible consistent with high reliability and reasonable cost.

The finished product, shown in Fig. 1, consisted of a 1.5-m (5-ft) rack and companion teletypewriter. Functionally, the system was subdivided into three distinct sections: ranging, interface, and computer units.

A. Ranging Unit

A photograph of the ranging unit appears in Fig. 27. This part is constructed in a 22-cm (8-3/4-in.) slide-out drawer and contains all subsections shown in Fig. 10 excepting the interface and PDP-11 computer. A front panel provides an indication of systems' operating status as well as serving as a useful tool for checkout and fault diagnosis.

Condition of the three coders is shown by the coder register indicator at the top. This display is subdivided into sections A, B, and C, each corresponding to one of the three 8-bit cards comprising a single coder. Column 00 denotes the 8-MHz code, while column 23 corresponds to the 1-Hz range code. Indication is by a light at the intersection of the component number and coder designation, showing which range code, or set thereof, is operative at a particular time. During the MVM'73 mission, Receiver 1 was generally assigned to S-band and Receiver 2 to X-band, although the system was designed to be operative on any two bands or with both channels on the same band. Lights preceding coder captions, together with the lights above particular segment letters (e.g., A,B,C), designate which coder banks have been enabled for manual entry from the front panel pushbuttons. For example, see in Fig. 1 that segment A of Receiver 1 and 2 coders has been enabled, and thereafter that component 4

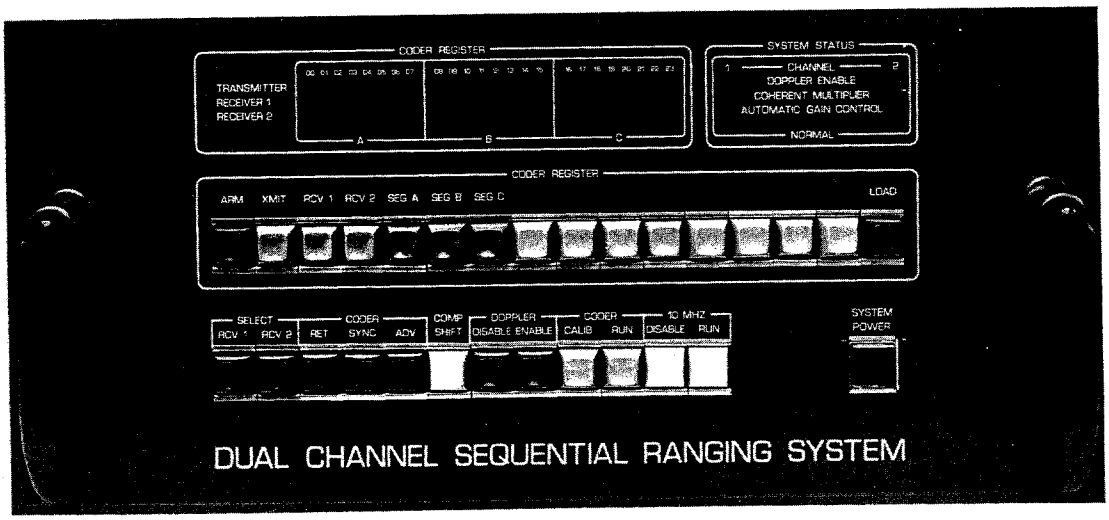

Fig. 27. Ranging unit

(500 kHz) has been selected in all coders, together with component 6 in Receiver 1 and 2 coders.

System status is shown by two columns of four lights corresponding to the two channels. Normal operation is indicated by a "light on" condition. When the doppler enable lamps are on, the local (receiver) range code is being rate aided by RF doppler supplied from the DSN receiver. This is a normal operating condition when the system is ranging with a spacecraft.

Since there is but one coherent multiplier for the two channels, both lights are connected in common to the phase-locked loops' lock detector circuitry, as discussed above. Whenever the static phase error exceeds a preset amount, the light is extinguished. Thus, if the 10-MHz station reference is inadvertently disconnected, the resulting malfunction will be immediately apparent on the indicator.

Likewise, the automatic gain control lights show whether the gain control (feedback) voltage is within the proper limits in each of the two AGC amplifiers. Again, should the 10-MHz IF signal lines be disconnected, the lights are extinguished, indicating improper operation.

Two unlabeled lamps at the bottom show the status of clocking signals. On the left, in the channel 1 column, will be found the 10-MHz indicator, while the 40-MHz light is on the right. Both indicate when their respective clocks are enabled, a necessary condition for proper system operation. As noted previously, 10 MHz is combined with code and chopper to provide a local reference for the arithmetic card, while 40 MHz is used to control the sample rate of the A/D converter.

The intermediate row of pushbuttons allows manual access to the coder registers. Commands are steered to the proper coder by first selecting which of the three coders (XMIT, RCV1, RCV2 or combination thereof) is to be loaded and thereafter, which segment (A, B, C) of the selected coder is to be changed. Segment selection also causes appropriate component numbers to appear above the eight buttons to the left of the "load" switch. Actual transfer is effected by pressing *first* the arm button and *thereafter* the load button. Note that this double lockout feature, which requires two hands to complete, precludes the inadvertent modification of the coders during a ranging operation. Changing the coders' contents from the front panel is prima facie evidence of intent to change their status.

Pushbuttons providing functional commands are located in the bottom row. Again the double lockout feature prevents the curious from disturbing the system's operation. All commands are confined to the receiver channels, and the two select buttons on the left serve to arm their respective channels. A command will only be transferred when the appropriate select button is depressed and held, and *thereafter* one of the command buttons is pushed.

The retard (RET) button causes the selected receiver coder to be delayed in phase by 7.5 ns, relative to the transmitter coder, each time it is pressed. Likewise, advance (ADV) causes the selected receiver coder to be advanced in phase by 7.5 ns. These correspond to the fine shifts supplied to the pulse adder from the computer and/or the doppler conditioning unit to position the local code relative to the received code.

The synchronization (SYNC) button causes the selected receiver coder to be aligned in phase with the transmitter coder. In addition to synchronizing the coder and pulse adder frequency divider chains, it also causes the doppler conditioning scalars to be set midway in their count. This should best approximate the expected value of elapsed time until the doppler produces a phase adjustment.

During acquisition of all components other than the first, the receiver coder may be called upon to invert the phase of that component. The component shift (COMP SHIFT) button performs this inversion and can be used to test the proper operation of the logic.

Doppler rate aiding to either channel can be enabled or disabled using the next set of buttons. A change in their condition is indicated by the doppler status lamps at the top of the panel.

In the calibrate mode, the coder outputs are disabled so that a measurement of the 10-MHz carrier phase can be obtained. Since code and 10 MHz are combined to provide a control signal for the arithmetic unit, the resulting complex waveform makes system checkout difficult. Therefore, a front panel control capability for both coder and 10 MHz was provided which allows the operator to selectively enable or disable either signal. In addition to facilitating operational readiness tests of the coder, coherent multiplier, and combiner logic, it also allows the system to be used for baseband ranging by disabling the 10 MHz.

The panel was designed to make the ranging unit independent of both computer and interface during testing. Since substantially all functions are controllable,

various operating modes can be simulated without resort to a special computer program. Additionally, the panel allows independent and simultaneous checkout of both the ranging unit and the computer program, a feature which was to prove invaluable in the field.

Power to the entire rack, including the ranging unit, is controlled by the system power switch on the right. Power amplification was included in the form of a power transfer relay located in the base of the rack.

Field experience indicates that substantial installation and debugging time was saved by the existence of the panel control/display capability. Absence of an equivalent feature on the earlier sequential ranging (Mu-I) system resulted in many wasted hours and not infrequent damage to the machine when a test probe or other tool would cause a short circuit. In retrospect, it has been argued that this control/display capability was one of the most useful features of the new system.

Figure 28 shows the top side construction of the ranging unit. Logic cards are of two types. First are the stitched wire welded cards containing low-frequency circuitry and interface subunits. The remainder are printed circuit cards, generally multilayer, containing high-frequency subsections. It was originally planned that all logic be placed on printed circuit cards, but while the designs exist, not all have been fabricated.

Most of the system was implemented using MECL 10,000 digital logic, although the A/D converter and parts of the pulse adder are mechanized with MECL III high-speed logic. Additionally, parts of the interface utilize 7400 series TTL integrated circuits for compatibility with the PDP-11 computer.

Since the 23 cards require considerable power—more than 30 A at 5 V—heat removal was a substantial problem. Cooling is provided by four centrifugal blowers mounted on opposing sides of the card cage. These are used to pressurize a plenum beneath the card cage, which results in cooling air being forced up between the cards. Tests using an infrared radiation monitor indicate that the warmest spots on any of the cards approximate 40°C, well within the safe operating range.

To the right rear of the card cage is a module containing the two AGC amplifiers. These were separated from the logic cards to provide shielding and to prevent the digital signals from increasing the noise level. A retrofit is planned whereby the A/D converter and the AGC amplifier are placed in a somewhat larger module in the same location. The intent is to further reduce any possibility of leakage of either code or 10-MHz signals through the normal signal path.

Three power modules are located to the rear of the chassis adjacent to the AGC amplifier. The two smaller units provide ±15 V for the AGC amplifier and A/D converter reference, and +5 V required by the TTL logic and MECL converters. In the left rear corner will be found the main power module supplying −5 V to the MECL circuitry, which comprises the bulk of this system. This unit is designed to provide 40 A at an 80°C base temperature. A thermistor mounted on the base indicates that the actual normal operating temperature is less than 45°C at the full load of approximately 35 A. Thus, the system appears to be operating well within its design limits.

Because the three power supplies generate substantial heat, thermal management was a primary concern during the design phase. The system utilizes a 0.953-cm (0.375-in.) thick aluminum chassis plate on which all power supplies, the card cage, and the amplifier module are mounted. This plate is thermally bonded to the side rails and rear panel of the drawer. The intent was to provide a monolithic thermal structure whereby heat generated by the various modules was first transferred to the base plate and then to the drawer frame itself. Cold air being drawn through the rack and exhausted at the top cooled the drawer and hence the entire system.

Figure 29 is a photograph of the ranging unit's underside. The card frame is in the forefront with its plenum cover removed to expose connectors and back plane wiring. The two rectangular holes on each side are exit vents for the fans used to pressurize the plenum. Note the perforated plate, whose 51% open area provides adequate air flow to cool the logic cards while still acting as an excellent ground plane. Generally, connections were made by wirewrap, and no substantial difficulty was encountered with the MECL signals even at frequencies as high as 40 MHz.

The several parallel lines visible on the back plane are bus bars. Judicious layout and placement of circuit cards allowed a large number of the interconnections to be bussed from one connector to the next. This resulted in a very material reduction in construction time since prepunched bus bars can simply be slipped over the wirewrap terminals.

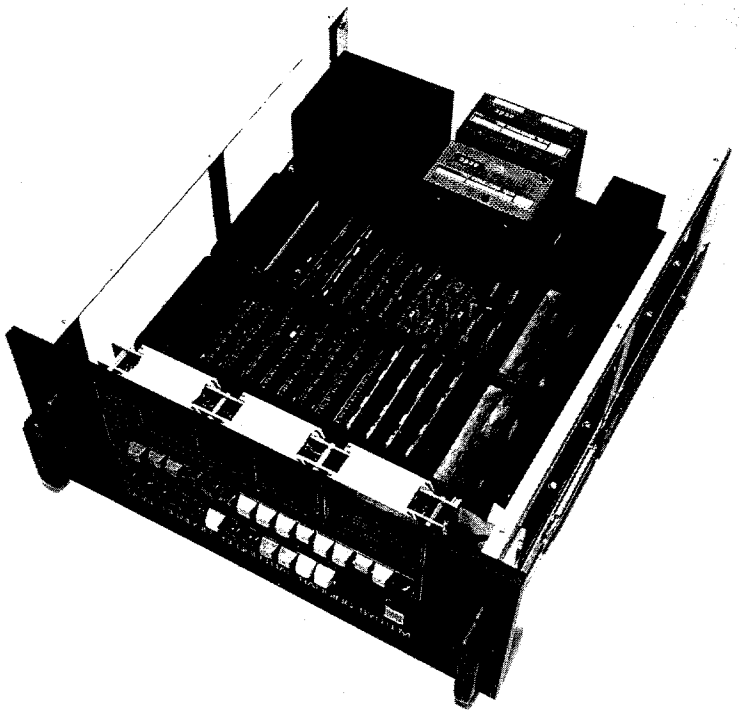

Fig. 28. Ranging unit, top view

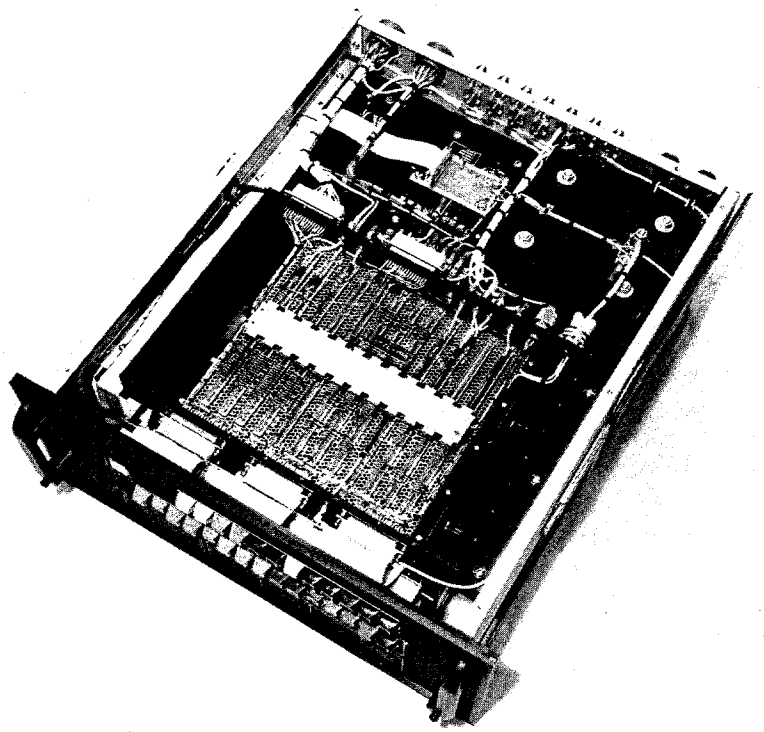

Fig. 29. Ranging unit, bottom view

Table 7. Required DSN interface signals

Name	Purpose	Signal characteristics	Impedance, Ω
RCVR 1	10-MHz input signal from DSN Receiver 1	-70 dBm $< P_S <$ $+15$ dBm	50
RCVR 2	10-MHz input signal from DSN Receiver 2	-70 dBm $< P_S <$ $+15$ dBm	50
10-Mc ref.	10-MHz sine wave coherent reference	0 to $+15$ dBm	50
66/132 Mc	66-MHz or 132-MHz reference from DSN exciter	0 to $+15$ dBm	50
DR1	Receiver 1 doppler reference (0 deg)	-10 to $+20$ dBm	50
DQ1	Receiver 1 doppler quadrature (90 deg)	-10 to $+20$ dBm	50
DR2	Receiver 2 doppler reference (0 deg)	-10 to $+20$ dBm	50
DQ2	Receiver 2 doppler quadrature (90 deg)	-10 to $+20$ dBm	50
XMIT code	Ranging code output to DSIF exciter	3 V p-p dc offset adjustable	50
E	1-s time tick from FTS	0 V quiescent, rising to $+5$ V (± 4 V) on the second tick	50
A	Spare		
B	Spare		
C	Spare		
D	Spare		

The rather large bar at the center is a 0.318-cm (0.125-in.) thick copper plate used to distribute –5 V throughout the system. Circuit cards in the two rows are faced in opposing directions so as to permit the common bus down the center. Ground connections are made to the perforated plane.

All electrical interfaces to or from the card cage are made via connectors to ensure an airtight seal for the pressurized plenum. Additionally, this facilitates removal and replacement of the entire card frame module while not disturbing the remainder of the system. Two power connectors are located on the right rear side of the card frame. Several OSM coaxial connectors are used for interface signals to or from other DSN subsystems. The rightmost 50-pin Cannon connector provides all communication with the interface unit and hence the PDP-11 computer. On the left, the remaining Cannon connector carries several important test signals to the rear panel so that proper system performance, or fault diagnosis, can be undertaken without opening the drawer.

The rather large block in the right rear corner of the chassis is, in actuality, a well for the –5-V power supply and was required because the supply's height exceeded available space above the chassis. As with other modules, a tight thermal bond was made with the chassis plate to ensure adequate cooling of the power supply.

Signal connections required for the ranging unit can be seen in the rear panel photograph (Fig. 30). A description of all external DSN subsystem interfaces, made via TNC coaxial connectors, may be found in Table 7. Additionally, 110 V ac is required for system power and enters through the ac power connector. Switched ac provides both a contact closure and switched 110 V ac to operate the power transfer relay mentioned earlier for the control of all system power. Critical signals, available on the test connector, are summarized in Tables 8 and 9. Command data connections with the interface unit are made using the computer connector.

B. Interface Unit

The interface unit serves (1) to connect the ranging drawer to the computer and (2) to connect the computer to the DSN timing signals and data ports. The front panel (Fig. 31) shows the unit power switch and operator interrupt buttons. The power switch is normally left "on" as system power is controlled by the ranging drawer. The two buttons cause specific interrupts to occur in the PDP-11. These are the "reacquire" interrupt and "command" interrupt discussed in Section V.

Figure 32 is a top view of the interface drawer. The card cage contains the TTL system data interfaces to the computer and the eight-level priority interrupt described earlier. The small box at the lower right contains timing

Table 8. Test connector signals

Pin No. Bendix test connector	Signal name	Description
A	Ground	Shield; transmitter code return
U	Transmitter code output	
B	R1 code ⊕ 10 MHz ⊖ 10 ms	Combiner output Ch. 1, 0 deg
V	R1 code ⊕ 10 MHz ⊖ 10 ms	Combiner output Ch. 1, 90 deg
T	Ground return combiners	
C	R2 code ⊖ 10 MHz ⊖ 10 ms	Combiner output Ch. 2, 0 deg
W	R2 code ⊖ 10 MHz ⊖ 10 ms	Combiner output Ch. 2, 90 deg
n	R1 doppler clock	Reconstructed Ch. 1 doppler reference
S	R1 doppler sign	Reconstructed Ch. 1 doppler direction signal
X	R1 doppler advance	Ch. 1 doppler advance to pulse adder
p	R1 doppler retard	Ch. 1 doppler retard to pulse adder
m	Ground return	Ground return for Ch. 1 doppler signals
Y	R2 doppler clock	Reconstructed Ch. 2 doppler reference
q	R2 doppler sign	Reconstructed Ch. 2 doppler direction signal
AA	R2 doppler advance	Ch. 2 doppler advance to pulse adder
k	R2 doppler retard	Ch. 2 doppler retard to pulse adder
D	Ground return	Ground return for Ch. 2 doppler signals
r	Ground return	Transmitter coder all zeros detectors
BB	T_a all 0's detector	All zeros detector transmitter coder C_0–C_7
z	T_b all 0's detector	All zeros detector transmitter coder C_8–C_{15}
R	T_c all 0's detector	All zeros detector transmitter coder C_{16}–C_{23}
Z	Ground return	Ch. 1 receiver coder all zeros detectors
CC	R1a all 0's detector	All zeros detector Ch. 1 receiver coder C_0–C_7
GG	R1b all 0's detector	All zeros detector Ch. 1 receiver coder C_8–C_{15}
j	R1c all 0's detector	All zeros detector Ch. 1 receiver coder C_{16}–C_{23}
E	Ground return	Ch. 2 receiver coder all zeros detectors
s	R2a all 0's detector	All zeros detector Ch. 2 receiver coder C_0–C_7
HH	R2b all 0's detector	All zeros detector Ch. 2 receiver coder C_8–C_{15}
y	R2c all 0's detector	All zeros detector Ch. 2 receiver coder C_{16}–C_{23}
a	Ground return	10-MHz coherent mult. reference, unswitched
DD	10-MHz	10-MHz coherent mult. reference, unswitched
FF	Ground return	20-MHz coherent mult. reference, unswitched
i	20-MHz	20-MHz coherent mult. reference, unswitched
F	Ground return	40-MHz coherent mult. reference, unswitched
t	40-MHz	40-MHz coherent mult. reference, unswitched
EE	Ground return	Not 1-s time tick
x	1-s time tick	Reconstructed 1-s time tick, inverted
N	Ground return	For interface chassis signals
b	CMDA	Enable A commands

Table 8 (contd)

Pin No. Bendix test connector	Signal name	Description
u	CMDB	Enable B commands
w	LTC	Load transmitter coder
h	LRC	Load receiver coder
c	Ground return	
v	DVM	Interface data valid
g	Ground return	Power supplies
G	+5 V	Positive 5-V supply
d	−5 V	Negative 5-V supply
f	+15 V	Positive 15-V supply
M	−15 V	Negative 15-V supply
H	YS1 thermistor	Base plate temp., −5 V supply*
e	YS1 thermistor return	Base plate temp., −5 V supply*

*See resistance vs. temperature characteristics in Table 9.

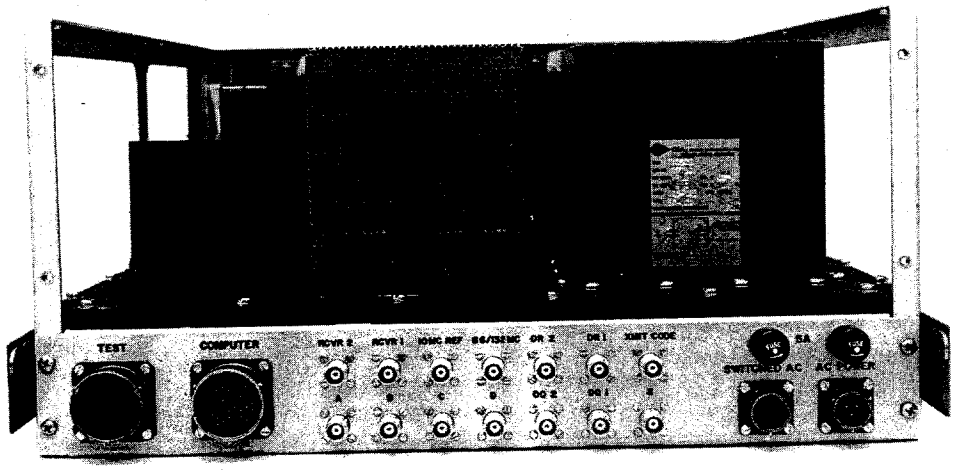

Fig. 30. Ranging unit, rear panel

Table 9. Thermistor resistance versus temperature characteristics

Temperature, °C	Resistance, Ω	Temperature, °C	Resistance, Ω	Temperature, °C	Resistance, Ω	Temperature, °C	Resistance, Ω	Temperature, °C	Resistance, Ω	Temperature, °C	Resistance, Ω
−40	884.6K	−4	116.0K	32	22.33K	68	5738	104	1840	140	701.2
39	830.9K	3	110.3K	33	21.43K	69	5545	105	1788	141	684.1
38	780.8K	2	104.9K	34	20.57K	70	5359	106	1737	142	667.5
37	733.9K	−1	99.80K	35	19.74K	71	5180	107	1688	143	651.3
36	690.2K	0	94.98K	36	18.96K	72	5007	108	1640	144	635.6
35	649.3K	1	90.41K	37	18.21K	73	4842	109	1594	145	620.3
34	611.0K	2	86.09K	38	17.49K	74	4682	110	1550	146	605.5
33	575.2K	3	81.99K	39	16.80K	75	4529	111	1507	147	591.1
32	541.7K	4	78.11K	40	16.15K	76	4381	112	1465	148	577.1
31	510.4K	5	74.44K	41	15.52K	77	4239	113	1425	149	563.5
30	481.0K	6	70.96K	42	14.92K	78	4102	114	1386	150	550.2
29	453.5K	7	67.66K	43	14.35K	79	3970	115	1348		
28	427.7K	8	64.53K	44	13.80K	80	3843	116	1311		
27	403.5K	9	61.56K	45	13.28K	81	3720	117	1276		
26	380.9K	10	58.75K	46	12.77K	82	3602	118	1241		
25	359.6K	11	56.07K	47	12.29K	83	3489	119	1208		
24	339.6K	12	53.54K	48	11.83K	84	3379	120	1176		
23	320.9K	13	51.13K	49	11.39K	85	3273	121	1145		
22	303.3K	14	48.84K	50	10.97K	86	3172	122	1114		
21	286.7K	15	46.67K	51	10.57K	87	3073	123	1085		
20	271.2K	16	44.60K	52	10.18K	88	2979	124	1057		
19	256.5K	17	42.64K	53	9807	89	2887	125	1029		
18	242.8K	18	40.77K	54	9450	90	2799	126	1002		
17	229.8K	19	38.99K	55	9109	91	2714	127	976.3		
16	217.6K	20	37.30K	56	8781	92	2632	128	951.1		
15	206.2K	21	35.70K	57	8467	93	2552	129	926.7		
14	195.4K	22	34.17K	58	8166	94	2476	130	903.0		
13	185.2K	23	32.71K	59	7876	95	2402	131	880.0		
12	175.6K	24	31.32K	60	7599	96	2331	132	857.7		
11	166.6K	25	30.00K	61	7332	97	2262	133	836.1		
10	158.0K	26	28.74K	62	7076	98	2195	134	815.0		
9	150.0K	27	27.54K	63	6830	99	2131	135	794.6		
8	142.4K	28	26.40K	64	6594	100	2069	136	774.8		
7	135.2K	29	25.31K	65	6367	101	2009	137	755.6		
6	128.5K	30	24.27K	66	6149	102	1950	138	736.9		
−5	122.1K	31	23.28K	67	5940	103	1894	139	718.8		

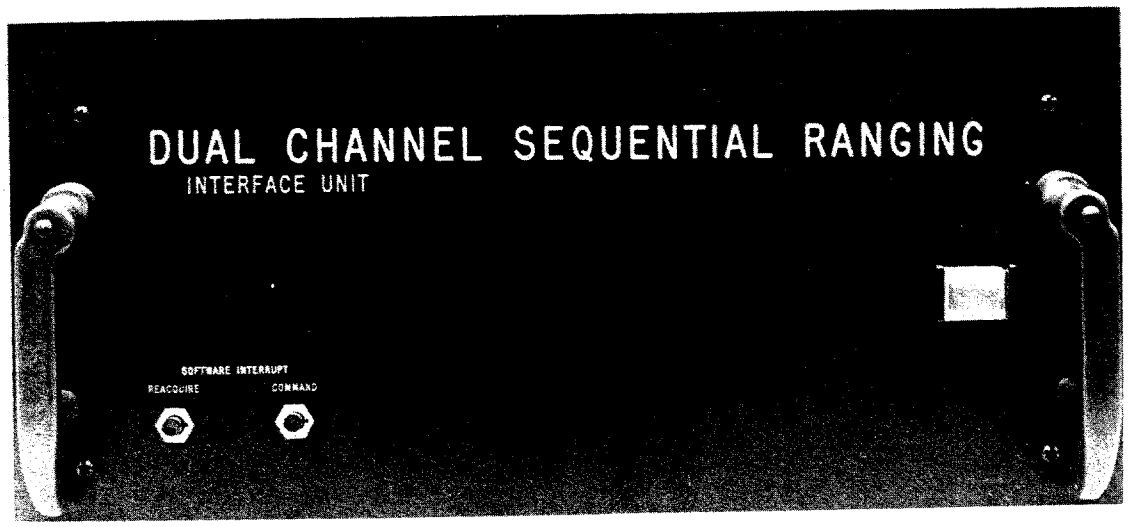

Fig. 31. Interface unit

signal conditioners to convert negative logic signals from the TDH/DIS and high positive voltage signals from the station Frequency and Timing System to TTL levels. The two gray boxes to the left are 5-V power supplies. Finally, note that two fans are used to cool the card cage. The bottom view (Fig. 33) shows the card cage plenum, back plane, and required cables and wiring.

Interconnections to/from the interface unit are apparent in Fig. 34. At the left is the connector which transports the 41 bits of data to the TDH. The FTS2 connector inputs the station's BCD time code. Two Bendix connectors service the Unibus cable to the PDP-11. Four TNC connectors receive timing and sample pulses. The four connectors marked IØ to I3 are spares. Finally, the Mu-II connector attaches the cable from the ranging drawer. External signal characteristics are shown in Table 10.

It should be noted that MECL to TTL and TTL to MECL conversions are done inside the ranging drawer. The high-speed (40-MHz) control portion of the interface is also in the ranging drawer because of the short interconnecting wire lengths required.

VII. System Performance

The Dual-Channel Sequential Ranging System was designed to support the MVM'73 radio science experiments. Experimental objectives included a study of the interplanetary plasma and an investigation of the solar corona.

A radio signal is delayed as it passes through a plasma field. The magnitude of this delay is dependent upon both the field's density and the frequency of the radio wave. Theoretically, the differential delay resulting from two radio signals of different frequencies passing through a common plasma field is proportional to the ratio of those frequencies squared. Thus, if the frequencies are known, measurement of the differential delay allows the unique solution of field density.

MVM'73 was the first space mission to fly a two-frequency (S- and X-band) ranging transponder. It provided a premier opportunity to measure the total columnar electron density as well as the plasma dynamics. Past missions have been restricted to the latter since they carried a single-frequency (S-band) transponder. While the plasma dynamics are scientifically interesting, the inability to determine total columnar electron density represented a potential source of error, preventing the full realization of other experimental objectives.

For example, both the Mariner 1969 and 1971 missions included a relativity experiment, wherein the objective was to differentiate between Einstein's Theory of General Relativity and a modification of that theory proposed by Brans–Dicke.

The experiment consisted of measuring the range over a protracted period in order to establish the spacecraft's orbit with a high degree of confidence. These range measurements continued as the spacecraft passed behind the Sun and the Sun–Earth–probe angle became small, on the order of 1 deg. As the signal's ray path approached the

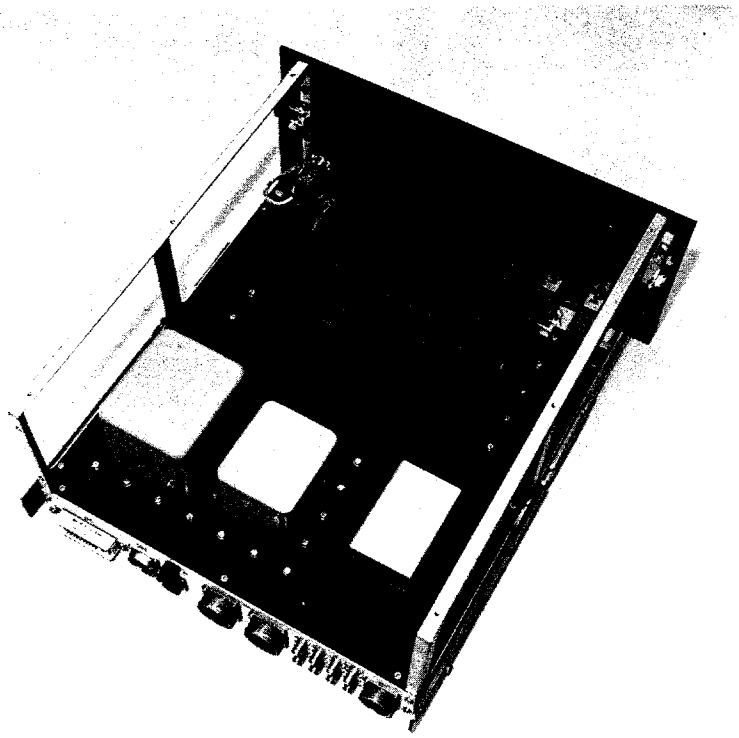

Fig. 32. Interface unit, top view

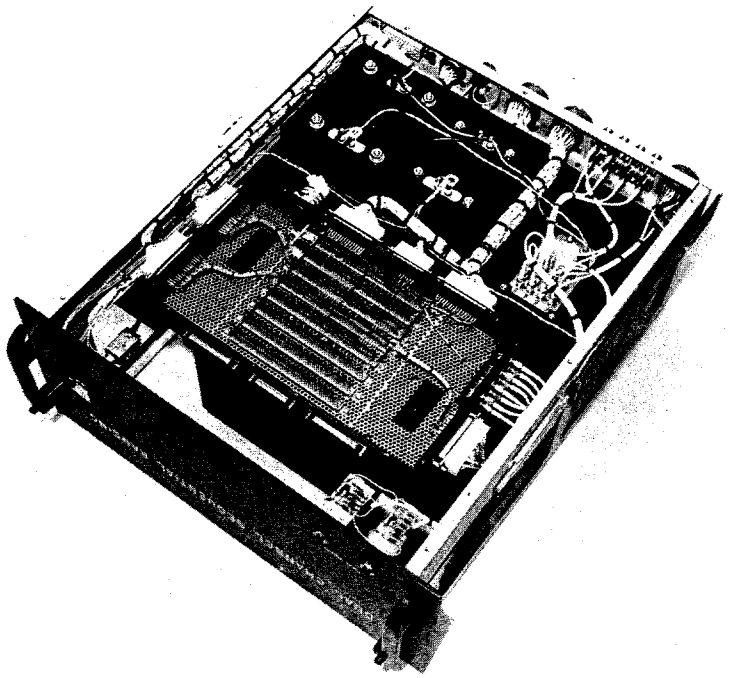

Fig. 33. Interface unit, bottom view

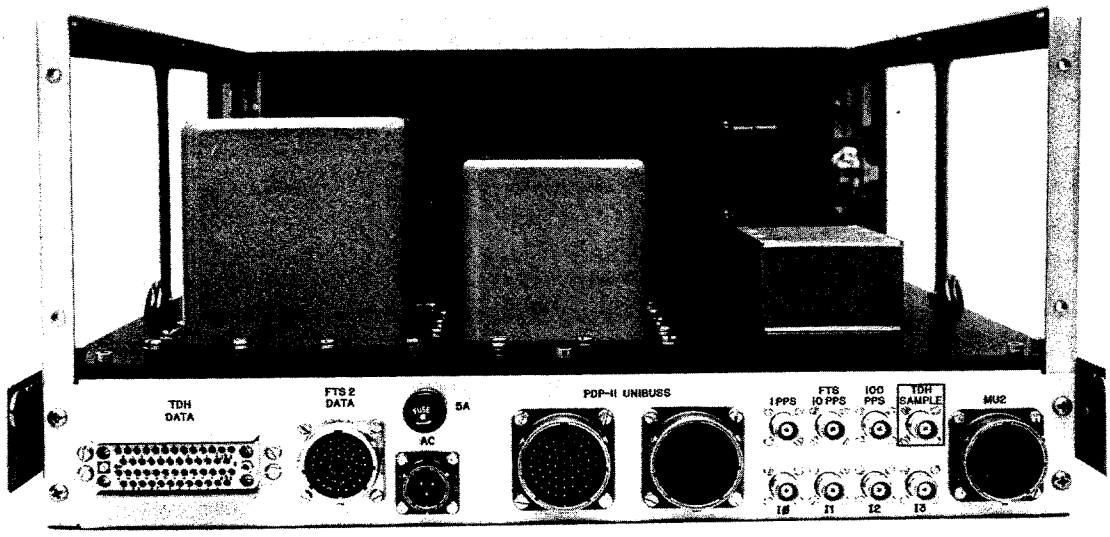

Fig. 34. Interface unit, rear panel

Table 10. Interface drawer: list of required DSN interface signal characteristics

Connector	Description	Remarks
FTS2 data	BCD time code	Positive voltage 0 to 12 V max, 6-V threshold
FTS 1 PPS[a]	1-s time pulse	0 to 12 V max, 6-V threshold
FTS 10 PPS	10 PPS	As above
FTS 100 PPS	100 PPS	As above
TDH sample	Interrupt from TDH	Normally −20 V, sample pulse goes to 0 V for 10 μs
TDH data	41 data lines from the Mu-II to the TDH	0 to −20 V

[a]Pulse per second.

Sun, the intense gravitational field resulted in a warping of the time–space field such as to make the apparent distance appear greater than that predicted by the spacecraft's orbit. This difference is due to the relativistic delay and is the subject of the theories promulgated by Einstein and Brans–Dicke.

Since only 7% separates the delays predicted by the two theories, a high degree of precision is required to differentiate between them. Unfortunately, plasma from the solar corona also introduces a delay in the received signal. While its magnitude is only a small fraction of the relativistic delay, the two are indistinguishable, and the size of the coronal delay is sufficiently large so it cannot be ignored. Thus, models have been formulated which attempt to quantify the coronal delay as a function of Sun–Earth–probe angle. The problem is that these are necessarily steady-state representations which approximate the average expected delay.

On the other hand, the solar corona is actually a highly dynamic body wherein day-to-day variations can reach a substantial fraction of the total coronal delay. Therefore, the modeling technique contains an intrinsic error limiting the accuracy of delay determination and hence the relativity experiment. Clearly, what is needed is an actual, daily measurement, not only to test the corona model but also for the correction of range data around superior conjunction. The dual-channel S-X ranging equipment provides this capability for the first time. But faith in the measurements made by this device must necessarily depend upon a trust in the ranging machine itself. Therefore, the remainder of this section is devoted to presenting and interpreting test data collected over a period of months with the Dual-Channel Sequential Ranging System.

To isolate the components introducing errors, correlation measurements were made in the Telecommunications Development Laboratory (TDL) using a variety of system configurations, including:

(1) The ranging equipment alone.

(2) The ranging equipment connected to a wideband 10-MHz modulator.

(3) The ranging equipment connected to a Block III exciter-receiver subsystem using a wideband zero delay device.

(4) The ranging equipment connected to a Block III exciter-receiver subsystem using an MVM'73 prototype transponder.

Figure 35 pictorially summarizes the four test configurations. Correlation curves are generated by connecting the equipment in one of the four modes. After acquiring the range in a normal manner, the local reference (receiver) coder is shifted by its smallest increment (7.5 or 15 ns, depending upon the reference frequency), and a new phase measurement is made. This process of shift and measure is continued through one complete code cycle. Both the 0- and 90-deg accumulators are integrated over the period of each phase measurement, and this number, representing the degree of correlation, is recorded at the conclusion of the measurement.

When plotted, the two channels represent the familiar code correlation curves discussed in Section III (see Fig. 3). Of course, Fig. 3 represents a theoretical, and hence idealized, correlation function. In actuality, bandpass limitations and nonuniform phase shifts between the fundamental code frequency and its harmonics cause a distortion of the correlation relationship. These nonlinearities can result from imperfections in the ranging equipment itself or from code waveform distortion occurring within the associated DSN exciter and receiver subsystems or within the spacecrafts transponder. Thus, the purpose of these tests was to investigate the contribution of each aforenamed subsystem to total system error.

During the first test, the ranging system transmitter code output was connected, through an attenuator, to its Receiver 1 input. Because of the AGC amplifiers' wideband characteristics (see Section IV), the range code is passed directly through to the analog-to-digital converter and thence to the correlator. To prevent a significant droop in the range code due to the amplifiers' low-frequency cutoff, a 2-MHz code was selected for this test.

Under normal operating conditions, the equipment receives a 10-MHz carrier, phase-modulated with the ranging code. Where, as here, the code is present without the 10 MHz, correlation against a model containing a 10-MHz reference will result in the integral of samples over the interval being zero. Thus, the internal reference must be disabled. Fortunately, this can easily be accomplished via the 10-MHz disable switch conveniently located on the machine's front panel.

Figure 36 summarizes the results of the "baseband" test. Since a 2-MHz code, rather than the usual 500-kHz code, was used for this test, only 32 steps were required to shift its phase through one complete cycle. This resulted in a rather large spacing between points, as will be observed in the quadrature channel, where the individual steps are plotted, and accounts for the roughness of the solid curve.

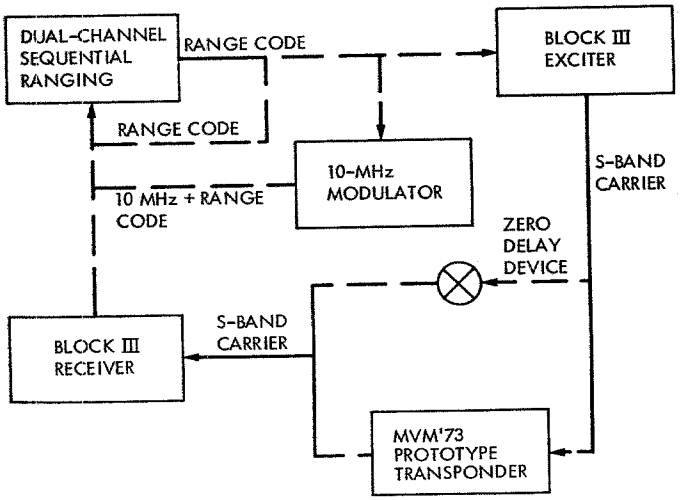

Fig. 35. Ranging test configurations

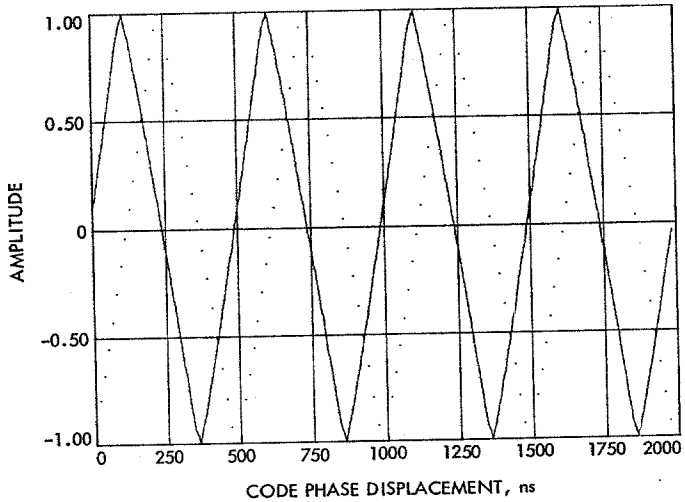

Fig. 36. 2-MHz code correlation characteristics

Note that the spacing of the peak points is different from all others. This is due to the local (receiver) code never being perfectly in phase with the transmitter code because the 15-ns shift available with a 66-MHz reference is too coarse. Thus, the correlator output at this point is less than it would have been had the two codes been in phase. This causes an apparent distortion in the correlation curve which is not actually present in the machine and is one of the reasons why a 132-MHz reference was selected in preference to the 44-MHz alternative available from the Block IV exciter. In the presence of noise, this apparent quantization does not reduce the accuracy of the range measurement.

The intrinsic accuracy of the machine is determined by the linearity of the correlation curve, for it is this relationship between reference and quadrature channels which translates into a phase measurement. Linearity in turn is affected by, among other things, code waveform both within and without the machine. It is useless to generate a perfect transmitter code and an ideal modulator, exciter, and spacecraft transponder if the local code used for correlation purposes is defective, for the result is but the product of the two waveforms, and the poorer will prevail. Thus, when one asks for a 1-ns accuracy in range, he is requesting a phase measurement to better than 0.05%, placing stringent requirements on code waveforms.

As discussed earlier, precision and stability were primary objectives. They were achieved by providing wide bandwidths and careful control over all code waveforms. High-speed logic was used to ensure that transition times were short and symmetry was good.

Comparing the phase calculated using the measured correlation curve (Fig. 36) with that obtained with a perfect square wave (and hence, an ideal correlation function) yields the error curve of Fig. 37. Note the peaks occurring at $\pi/2$ intervals due to the distortion in the correlation function at its maximum and minimum values. As discussed above, this distortion is a product of the quantization and delay experienced in this particular test and would be expected to disappear under normal operating conditions. Thus, the slight difference in amplitude of the error function due to slightly greater distortion in the reference channel would probably disappear also.

The important information presented by Fig. 37 can be summarized as follows: First, the error function is substantially periodic at $\pi/2$ intervals. Second, the error at the actual tracking point ($\pi/4 + n\pi/2$) is virtually nonexistent. Third, the average value over 2π is approximately zero, showing that the machine contains no biases. Fourth, the maximum error experienced was on the order of 2 ns, and this was probably due to quantization.

In order to ascertain the degradation in performance resulting from the interconnection with other equipment, similar tests were run using a more normal operating mode. Figure 38 shows the test results using the 10-MHz wideband modulator (see Fig. 35). This is similar to the previous test in that only the ranging equipment is under test; however, now the input is receiving a 10-MHz phase-modulated carrier as it does when connected with a DSN receiver. Additionally, the typical 500-kHz range code is employed rather than the 2-MHz code.

Observe the high degree of linearity in the sides of the correlation function. The slight rounding at the peaks is due to bandpass restrictions in the modulator; however,

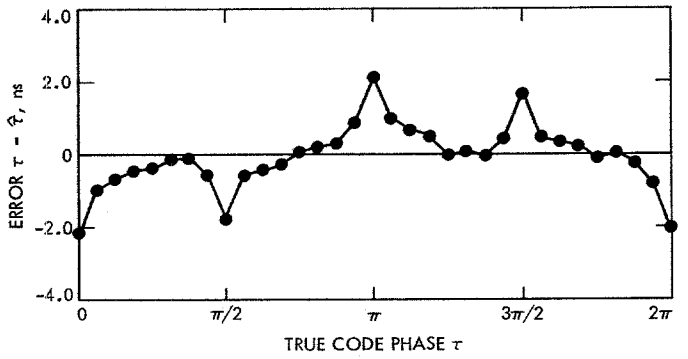

Fig. 37. Baseband test, error in tau estimate, 2-MHz code

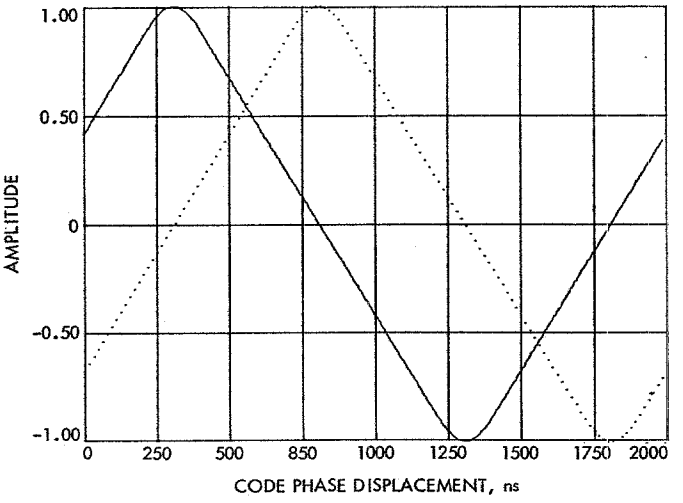

Fig. 38. 500-kHz code correlation using wideband modulator

this distortion is small compared with that which appears using other configurations.

The error function (Fig. 39) is plotted for one half of the period (0 to π). Its maximum amplitude is approximately the same as that measured during the baseband test and occurs at the peaks of the correlation function. At other locations, the error is substantially zero. Figure 39 also includes an apparent negative bias, which results from the method by which code phase is established. In fact, it is part of the system delay, which has not been removed and therefore should be ignored.

Continuing with the system tests, Fig. 40 is a plot of the correlation function when the system is connected to a standard DSIF Block III exciter-receiver subsystem through a zero delay device (see Fig. 35). A zero delay device consists of a wideband crystal mixer, which converts a part of the transmitted energy to the receive frequency and is so named because its throughput time is exceedingly small.

Careful inspection of Fig. 40 reveals some nonlinearity in the correlation function. This is likely due to a nonuniform shift in the phase of the higher-order range code harmonics with respect to the fundamental frequency. Note also the somewhat greater rounding at the peaks of the correlation curves. This is consistent with the nonuniform phase shift theory in that the rounding is indicative of poor high-frequency response in the system. As the response begins to roll off, it becomes uneven, with the result that the phase–frequency characteristic is nonlinear. This in turn results in a disproportionate phase shift in the high-order harmonics and the nonlinear correlation curve.

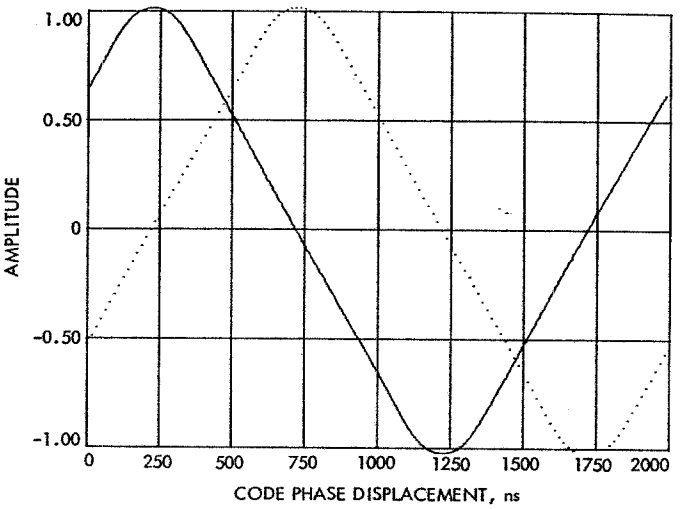

Fig. 40. 500-kHz code correlation characteristics using Block III receiver-exciter/zero delay configuration

The effect is clearly evident in the error curve shown in Fig. 41. Here the amplitude has increased from approximately 2 to more than 7 ns. Note also that the area under the error function is substantially greater than that indicated in Figs. 37 and 39. This results not only from the increased amplitude but also from an increase in the error value at all code phases. The latter results from the

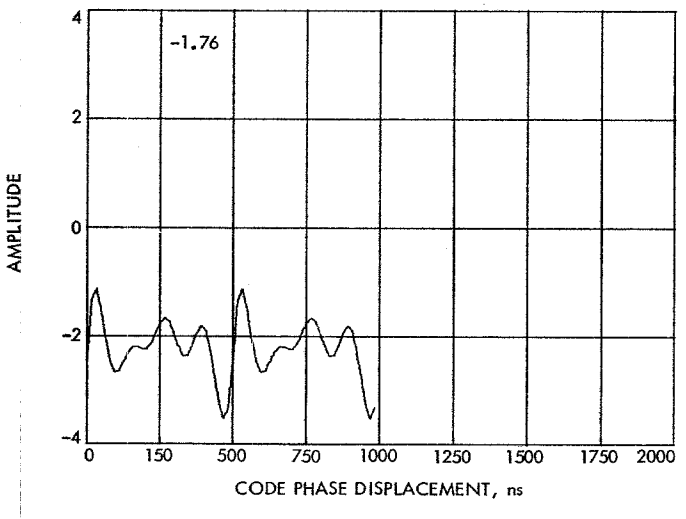

Fig. 39. Error in tau estimate for Fig. 38

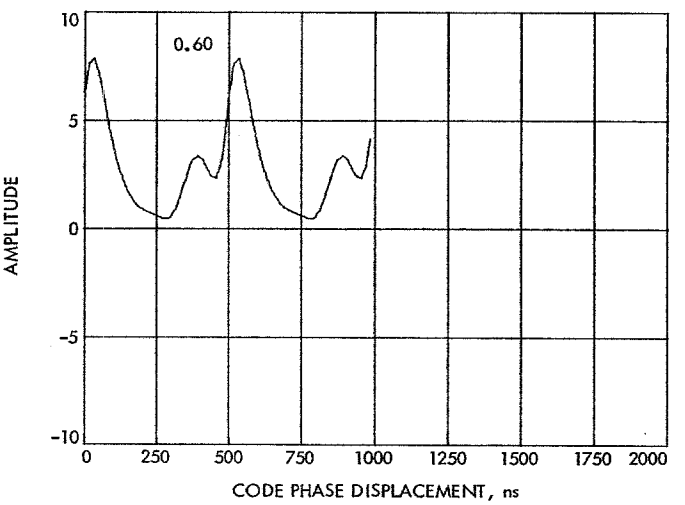

Fig. 41. Error in tau estimate for Fig. 40

nonlinearity in correlation function caused by nonuniform harmonic phase shift.

The final system test results appear in Fig. 42. For this measurement, a Block III exciter was connected to a Block III receiver via the MVM'73 prototype transponder (see Fig. 35). This, then, represents a hardware complement similar to that which would be found in the field during an actual mission track. The tests were run at relatively strong ranging signal levels in order to properly identify the system's characteristics. However, the total uplink power was kept at –120 dBm in order to ensure a noise-limited condition at the spacecraft transponder's limiter and, hence, linear performance (i.e., no material reconstruction of the range code).

Here the degradation is readily apparent by comparing Fig. 42 with any of the preceding correlation curves. Not only has the linearity suffered badly, but also the peak rounding is so great that the curve is becoming nonlinear at the equal power points for the reference and quadrature channels. Moreover, careful inspection reveals that this rounding is asymmetrical with respect to the true peak. Again, this follows from the restricted bandwidth; however, in this case, the spacecraft is the limiting element.

The degradation is clearly evident in the error function (Fig. 43). The amplitude is some eight times greater than that measured in the baseband test. Moreover, the magnitude remains fairly high for all code phases, indicating substantial high-order harmonic phase shift.

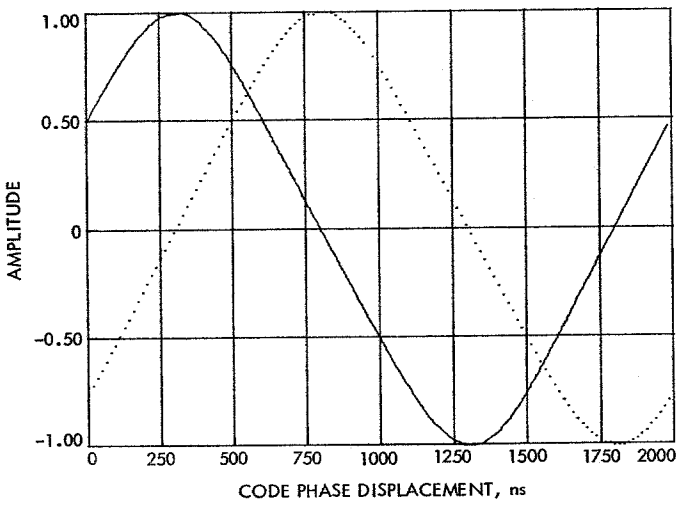

Fig. 42. 500-kHz code correlation characteristics using Block III receiver-exciter/MVM transponder configuration

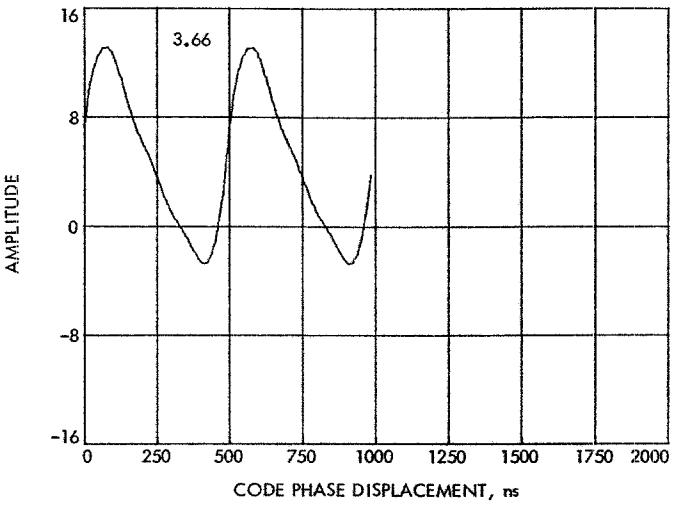

Fig. 43. Error in tau estimate for Fig. 42

Further indication of this shift appears from the asymmetrical character of the error curve, that is, the sharp increase followed by the relatively slow decline. The message here is that the correlation function is not symmetrical with respect to its peak, with the result that the optimal tracking point has been shifted from the normal, $\pi/4$, point.

Thus, one is led to the inescapable conclusion that the spacecraft transponder is the weak link in the total system. A further discussion of this point will be found at the conclusion to this section.

Another aspect of accuracy is stability. By this is meant the system's ability to produce the same result over a period of time where conditions remain relatively unchanged. Stability can be further subdivided into short-term and long-term components.

Short-term stability may be defined as the capacity to remain invariant over periods from 8 to 12 h, such as would be experienced during a single pass. This characteristic is important because the equipment is calibrated only prior to, and occasionally after, each track. Changes occurring during the pass are indistinguishable from the parameter being measured, either range or the change in range due to particle dynamics (DRVID). These variations impose an upper bound on the system's accuracy, and every effort should be made to minimize them.

Long-term stability refers to the system's ability to produce consistent results over a period of months. This is, of course, inexorably related to short-term stability in

many respects, for most of the factors influencing one will also affect the other. Frequently, a situation will arise which prevents a ranging calibration either prior to or following a pass. The reasons can vary from overcommitment of station tracking time to equipment malfunctions which require repair during the normal calibration periods. In a situation such as this, it is desirable to use the calibration of the previous day, or perhaps the previous week if tracks are infrequent. This is possible only if the delay will not have changed during the period, and therefore long-term stability becomes very important.

As noted in an earlier section, considerable care was taken to ensure high stability in the ranging subsystem. To evaluate the success of this effort, the range code was connected, via the wideband 10-MHz modulator, to the ranging unit input (see Fig. 35). This utilized the minimum amount of external equipment necessary to make a meaningful stability measurement.

A normal range acquisition was made, and the machine was allowed to continually remeasure the range at 10-min intervals for more than 16 h. The results are plotted in Fig. 44. During the entire period, the peak-to-peak variation was less than 60 ps (60×10^{-12} s). Moreover, the average variation during the same period was on the order of 30 ps. This corresponds to a change in one-way range of less than 5 mm (1/4 in.) over the 17-h period!

While the relative contributions of the modulator and ranging subsystem are inseparable, the size of the change probably makes further consideration of this matter unnecessary. Unless one is willing to postulate larger drifts in opposite directions for each piece of equipment, which almost perfectly compensate one another, and which situation is highly unlikely, then the only conclusion left is that neither equipment changes significantly.

Long-term stability of the *entire ground system* was evaluated by plotting ranging calibration data obtained at DSS 14 over a period of several months. The particular configuration consisted of the ranging system herein described, a standard Block III exciter, and the new Block IV receiver. The zero delay device at DSS 14 had been improved so as to eliminate the air path and therefore a problem with RF reflections which had been found near the face of the dish.

The calibrations, made at S-band, are plotted in Fig. 45 for a period from February through the middle of June 1974. Because of different path lengths, only data obtained with the 100-kW transmitter was plotted.

Note the remarkable consistency throughout the entire period. The average delay was found to be 3.470 μs and the standard deviation was less than 4 ns (approximately 1/2 m in one-way range). One can discern evidence of cyclic behavior whose period is approximately 25 days. After the system had stabilized following day 70, the day-to-day variation was extremely small compared with the cyclic characteristic. Some effort should be expended to identify the source of this change, whereafter the total variation (peak-to-peak) could probably be reduced to less than 5 ns. If this were done, daily calibration might be found unnecessary.

As a further check on long-term stability, differential group delay was plotted for a somewhat longer period using both the 100- and 20-kW transmitters. The results appear in Fig. 46. Here the data can be separated into three distinct groups. During the early part of the year, just prior to Mercury encounter, there was considerable activity at DSS 14 in readying the new Block IV receiver for the critical period. The effect of this activity is evident as an increased instability in differential delay prior to day 70.

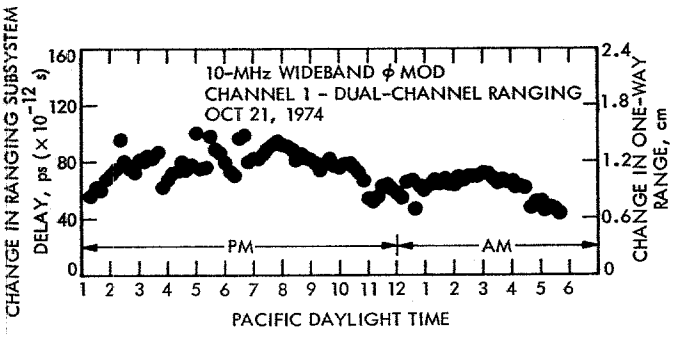

Fig. 44. Ranging subsystem stability test

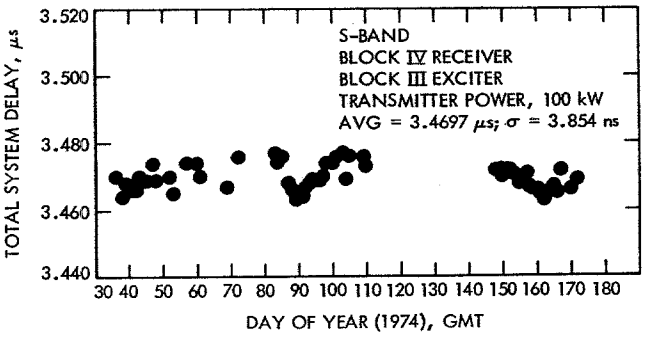

Fig. 45. Mu-II ranging zero delay calibrations at DSS 14

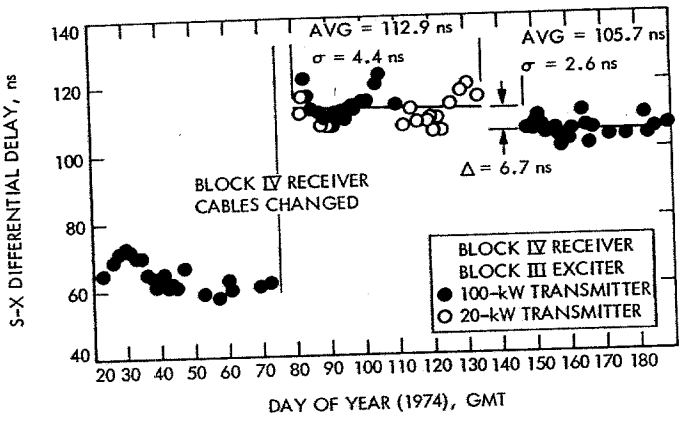

Fig. 46. Mu-II ranging zero delay calibrations, S-X differential delay at DSS 14

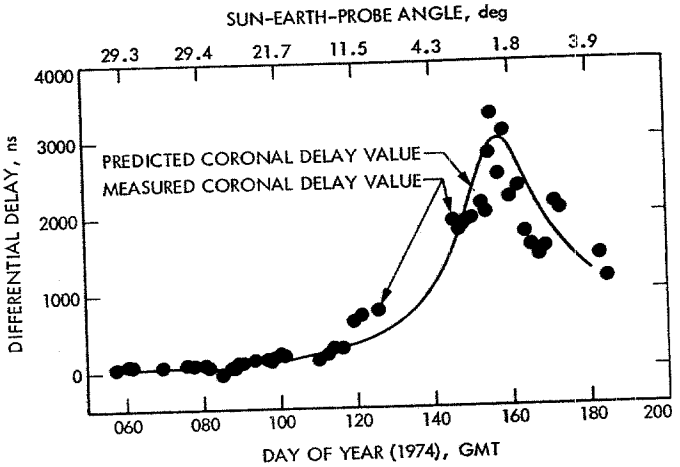

Fig. 47. Mariner 10 S-X differential range, DSS 14

On or about day 75, cables traversing the elevation bearing were replaced, resulting in a substantial change in differential delay. Thereafter, the day-to-day variation became smaller and the cyclic behavior more evident. From day 80 through day 135, the average delay diminished by only 1 ns, although the periodic signature resulted in a standard deviation of about 4.5 ns.

The station was inactivated for a time following day 135. During this period, certain unidentified changes took place causing the differential delay to decrease by 6.7 ns. This reconfiguration also appears to have had a stabilizing effect in that the average delay remained unchanged during the following 1-1/2 months. Moreover, the cyclic variation appears increased in frequency and reduced in amplitude. Thus, careful scrutiny of the alterations made during this period may provide a clue as to its cause.

The conclusion reached from this compendium of information is that the entire ground system exhibits fairly stable behavior over substantial periods of time, particularly if left undisturbed. Further work should be undertaken to identify the source of the cyclic behavior.

In the final analysis, the test of any system is in the utility of information which it produces. As noted in the introduction to this section, one limitation on the accuracy of relativity experiments has been the absence of a dynamic corona model. Obviously, the best model is obtained from actual measurements made through the time near superior conjunction.

The two-frequency capability of this system provided a unique opportunity to measure not only the dynamics but also absolute coronal delay. The effect of the solar corona upon group delay will be found in Fig. 47 (presented through the courtesy of T. Howard of Stanford University, team leader of Mariner 10 Radio Science Experiments).

No attempt will be made to interpret this data, which is far beyond the purpose or scope of this presentation. Suffice it to say that the graph amply demonstrates the system's ability to resolve not only the magnitude of delay but also its day-to-day variation. Theoretical computations have confirmed the correctness of the data contained in the figure.

One final measurement deserves mention. On day 171, approximately 2 weeks after superior conjunction, the ranging equipment was configured to provide rapid multiple acquisitions. Only three range code components were employed which were sufficient to resolve the differential delay resulting from the solar corona. Some 25 points were obtained over a 4-h period, approximately one point every 10 min. The purpose here was to demonstrate the machine's ability to resolve high frequency fluctuations in coronal density which caused

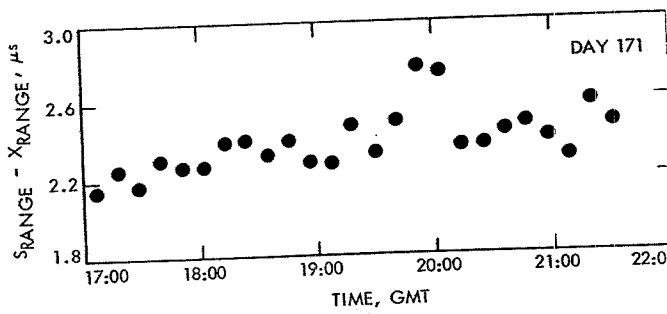

Fig. 48. High-frequency coronal fluctuations as shown by differenced S-X ranging

changes in differential group delay. The data is plotted in Fig. 48.

The predicted signal level available on day 171 was such that the expected variation in delay due to noise was small compared with the changes actually observed. Again, interpretation of this data is not within the purpose of this work and the data is included simply to show the capabilities of the equipment.

VIII. Conclusions

All this leaves the question as to what can and should be done to improve the entire system's accuracy. The foregoing evidence suggests several conclusions.

First, the ranging equipment, standing by itself, appears quite adequate. The tests have shown that improvements in this subsystem would not materially affect the overall system performance.

Second, accuracy and stability with the Block III exciter-receiver subsystem are fairly good. While bandwidth limitations are clearly present and some nonlinearity exists due to nonuniform harmonic phase shift, these distortions do not appear to have a substantial effect on stability. Work should be undertaken to eliminate the nonuniform phase shifts which probably occur within the exciter. Because it was unavailable for these tests, no conclusions are reached with respect to performance with the Block IV equipment.

Third, the dominant source of error is within the spacecraft transponder. It follows that the maximum yield in terms of performance improvement for manpower invested would be obtained by concentrating on this unit.

If one accepts these conclusions as true, then the only reasonable course lies in spacecraft transponder development. To attempt alternate "fixes" with respect to the ground equipment is to treat symptoms and not causes, and it will prove both expensive and relatively unproductive in the long term. The underlying problem is one of bandwidth. It is too narrow. A limited bandwidth may have had merit in the days of 26-m (85-ft) antennas, 10-kW ground transmitters, and pseudo-noise ranging systems. Today there are 64-m (210-ft) antennas, 100-kW transmitters, and sequential ranging equipment, and the relevant considerations have changed accordingly. Now the question is no longer whether we can measure range at all but rather how accurately we can measure it. Whereas a 20-m accuracy was sufficient but a few years ago, now uncertainties greater than 5 m can invalidate whole experiments. Tomorrow the requirements will press to a few centimeters.

Viewed from this perspective, the answer seems clear: widen the bandwidth. Increasing the present 1.5-MHz transponder bandwidth to 12 MHz would result in less than a 10-dB loss in signal-to-noise ratio. To produce the same uncertainty in phase, the already short integration time would have to be increased by a factor of 8, provided that the code frequency remained constant. However, if channel bandwidth limitations imposed by the Federal Communications Commission permitted, the code frequency could, and should, be increased.

Remembering the equation for phase uncertainty (Ref. 1)

$$\sigma = 2T\sqrt{\frac{N_0}{2st}}$$

where T is the code bit period, it is obvious that increasing the code frequency to 2 MHz will result in the same phase noise without changing integration time! But the higher code frequency will have resulted in improved accuracy for the reason that time, and hence range, has been quantized into smaller units. Thus, the answer is not one of patching an existing and outmoded system but rather reevaluation and change of that system in light of today's experimental results and tomorrow's experimental requirements.

References

1. Goldstein, R. M., "Ranging With Sequential Components," *Space Programs Summary* 37-52, Vol. II, pp. 46–49, Jet Propulsion Laboratory, Pasadena, Calif., July 31, 1968.
2. Martin, W. L., "Information Systems: A Binary-Coded Sequential Acquisition Ranging System," *Space Programs Summary* 37-57, Vol. II, pp. 72–81, Jet Propulsion Laboratory, Pasadena, Calif., May 31, 1969.

3. Martin, W. L., "Information Systems: Performance of the Binary-Coded Sequential Acquisition Ranging System of DSS-14," *Space Programs Summary 37-62*, Vol. II, pp. 55–61, Jet Propulsion Laboratory, Pasadena, Calif., March 31, 1970.

4. MacDoran, P. F., "A First-Principles Derivation of the Differenced Range Versus Integrated Doppler (DRVID) Charged Particle Calibration Method," *Space Programs Summary 37-62*, Vol. II, pp. 28–34, Jet Propulsion Laboratory, Pasadena, Calif., March 31, 1970.

5. MacDoran, P. F., and Martin, W. L., "DRVID Charged-Particle Measurement With a Binary-Coded Sequential Acquisition Ranging System," *Space Programs Summary 37-62*, Vol. II, pp. 34–41, Jet Propulsion Pasadena, Calif., March 31, 1970.

6. Molinder, J., "Digital Telemetry and Command: Mean-Square Error and Bias of Phase Estimator for JPL Sequential Ranging System," *Space Programs Summary 37-64*, Vol. II, pp. 27–28, Jet Propulsion Laboratory, Pasadena, Calif., August 31, 1970.

7. *DSN System Requirements, Detailed Interface Design, TRK 2-8, DSN Tracking System Interfaces, 26 Meter and 64 Meter Standard Station HSD Interfaces,* Document 820-13, Rev. A, Jet Propulsion Laboratory, Pasadena, Calif. (JPL internal document); also: R. E. Edelson, *S/X R&D Ranging Data on the HSDL,* Memo 3396-72-166, Jet Propulsion Laboratory, Pasadena, Calif., June 20, 1972 (JPL internal document).

Appendix A
Mu-II Operating Instructions

I. Power

(1) To power up:

(a) Computer HALT/ENABLE switch in HALT.

(b) Press SYSTEM POWER switch located on topmost chassis.

(2) To power down:

(a) Computer HALT/ENABLE in HALT.

(b) Press computer START switch.

(c) Press SYSTEM POWER button.

II. Loading

Loading should not normally be required. If for some reason program integrity is suspect, follow the loading instructions in the Addendum.

III. Program Start

The following procedure starts the program. The program start address is 600_8.

(1) Place 600_8 in the SWITCH REGISTER (switches 8 and 7 up, all the rest down).

(2) Press LOAD ADDR (load address).

(3) 600_8 should now appear in the ADDRESS REGISTER lights.

(4) HALT/ENABLE switch to ENABLE.

(5) Press START.

(6) The computer should now type "MU2V3A1 READY***". This indicates that the program is ready to run.

IV. Parameter Entry

If the computer has just been reloaded, all parameters must be entered. Otherwise, the computer will "remember" the last parameters used. This is true even if the machine has been powered down. Parameters are entered via a technique known as "Tutorial Input".

A. Tutorial Input

There are basically two parts to an input using the Tutorial technique. First, a command is typed to designate the type of entry; second, the parameter or parameters are entered. The Mu-II commands are listed in Table A-1. The Mu-II parameters are listed in Table A-2.

The operator first notifies the PDP-11/20 that command input is desired by pressing the COMMAND interrupt button. When the program scheduler finds time for the operator, the computer responds by typing a pound sign (#). The operator may now type an input line terminated by a carriage return. The first field to be typed is a command followed by a slash (/). If the command is acceptable, the software looks to see if anything else is in the input line. If more characters are typed, they are used. If not, the operator is queried by a specific message for the appropriate parameter of the now-active command. This is true every time a field containing a command or parameter has been used. If more characters are in the input line, they are processed; if not, and more parameters are required, the operator is queried.

The field delimiters used are a slash between a command and parameters and commas between multiple parameters. Note that the whole line is used. This allows commands to be entered contiguously.

By way of demonstration, the following are equivalent command and parameter entries (computer printouts are underlined):

Example 1

#A/↵
TOF:↵
#1200↵
SYN FREQ:↵
#44.01234↵
T1:↵
#20↵
T2:↵
#20↵
T3:↵
#20↵

TC: ↵
#12 ↵
C1: ↵
#4 ↵
C2: ↵
#19 ↵
CN: ↵
#3 ↵
MODE: ↵
#- ↵

Example 2

#A/1200,44.01234,20,20,20,12,4,19,3,- ↵

Example 3

#A/1200,44.01234,20,20,20 ↵
TC: ↵
#12,4,19 ↵
CN: ↵
#3,- ↵

Example 1 shows how the operator can be lead through the input parameters. In Example 2, an experienced operator has entered all parameters without software prompting. The operator in Example 3, after losing his place, has let the computer request the remaining required numbers.

Multiple commands may be entered on a single line. In order to change the mode and number of components, for instance, one could enter

#M/124,C/3,10,50 ↵

or equivalently,

#M/124,C/ ↵
C1: ↵
#3,10,50 ↵

An asterisk (*) may be entered for a parameter. This causes the parameter to retain its previous value.

B. Line Editing

The following control characters can be used to correct or erase input errors if such errors are caught before the carriage return is typed. (A control character is one where the control key is held while the character key is pressed.)

(1) *Deleting a character.* C^c (Control C) may be used to delete the preceding character. It may be used more than once. The computer responds with ← ← to indicate a character deletion. For example,

#B/← ←A/ ↵

is the same as

#A/ ↵

(2) *Deleting a line.* E^c causes the current line to be deleted. The computer responds with a carriage return and → on the new line. For example,

#M/27KA(E^c)
⇉M/275 ↵

(3) *Cancelling the input.* R^c causes the whole input sequence to be cancelled. The computer returns to normal processing.

C. Errors and Time-Out Messages

(1) *Time out.* Because of timing limitations, a maximum of 15 s is allowed to elapse between any two input characters. If the interval exceeds 15 s, the computer types

TIME OUT

and exits the command routine. It is necessary to press the COMMAND interrupt again and redo the entire entry sequence.

(2) *Input error.* This is a generalized error for mistakes such as entering a decimal point in a number where an integer is expected, etc. The recovery is to redo the entire input sequence.

(3) *No such command.* The command is unacceptable. Redo the entire input sequence.

D. Special Parameter Entries

(1) *Time entries.* Time-of-Flight (TOF) and all integration times (T1,T2,T3,TC) may be entered as either seconds or hour-minute-seconds. A colon (:) is used to distinguish between the two. For example,

#TF/180

and

#TF/3:00

are identical entries for time of flight. Legal formats are seconds, HH:MM:SS, H:MM:SS, MM:SS, or M:SS, where H is an hours digit, M is a minutes digit, and S is a seconds digit.

The real-time entries TX/ and TZ/ (to be discussed later) can be entered as HH:MM:SS, or HH:MM.

(2) *Mode.* MODE is a special parameter which configures the ranging system. There are two ways to enter an option into this parameter. One way is simply to type a sequence of numbers from 0 to 9, each digit describing a particular option. For instance, to configure the system with options 1, 3, and 5, you may type the single digit number 135 or 153 or 315, i.e., in any order. Entering a hyphen for this parameter causes no options to be selected. The second way to enter a parameter for MODE is to set the appropriate switch on the SWITCH REGISTER to one, that is, up, and type S as the MODE parameter. For instance, to enter 1, 5, and 3, set switches 1, 5, and 3 up, and type S for the parameter entry. Options 10 through 15 can only be entered through the SWITCH REGISTER. Special entries for the MODE also control termination of the current range sequence and reinitialization of the program. To reinitialize the program in such a way as to empty the TDH buffer, enter FIN for MODE; for instance, #M/FIN. The program will terminate when the buffer empties or after 3 min, whichever comes first. To reinitialize the program immediately without emptying the buffer, enter STOP for MODE, #M/STOP. The various options are shown in Table A-3.

(3) *Teletype control.* Data output to the teletype can be turned off by

#Y/OFF)

It can be turned back on by

#Y/ON)

Error messages and headers will still be typed. Command inputs are unaffected. Only the data can be shut off.

V. Acquisitions and Reacquisitions

After initialization and parameter entry, the program waits for the operator to start the first acquisition. He has three means to accomplish this. First he can simply press REACQUIRE, second he can enter a requested TO, or third he can enter a time to start transmission.

TØ entry is accomplished by use of the TZ command. The following are valid:

#TZ/22:13)

or

#TZ/)

TØ(HHMM):)

#22:13)

There are two possible messages after a TZ/ command. The first is

TØ TOO SOON

This implies that not enough time is available for an RTLT, calibrate, and sync to meet the requested TØ. The entry is ignored. The second possible type-out is

NEXT DAY

In this case, the requested TØ is earlier than the current time, so the program assumes that the time is for the next GMT day.

A particular transmit time can be requested by the TX/ entry, e.g.,

#TX/20:56)

As for the TO entry, if the input time is before the current time, the next GMT day is assumed, and NEXT DAY is typed.

After the first acquisition, the computer automatically reacquires the range code after each set of "CN" DRVID measurements. Whenever a transmit sequence starts, the program prints

XMIT****HHMMSS

This is the start transmit time for an acquisition. At this time, all parameters are fixed for that acquisition, and the automatic reacquisition time is computed. It is important to note that the program remembers only one transmit acquisition ahead. That is, if an automatic acquisition is waiting and a requested TØ is input, that TØ request will replace the automatic reacquisition. Similarly, if the reacquisition button is pushed prior to the start transmit time of a requested TØ acquisition, the requested TØ acquisition will be replaced by the push button acquisition.

VI. System Errors

(1) *Power failsafe.* If the ac power fails and returns, the computer will type

POWER FAILSAFE*

and ring an alarm. Pressing the COMMAND button at this time restarts the program. Even though the ranging sequence is destroyed, all parameters are preserved.

(2) *Trap errors.* If the computer should type

**TRAP ERROR #

a major computer or hardware error has occurred. The error can be caused by destroyed core memory contents or a hardware failure. The recovery procedure is as follows:

(a) Put the computer HALT/ENABLE in HALT.

(b) Attempt to reach the cognizant system engineer.

(c) If unable, press START and follow Section III to restart the program.

(d) If unable, do a reload, as shown in the Addendum.

Addendum

A. Reloading the Mu-II Program

(1) Computer HALT/ENABLE (H/E) to HALT.

(2) Place ABSOLUTE LOADER in reader with punched (not sprocket only) leader under head (reader switch to START).

(3) Put 173000 in switch register (SWR).

(4) Press load address (LOAD ADDR).

(5) Enable H/E switch.

(6) Press START.

(7) When tape stops, H/E to HALT.

(8) MATH PACKAGE to reader (sprocket hole only leader).

(9) 37500_8 in SWR.

(10) Press LOAD ADDR.

(11) H/E to ENABLE.

(12) Press START.

(13) When tape stops, repeat steps 7–12 with "program" tape. Now program is loaded.

B. Typeout Format Description

Figure A-1 contains a typical printout for a "pre-cal" on the Mu-II. Note that the first seven lines are an operator input sequence. After parameter entry, the operator initiated an acquisition by pushing the REACQUIRE button. The transmit time for the acquisition is shown as line 8. The time is read as 07 h, 21 min, and 56 s, GMT. At the start of the RECEIVE sequence, the day-of-year is printed. In this case, it is day 90, again GMT. Next, the 10-MHz phase relationship between the IF carrier and the station reference is printed as the angle's sine and cosine for S- and X-band.

The MODE line shows a binary representation of the options selected. The bits are numbered 0 through 15 from right to left. If, for instance, option 5 were selected, the printout would be

MODE: 0 000 000 000 100 000

Following the MODE line is the TO time, in this case 07:22:22. This is the time to which the range point is referenced.

Ranging data is output in blocks of two lines as follows. On the first line, reading left to right, is the time tag, S-band in-phase correlation voltage, S-band quadrature voltage, S-band DRVID, and S-band PR/N_0. On line two, the sequence is: block number, code component, X-band in-phase correlation voltage, X-band quadrature voltage, X-band DRVID, and X-band PR/N_0.

After the range acquisition is complete, the range number is printed in the form:

***S-RANGE X-RANGE

As for DRVID, the range values are in microseconds.

The TDH overflow indicator appears on the printout because the TDH was not connected to the Mu-II, and therefore data was not removed from the output buffer. Hence, the buffer overflowed.

For more information on the formats, see Section V of the text.

Table A-1. Commands

Command	Parameter entered
A/	TOF,SYN FREQ, T1,T2,T3,TC, C1,C2,CN, MODE
TF/	TOF
C/	C1,C2,CN
C1/	C1
C2/	C2
CN/	CN
T/	T1,T2,T3,TC
T1/	T1
T2/	T2
T3/	T3
TC/	TC
S/	SYN FREQ
M/	MODE
TZ/	Request T0 time
TX/	Start transmit time
M/FIN	Play out TDH buffer or wait 3 min, then reinitialize program
M/STOP	Reinitialize program
Y/	Typewriter data output ON or OFF

Table A-2. Parameters

TOF	Time of flight[a]
SYN FREQ	Exciter synthesizer frequency[b]
T1	First computer integration time[a]
T2	Second through C2 component integration time[a]
T3	Post-acquisition C1 integration time[a]
TC	Calibrate integration time[a]
C1	First component
C2	Last component
CN	Number of post-acquisition DRVIDs
MODE	See Table A-3
TRANSMIT TIME	Time to start transmission[c]
REQUEST TØ TIME	Time to start receiving an acquisition[c] (TX time is automatically calculated.)

[a]These parameters may be entered in seconds, HH:MM:SS, H:MM:SS, MM:SS, or M:SS.

[b]SYN FREQ is entered as a floating point number, i.e., 44.2635.

[c]Enter as HH:MM:SS or HH:MM.

Table A-3. Mode options

Options	Function
-	(Hyphen)—no options selected
0	Code servo disable
1	Disable DRVID during acquisition
2	Invert S-band code
3	Invert X-band code
4	Reacquire without resynchronization
5	(Reserved)
6	Set S-band power meter bandwidth for BLOCK III
7	Set X-band power meter bandwidth for BLOCK III
8	Not assigned
9[a]	No transmit code during calibration
10[a]	Calibrate on Q channels
11[a]	Track DRVID at peak instead of equal-power point
12[a]	Substitute voltages for SIN, COS
13[a]	Post-acquisition S curve
14[a]	Reverse calibrate SIN, COS internally (90-deg phase shift)
15[a]	Set COS = 1, SIN = 0 internally (use 15 and 14 for COS = 0, SIN = 1)[b]

[a]These are maintenance options.

[b]TC must be zero for this option.

```
MU2V3A1 READY
# A/
TOF:
# 0
CANCEL INPUT
# A/0,44.,16,16,16,16,4,8,2,-

# S/43.97416

XMIT****072156


****DOY 090*****
S SIN:    0.52317D 00    COS:   0.85223D 00
X SIN:   -0.67443D 00    COS: -0.73834D 00


MODE:    0 000 000 000 000 000

T0**072222

072236     -2.14936D 05 -8.31218D 05 -5.84806D-01   56.7D 00
   1     4 -2.36805D 05 -3.73866D 05 -6.73258D-01   51.5D 00

072252     -9.74433D 05 -1.19638D 04 -5.84806D-01   56.0D 00
   2     5 -5.99061D 05 -5.42566D 03 -6.73258D-01   51.4D 00

072308      9.66404D 05  6.76868D 02 -6.11093D-03   55.8D 00
   3     6  5.92319D 05 -2.19591D 03 -3.17279D-03   51.3D 00

072324      9.65737D 05  1.04364D 02 -6.39806D-03   55.8D 00
   4     7  5.89573D 05 -2.81089D 03 -3.68287D-03   51.3D 00

072340      9.65672D 05 -9.90606D 01 -6.50024D-03   55.8D 00
   5     8  5.88052D 05 -3.19056D 03 -3.99884D-03   51.3D 00
***   3.29626128271D 00   3.20780939319D 00
TDH OVERFLOW

072356      5.03433D 05 -4.99018D 05 -5.38220D-03   56.2D 00
   6     4  3.03439D 05 -3.04009D 05 -1.60867D-03   51.5D 00

072412      5.02650D 05 -4.98373D 05 -5.41408D-03   56.2D 00
   7     4  3.02644D 05 -3.03634D 05 -1.77732D-03   51.4D 00
XMIT****072414
```

Fig. A-1. Typical "precal" printout

Appendix B*

"Tutorial Input"—Standardizing the Computer/Human Interface

A. I. Zygielbaum
Communications Systems Research Section

This article describes a new technique for implementing a human/computer interface for computer-based subsystems for the DSN. Known as "tutorial input," this technique provides convenient short input procedures for the experienced operator and a helping hand for the novice. From the programmer's viewpoint, the technique is implemented in a compact, modular, easily modified table-driven structure. The technique has been successfully used through two generations of R&D ranging machines.

I. Motivation

Though much time is spent by programmers in producing efficient, clean, and ego-pleasing code, very little time is spent in developing an efficient, reliable human/computer interface. From an operational standpoint, this interface is the most important and least understood in DSN subsystem programming. With a view toward minimizing operator error and increasing subsystem efficiency, this article will present the technique for human/computer communication successfully used in two generations of R&D ranging systems.

In a typical subsystem program, the operator must provide operating parameters, critical times and perhaps limits to the software. Two interface techniques are generally used. With the first technique the operator may be queried on an input-by-input basis. For instance,[1]

ENTER T1: ↵
26
ENTER T2: ↵
15
ENTER T3: ↵
15

A second technique is the preset format wherein the operator must enter numbers in accordance with some specified template. An analogous entry to the one given above could be

*/26/15/15$

The first technique has the advantage that a format need not be memorized or followed. Given the parameters, an operator just follows directions. The disadvantage is that at the 10 characters per second of the usual tele-

[1]Computer typeouts are underlined.

*Reprinted from JPL Deep Space Network Progress Report 42-23, October 15, 1974.

typewriter, the questions sometimes waste an unacceptable amount of time. The second technique is clearly faster but requires a thorough a priori knowledge of the format. This leads to increased training time and a greater chance of operator error from misplaced fields.

Overriding the problems and tradeoffs inherent in these techniques is the multitude of programs involved in a typical DSN operation. An operator may have to communicate with a variety of programs, each designed with a different input philosophy and format. This situation naturally leads to an increased probability of human error.

In a real-time mission environment, an incorrect program entry can be just as disastrous as an equipment malfunction. A specific example occurred to ranging during the Mariner Mars 1971 (MM'71) mission. The software for command and telemetry running on the XDS 920 Telemetry and Command Processors (TCPs) used a dollar sign for a line terminator, whereas the software for the Mu ranging system used a carriage return. On at least two occasions, range data were lost because the operator typed a dollar sign at the end of an input line and walked away thinking his task complete. The ranging software waited the time-out period and then cancelled the necessary input. A simple modification to the software to allow it to recognize both a dollar sign and carriage return as a terminator saved a significant amount of data.

II. Proposal

Usually the subsystem operator is treated as a button-pusher who is taught to run specific software and devices. This view was believed incorrect, and software to support both the Mu-I and Mu-II ranging systems was developed with the direct cooperation and interaction of the operators. The input routine devised in this effort has been shown to be easy to learn as well as easy to operate. It uses a table-driven structure which makes it highly visible to the programmer who must implement it and relatively easy to modify and enlarge. This algorithm, known as "tutorial input," is presented here.

III. Tutorial Input as Viewed by an Operator

There are basically two parts to an input using the "tutorial" technique. First, a command is typed to designate the type of entry; second, the parameter or parameters are entered. For clarity, consider the commands used with the Mu-II system given in Table 1. (Parameter definitions are given in Table 2 for completeness.)

To input commands and data, the operator first notifies the PDP 11/20 that command input is desired by pressing an interrupt button (this could be a breakpoint on the XDS 9-series machines). When the machine responds with a pound sign (#) he types an input line terminated with a carriage return. The first field is a command followed by a slash (/). If the command is acceptable, the software looks to see if anything else is in the input line. If more characters have been typed, they are used. If not, the operator is queried by a specific message for the appropriate parameter of the now-active command. This is true every time a field containing a command or parameter has been used. If more characters are in the input line, they are processed; if not, and more parameters are required, the operator is queried.

The field delimiters used are a slash between a command and parameters and commas between multiple parameters. Note that the whole line is used. This allows commands to be entered contiguously.

The following are equivalent ways to initialize all ranging parameters:

Example 1:

#A/ ↵
TOF: ↵
#1200 ↵
SYN FREQ: ↵
44.01234 ↵
T1,T2,T3,TC: ↵
20,20,20,12 ↵
C1,C2,CN: ↵
4,19,3 ↵
MODE: ↵
- ↵

Example 2:

#A/1200,44.01234,20,20,20,12,4,19,3,- ↵

Example 3:

#A/1200,44.01234,20,20,20 ↵
TC: ↵
#12,4,19 ↵
CN: ↵
#3,- ↵

Example 1 shows how the operator can be led through the input parameters. In Example 2, an experienced operator has entered all parameters without software prompting. The operator in example 3, after losing his place, has let the computer request the remaining required numbers.

Multiple commands may be entered on a single line. In order to change the mode and number of components, for instance, one could enter

#M/124,C/3,10,50 ↵

or

#M/124,C/ ↵
C1,C2,CN: ↵
#3,*,50 ↵

The asterisk (*) entered for C2 causes the previous value of C2 to remain unchanged.

A further provision to ease the operator's task is error correction. Input cancellation (control R—R^c) results in immediately exiting the input routine. Character deletion (C^c) causes the program to type ← and results in the deletion of the last character entered into the string. Character deletion may be used more than once, e.g., to delete the last three characters so that they can be retyped. Line deletion (E^c) deletes the line, upspaces, types →, and allows the whole line to be retyped. Error correction can also be accomplished by use of the command to change a particular parameter.

IV. Tutorial Input as Viewed by a Programmer

Although written in machine language for a PDP-11/20, via the SAPDP Xerox Sigma 5 cross assembler (Ref. 1) the routine is amenable to coding in another machine language or in a higher level language such as BASIC or FORTRAN. In this discussion the interaction of the input routine with other real-time processors will not be covered. The Mu-II software required interfaces to a teletype output routine and to a real-time scheduler. These topics will be documented in a forthcoming article on the Mu-II system software.

Though perhaps not meeting the letter of structured programming, which is difficult, if not impossible, in a real-time environment, tutorial input does realize all advantages normally claimed for structured programming. Through the use of a table-driven technique, the input sequencing and programming is straightforward, easily modified, and simply documented.

The technique involves two tables. The first table is the command list. Each entry in the list takes three words in the Mu-II realization. There is one entry for each command. The first word has the two characters of the command, e.g., "A/" or "TF," the second a pointer to a word in the second table, and the third word a number equal to the number of parameters to be entered with the particular command.

The second table is the parameter list. Each entry in this list takes four words. There is one entry for each parameter. The first word of the entry contains the number of characters in the message associated with each parameter, while the second contains the message location. (The messages are the queries shown earlier, e.g., TOF: ↵.) The third word gives the location of the decoding subroutine (integer, floating point, etc.) to convert the parameter's ASCII character string to binary. The fourth and final word contains the location of the destination for the binary number. Figure 1 contains a listing of the two tables in the Mu-II software.

The algorithm which interprets these tables is described structurally in Fig. 2 and in a detailed flow chart in Fig. 3.

As an example of the algorithm, let us consider that a command "T/" has been input and follow the algorithm operation. Scanning the command list (Fig. 1), a match is found (line 334) giving the parameter table location as SCT1 and the number of parameters to be input as four. The program looks to see if there are any more characters in the input string. If not, the message TMSG, containing 14 characters, is typed as shown by the SCT1 entry in the parameter list. If input already exists, the message is skipped. In either case, the input parameter is processed by INGR which is the integer decoding subroutine and the result stored in IT1.

Thus far, one parameter has been processed and three more are left. The program proceeds directly to the SCT2 entry in the parameter table and repeats the input process. This continues until all parameters are entered.

Once again the algorithm checks to see if there are more characters in the input stack. If there are none, the routine exits. If there are more, the first field is used to search the command stack as the program assumes that another command is in the input string. The process goes on until an error occurs or until the input line is exhausted.

The input logic flow is readily observable by following the driving tables. The tables are also a simple documentation of the input sequences. The ease with which commands and entries can be modified or deleted is shown by a program change that occurred during the Mariner Venus/Mercury 1973 (MVM'73) mission.

As originally written, an operator could modify any parameter or set of parameters individually except for time of flight (TOF). The only way to change this parameter was through the "enter all parameters" A/ command. As the mission proceeded, the TOF changed by several seconds each day. It was obvious that going through the entire initialization sequence to change TOF was a waste of time. The decision was made to add the TF/ command so that TOF could be changed individually.

Because of the table-driven structure, only three cells were actually needed. These were, from Fig. 1, lines 346–348:

"TF"	Command
SCTOF	Parameter Table Pointer
1	Number of parameters to be entered.

This simple modification changed a tedious operation into a trivial one.

V. Summation

Data will continue to be lost due to incompatibilities, indeed contradictions, between input formats in various DSN software systems. This coupled with the trend toward smaller station operational crews, automation, and the continued proliferation of minicomputers in the DSN makes standardization increasingly important. The algorithm presented herein is a candidate to aid in that task.

A final comment, tutorial input has been used in ranging software throughout the MVM'73 mission. It has shown itself to be an easy-to-use as well as an easy-to-learn input technique. The extra time taken to interact with experienced ranging operators during its development has been paid back many fold through simplified training and the low probability of human error. This programming effort clearly shows the value of bringing the system operators into the software design process at a very early stage. Many times the operators were able to point out features which were not helpful and could be discarded as well as request features which would simplify their task. The success of the Mu-II system programming is largely due to this cooperation between the programmer and the system operators.

Reference

1. Erickson, D. E., "The SAPDP Program Set for Sigma 5 Assembly," in *The Deep Space Network Progress Report*, Technical Report 32-1526, Vol. VII, pp. 91–96, Jet Propulsion Laboratory, Pasadena, Calif., Feb. 15, 1972.

Table 1. Mu-II commands

Command	Parameter to be entered
A/	All operational parameters: TOF, SYN FREQ, T1,T2,T3,TC,C1,C2,CN,MODE
TF/	TOF
C/	C1,C2,CN
T/	T1,T2,T3,TC
S/	SYN FREQ
M/	MODE
Z/	Requested TØ time
Y/	Typewriter printout ON/OFF: i.e., Y/ON Y/OFF

Table 2. Parameter definitions

Abbreviation	Meaning
TOF	Round-trip light time
SYN FREQ	Exciter synthesizer frequency
T1	First component integration time
T2	Lower-frequency components integration time
T3	Post-acquisition DRVID integration time
TC	10-MHz calibration integration time
C1	Highest-frequency component
C2	Lowest-frequency component
CN	Number of post-acquisition DRVID points before automatic reacquisition
MODE	Select configuration (i.e., Block III or IV receiver phasing, reacquisition with or without coder sync, etc.) "-" results in standard configuration
TØ	Coder synchronization time

```
FOO   14:51  APR 05, '7?                                        SUPER MU II
     326*                                        PAGE
     327*                                  *COMMAND LIST
     328*  01 00782 2  C1        A  COMSCAN BYTE   8'301',8'257'   A/
           01 00782 3  AF        A
     329*  01 00783    1EFA      N          WORD   SCT0F
     330*  01 00783 2  000A      A          WORD   10
     331*  01 00784    C3        A          BYTE   8'303',8'257'   C/
           01 00784 1  AF        A
     332*  01 00784 2  1F2A      N          WORD   SCC1
     333*  01 00785    0003      A          WORD   3
     334*  01 00785 2  D4        A          BYTE   8'324',8'257'   T/
           01 00785 3  AF        A
     335*  01 00786    1F0A      N          WORD   SCT1
     336*  01 00786 2  0004      A          WORD   4
     337*  01 00787    D3        A          BYTE   8'323',8'257'   S/
           01 00787 1  AF        A
     338*  01 00787 2  1F02      N          WORD   SCSYNF
     339*  01 00788    0001      A          WORD   1
     340*  01 00788 2  DA        A          BYTE   8'332',8'257'   Z/
           01 00788 3  AF        A
     341*  01 00789    1F4A      N          WORD   SCTO
     342*  01 00789 2  0001      A          WORD   1
     343*  01 0078A    CD        A          BYTE   8'315',8'257'   M/
           01 0078A 1  AF        A
     344*  01 0078A 2  1F42      N          WORD   SCMDE
     345*  01 00788    0001      A          WORD   1
     346*  01 00788 2  D4        A          BYTE   8'324',8'306'   TF
           01 00788 3  C6        A
     347*  01 0078C    1EFA      N          WORD   SCT0F
     348*  01 0078C 2  0001      A          WORD   1
     349*  01 0078D    D9        A  COMEND  BYTE   8'331',8'257'   Y/
           01 0078D 1  AF        A
     350*  01 0078D 2  1F52      N          WORD   TYCMD
     351*  01 0078E    0001      A          WORD   1
     352*                                        PAGE
     353*                                  *PARAMETER LIST
     354*  01 0078E 2  0006      A  SCT0F   WORD   6
     355*  01 0078F    1F5A      N          WORD   T0FMSG
     356*  01 0078F 2  1BF0      N          WORD   INGR
     357*  01 007C0    2872      N          WORD   IT0F
     358*  01 007C0 2  000E      A  SCSYNF  WORD   14
     359*  01 007C1    1F60      N          WORD   SYNFMSG
     360*  01 007C1 2  1C3E      N          WORD   INDPFP
     361*  01 007C2    2874      N          WORD   ISYNF
     362*  01 007C2 2  000E      A  SCT1    WORD   14
     363*  01 007C3    1F6E      N          WORD   TMSG
     364*  01 007C3 2  1BF0      N          WORD   INGR
     365*  01 007C4    2864      N          WORD   IT1
     366*  01 007C4 2  0006      A  SCT2    WORD   6
     367*  01 007C5    1F80      N          WORD   T2MSG
     368*  01 007C5 2  1BF0      N          WORD   INGR
     369*  01 007C6    2866      N          WORD   IT2
     370*  01 007C6 2  0006      A  SCT3    WORD   6
     371*  01 007C7    1F86      N          WORD   T3MSG
     372*  01 007C7 2  1BF0      N          WORD   INGR
     373*  01 007C8    2868      N          WORD   IT3
     374*  01 007C8 2  0006      A  SCTC    WORD   6
     375*  01 007C9    1F8C      N          WORD   TCMSG
     376*  01 007C9 2  1BF0      N          WORD   INGR
     377*  01 007CA    286A      N          WORD   ITC
     378*  01 007CA 2  000E      A  SCC1    WORD   14
     379*  01 007CB    1F7C      N          WORD   CMSG
     380*  01 007CB 2  1BF0      N          WORD   INGR
     381*  01 007CC    286C      N          WORD   IC1
     382*  01 007CC 2  0006      A  SCC2    WORD   6
     383*  01 007CD    1FC2      N          WORD   C2MSG
     384*  01 007CD 2  1BF0      N          WORD   INGR
     385*  01 007CE    2862      N          WORD   IC2
     386*  01 007CE 2  0006      A  SCCN    WORD   6
     387*  01 007CF    1FC8      N          WORD   CNMSG
     388*  01 007CF 2  1BF0      N          WORD   INGR
     389*  01 007D0    286E      N          WORD   ICN
     390*  01 007D0 2  000A      A  SCMDE   WORD   10
     391*  01 007D1    1F8A      N          WORD   MMSG
     392*  01 007D1 2  1CC0      N          WORD   INMDE
     393*  01 007D2    2870      N          WORD   IMDE
     394*  01 007D2 2  000E      A  SCTO    WORD   14
     395*  01 007D3    1F94      N          WORD   TOMSG
     396*  01 007D3 2  1D60      N          WORD   INTO
     397*  01 007D4    288C      N          WORD   ITO
     398*  01 007D4 2  000F      A  TYCMD   WORD   14
     399*  01 007D5    1FA2      N          WORD   TYMSG
     400*  01 007D5 2  1C92      N          WORD   CNTRL
     401*  01 007D6    287C      N          WORD   ITYSWT
```

Fig. 1. Mu-II software listing

```
Command, IF command request DO.
    Save current parameters.
    Input line.
    DO UNTIL input stack empty.
        Separate next input field.
        Search command table for match.
        IF NOT match.
            Notify operator.
            EXIT command.
        ELSE.
            Location ← command table (match +1).
            Count ← command table (match +2).
      Parameter, DO UNTIL count = 0.
        If input stack NOT EMPTY.
            Separate next input field.
        ELSE
            Print parameter table (location) characters from
              string addressed by parameter table (location +1).
            Input line.
        Location ← location +2.
        DO SUBROUTINE addressed by parameter table (location).
        Location ← location +1.
        Store result in parameter addressed by parameter table (location)
        Location ← location +1.
        Count ← count -1
      END
    END
END
```

Fig. 2. Structured representation

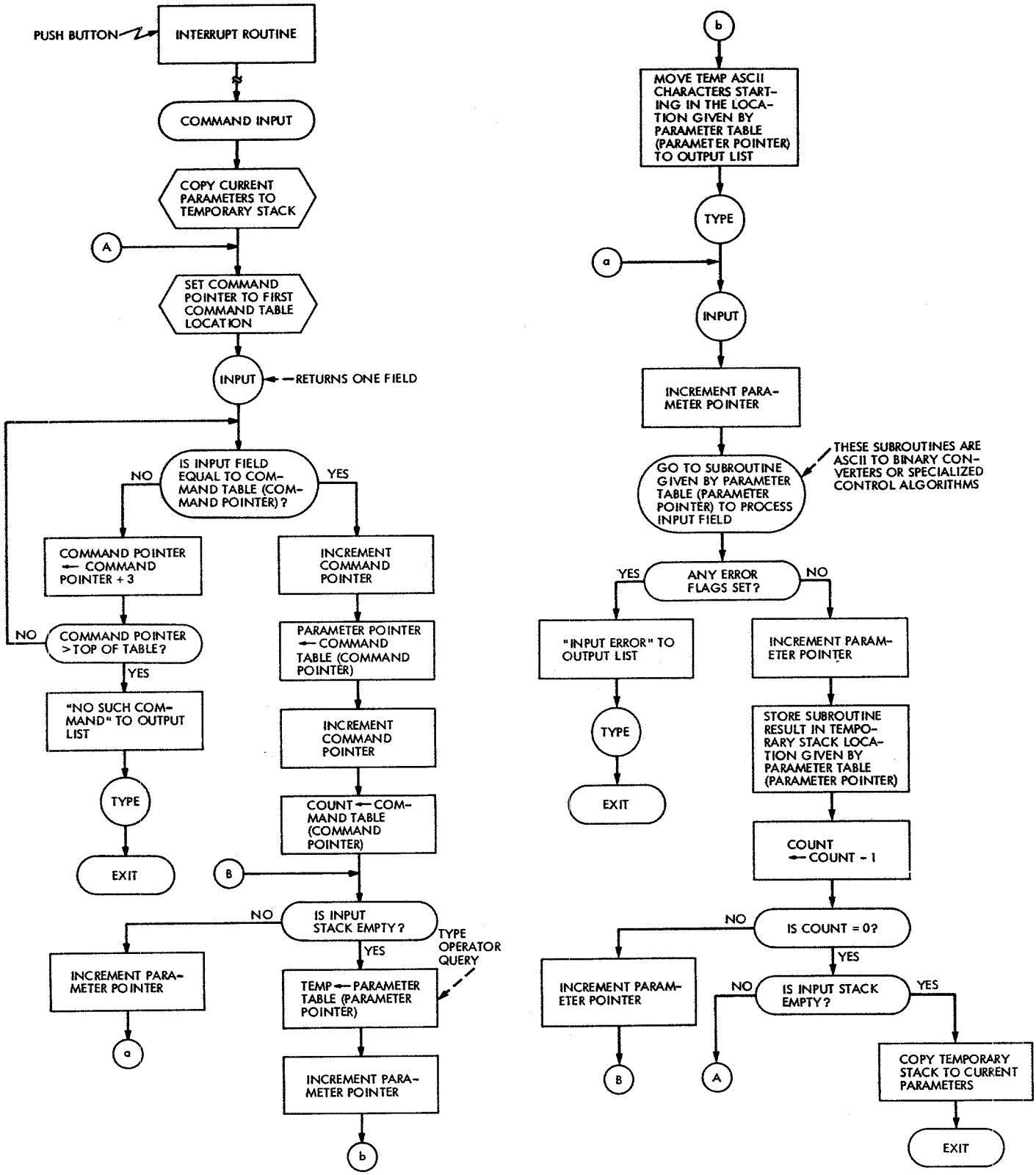

Fig. 3. Tutorial input schematic flowchart (Mu-II realization)

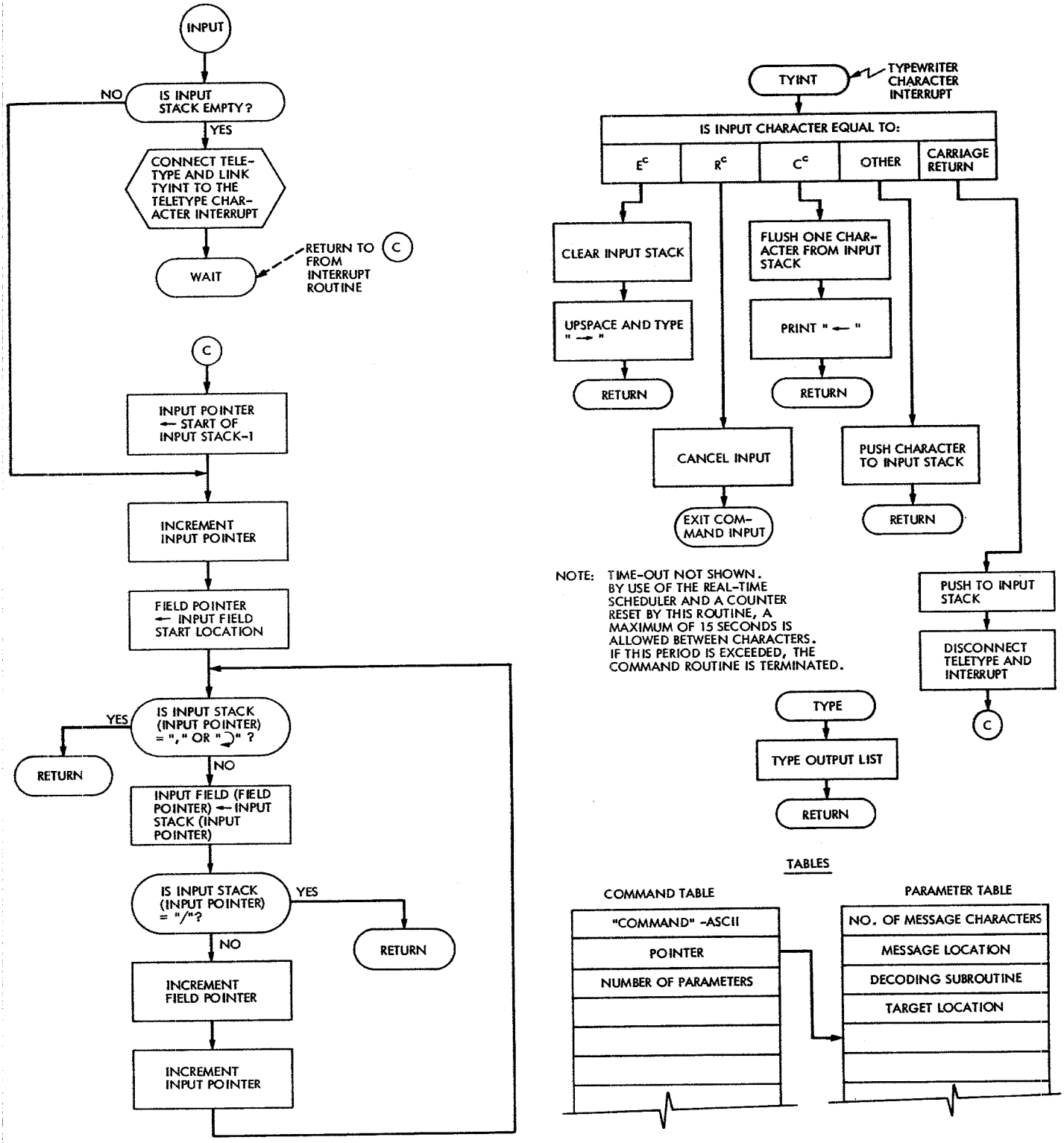
INPUT
NO
IS INPUT STACK EMPTY?
YES
CONNECT TELETYPE AND LINK TYINT TO THE TELETYPE CHARACTER INTERRUPT
WAIT
RETURN TO FROM INTERRUPT ROUTINE
C
C
INPUT POINTER ← START OF INPUT STACK-1
INCREMENT INPUT POINTER
FIELD POINTER ← INPUT FIELD START LOCATION
YES
IS INPUT STACK (INPUT POINTER) = "," OR "↵" ?
RETURN
NO
INPUT FIELD (FIELD POINTER) ← INPUT STACK (INPUT POINTER)
IS INPUT STACK (INPUT POINTER) = "/"?
YES
RETURN
NO
INCREMENT FIELD POINTER
INCREMENT INPUT POINTER
TYINT
TYPEWRITER CHARACTER INTERRUPT
IS INPUT CHARACTER EQUAL TO:
E^C
R^C
C^C
OTHER
CARRIAGE RETURN
CLEAR INPUT STACK
UPSPACE AND TYPE " → "
RETURN
FLUSH ONE CHARACTER FROM INPUT STACK
PRINT " ← "
RETURN
CANCEL INPUT
EXIT COMMAND INPUT
PUSH CHARACTER TO INPUT STACK
RETURN
PUSH TO INPUT STACK
DISCONNECT TELETYPE AND INTERRUPT
C
NOTE: TIME-OUT NOT SHOWN. BY USE OF THE REAL-TIME SCHEDULER AND A COUNTER RESET BY THIS ROUTINE, A MAXIMUM OF 15 SECONDS IS ALLOWED BETWEEN CHARACTERS. IF THIS PERIOD IS EXCEEDED, THE COMMAND ROUTINE IS TERMINATED.
TYPE
TYPE OUTPUT LIST
RETURN
TABLES
COMMAND TABLE
"COMMAND" -ASCII
POINTER
NUMBER OF PARAMETERS
PARAMETER TABLE
NO. OF MESSAGE CHARACTERS
MESSAGE LOCATION
DECODING SUBROUTINE
TARGET LOCATION

Fig. 3 (contd)